MODELING OF EXTENSIONAL BEHAVIOUR OF POLYMERS

MODELING OF EXTENSIONAL BEHAVIOUR OF POLYMERS

By

JOHN POCHER, B.SC., B.ENG.

A Thesis

Submitted to the School of Graduate Studies

in Partial Fulfillment of the Requirements

for the Degree

Master of Engineering

McMaster University

Master of Engineering (1996)
(Civil Engineering)

McMaster University
Hamilton, Ontario

TITLE: Modeling of Extensional Behaviour of Polymers

AUTHOR: John Peter Pocher, B.Sc. (University of British Columbia), B.Eng. (McMaster University)

SUPERVISORS: Dr. J. Vlachopoulos
Dr. B. Koziey

NUMBER OF PAGES: xi, 111

ABSTRACT

The use of polymeric materials in the manufacturing industry has vastly increased since the 1950's. Because of the large amounts of material involved in modern processing operations, attempts have been made over the years to numerically simulate the processes, in the hope of optimizing operating parameters. However, in contrast to other, more traditional materials such as steel or glass, there is not a well understood connection between the microscopic structure and the (highly non-linear) macroscopic physical response of polymers. Because of this lack of microscopic cause - macroscopic effect knowledge, many descriptions of the physical response of polymers are largely phenomenological ones; that is, the equations used to model the stress/strain response make no attempt to convey information about the microscopic structure of the material.

In the present work, five constitutive equations - Mooney-Rivlin, Ogden, G'Sell Two-term Polynomial and K-BKZ - are used to model the stress/strain response of two different polymers commonly used in thermoforming and blowmolding operations, ABS and HDPE, to uniaxial elongation and equibiaxial extension. The models are compared to experimental stress/strain data obtained from an industrial source, and the applicability of their predictions are investigated with regards to variations in strain, strain rate and temperature. Lastly, since the vast majority of real processes involve biaxial, not uniaxial, deformations, the ability of the models to predict equibiaxial response using parameters fit solely to uniaxial data is considered, in order to

investigate the possibility of being able to forego the need for expensive, difficult biaxial tests.

ACKNOWLEDGMENTS

In presenting this thesis, I wish to express my sincere appreciation to the following individuals and organizations who have helped in its completion:

My supervisors, Dr. John Vlachopoulos, of the Department of Chemical Engineering, and Dr. Brad Koziey, of the Department of Civil Engineering, for their great enthusiasm, interest and assistance throughout.

The late Dr. Farooque Mirza, whose seemingly endless supply of enthusiasm, knowledge and patience inspired me to pursue graduate work in this area.

The Department of Civil Engineering and the National Science and Engineering Research Council for financial support in the form of scholarships.

My contacts in industry who very generously supplied the raw data for this work, and assisted with many helpful discussions, suggestions and comments on extensional data fitting.

Lastly, and most importantly, I would like to acknowledge the continuous support and confidence provided to me by my wife, Teresa, which made the completion of this work possible.

TABLE OF CONTENTS

LIST OF FIGURES

LIST OF TABLES

CHAPTER 1

1.1 Introduction

The ever increasing use of polymers in the fabrication of both expensive, specialized parts, as well as for everyday items, has led to a need to better understand and predict their physical response during processing operations, and during extended use.

Polymers are materials composed of giant molecular chains. The word "polymer" comes from Greek, and is indicative of their basic physical structure; "poly" meaning many, and "mer" coming from the word "meros", meaning "a part". Many of these parts, called monomers, combine with strong carbon-carbon bonds to form the chains [1].

There are many naturally occurring polymers that have been used by mankind since pre-historic times, such as leather, wool, bone and wood. However, these materials were taken as they were found, and were in no way engineered for any specific purpose. It was not until the early 1800's that workers in the field began to look closely at polymers such as rubber. In 1839, Charles Goodyear invented the process of vulcanization, whereby the extreme softening and hardening of rubber with temperature was greatly lessened, which allowed the production of high durability products. Further development followed, leading to John Wesley Hyatt, in 1869,

producing the first synthetic plastic material, called celluloid, from cellulose nitrate and camphor.

While the early work of researchers and industrialists greatly increased the knowledge of polymer technology, a clear picture of the nature of these materials did not evolve until the 1920's, when the German chemist Hermann Staudinger clearly demonstrated the macromolecular concepts of long chains of repeating units. Indeed, his work was of such importance, that it is from the 1932 appearance of his book, "Die Hochmolekularen Organischen Verbindungen", that one can mark the start of a new era in polymer science and technology.

There are many different types of polymers in use today, and many different classifications to identify them. One such classification is the distinction between polymers which are amorphous and those which are semi-crystalline. Amorphous polymers are composed of randomly packed molecular chains, whereas semi-crystalline polymers possess both amorphous and crystalline regions, and are generally stiffer than those of the amorphous type. Amorphous polymers are identified by major variations in physical response due to temperature changes: the so-called "glass transition temperature", T_g, is the temperature at which they change from brittle, glassy solids to rubberlike materials, and the melt temperature, T_m, is where they become viscous liquids, although they may still exhibit elastic response (this is the subject of viscoelasticity). Another classification is the distinction between: thermoplastics, which can be repeatedly melted by heating and solidified by cooling, without affecting their basic nature; thermosets, which react upon application of heat and pressure, to form stiff, cross-linked networks, which are not able to be softened to make them flow; and

elastomers, which are highly deformable, almost completely elastic, cross-linked materials [1]. Although thermosets and elastomers are important in their own right, and are found in many applications, the type of polymers that are considered in this thesis are the thermoplastic type, which are used in thermoforming and blowmolding operations.

Some of the more common polymers, their uses and their glass and melting temperatures are listed in Table 1.1. As can be seen, they cover a very broad range of applications, and are processed in a myriad of different ways. Their use is increasing yearly, as refinements and advancements occur in both the materials themselves and their manufacturing processes.

Table 1.1: Glass and Melt Temperatures of Commonly Used Polymers, and Their Main Uses (from [1])

Polymer	Abbreviation	T_g (°C)	T_m (°C)	Main Uses
High Density Polyethylene	HDPE	-110	134	Extruded and injection molded articles, bottles and containers
Low Density Polyethylene	LDPE	-110	115	Flexible packaging film; flexible extruded and molded articles
Polystyrene	PS	90-100	–	Transparent extruded and molded articles; foamed articles
Polyvinylchloride	PVC	87	–	Extruded rigid and plasticized articles
Polypropylene	PP	-10	165	Rigid extruded and molded articles
Polyethylene terephthalate	PET	70	260	Fibres and transparent strong films

While the use of polymers has steadily increased over the years, they are not without inherent disadvantages with respect to more traditional materials. These disadvantages include: having low strength and stiffness; having temperature limitations (at low temperatures they are brittle, at high temperatures they soften); and under sustained load they creep. These drawbacks, however, are counter-balanced by

their advantages, including: they are easily shaped or molded into complex shapes with minimum fabrication and finishing; they have high strength to weight ratios; they can act as thermal or electrical insulators; and it is possible to impart special characteristics (optical, physical or chemical) to them through their production or processing stages. Some physical characteristics of commonly used polymers and other traditional materials are listed in Table 1.2.

Table 1.2: Tensile Moduli of Polymers and Other Engineering Materials (from [1,2])

Material	Modulus, E ($N/m^2 x10^{-9}$)	Density, ρ ($kg/m^3 x10^{-3}$)	Specific Modulus E/ρ ($x10^{-6}$)
Commonly processed HDPE	1-7	1	1-7
"Extrusion drawn" HDPE fibres	~70	1	~70
Specially cold drawn HDPE fibres	68	1	68
DuPont "Kevlar" fibres	132	1.45	92
Theoretical limit of polymers other than HDPE and PVA - fully extended	<140	~1	<140
Theoretical limit of HDPE and PVA - fully extended	240-250	1	240-250
Aluminum alloys	<70	~2.7	~26
"E" glass fibre	63	2.54	35
Steels	~200	~7.9	~25

In addition to their physical properties, polymers have unique responses to deformations which further set them apart from traditional materials. Figures 1.1 and 1.2 illustrate the common stress-strain response of polymers (in this case high impact polystyrene, or HIP, and Polyethylene Terephthalate, or PET), showing the variation with respect to changes in strain rate and temperature [3,4]. The characteristics shown in these plots are relatively easy to understand and are intuitive from a physical viewpoint; less easily understood are the more complicated physical manifestations of the complex nature of polymers. These include: shear thinning; first and second normal stress differences; stress relaxation; stress overshoot; and extensional viscosity.

Figure 1.1: Uniaxial Elongational True Stress as a Function of True Strain, HIP, 122 deg. C,
Showing Typical Variation of Stress with Strain Rate

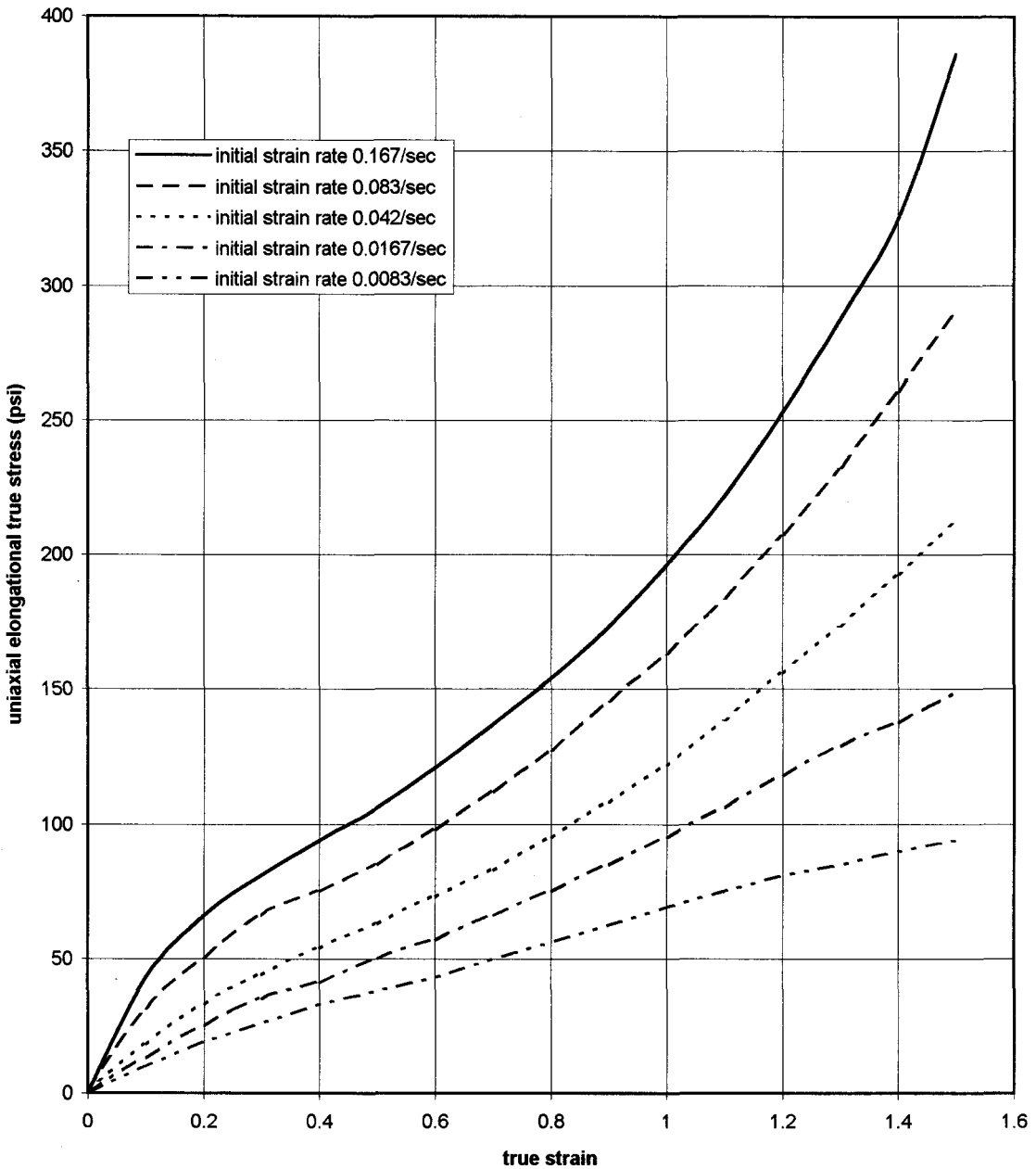

Figure 1.2: Uniaxial Elongational True Stress as a Function of True Strain, PET, Strain Rate 0.95/sec
Showing Typical Variation of Stress with Temperature

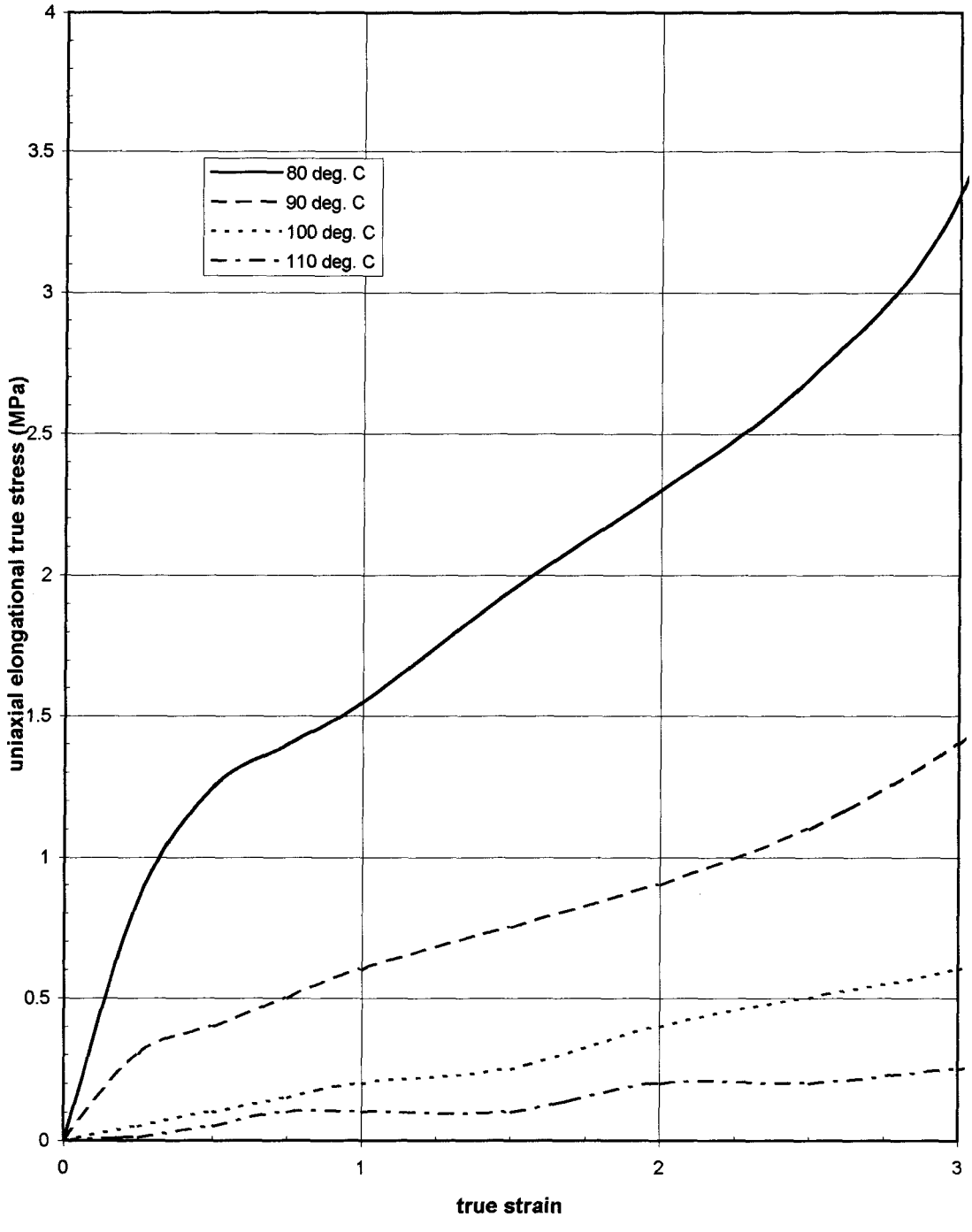

The subject of rheology has been employed extensively over the past 40 years in the study of constitutive models in order to model these unique non-Newtonian phenomena; to date there has been no success in accounting for all of them with one constitutive model.

1.2 Polymer Processing Operations

The types of flows studied in this thesis are elongational flows, both uniaxial and equibiaxial. While there are a great many processes in which these types of flows occur (such as film blowing, calendering and fibre spinning), this work is largely concerned with the application of constitutive models to the numerical simulation of thermoforming and blowmolding. A brief description of each of these processes follows.

1.2.1 Thermoforming

In thermoforming, a flat sheet of polymer is heated slightly above its melting or glass transition temperature, clamped along the mold perimeter, and then forced into the mold cavity by one of the following means: vacuum, applied through holes or channels in the mold - this is called *vacuum forming*; pressure, which forces the polymer sheet into the mold - this is called *pressure forming*; a force applied by a plunger or plug, which has a shape matching that of the mold - this is called *matched mold forming*, or *plug assisted thermoforming*, when it is used in conjunction with either the pressure or vacuum methods [1,6]. These thermoforming processes are shown schematically in Figures 1.3 and 1.4 (from [5]).

1.2.2 Blowmolding

Blowmolding is a very important process which is used to produce hollow articles such as bottles. In this process, a hollow sleeve of molten material, called a parison, is extruded between two halves of a mold. Air is then blown into the parison, causing it to expand like a balloon, taking the shape of the mold, and quickly solidifying as it touches the cold mold surface [1]. The process is shown schematically in Figure 1.5 (from [5]).

One of the main advantages of blowmolding is that it can achieve quite high outputs, since the cooling step can be made very short. Its main disadvantage is one that it shares with many processing operations, in particular thermoforming, and that is the thickness distribution along the walls of the finished part can vary greatly, depending on the shape of the item. There are two solutions to this commonly occurring problem: the first involves a method of trial and error, whereby the initial thickness of the sheet or parison is "programmed" to account for the eventual uneven thinning [1]; the second involves numerically simulating the process, with the aid of accurate, realistic constitutive models, and altering the conditions under which the process operates in order to produce a part with the desired thickness distribution. It is this second method to which the present work is intended to apply.

1.3 Constitutive Models

As mentioned above, constitutive models play a large role in the study of polymer processing and rheology. The relationship between applied stimulus and physical response is characteristic of the unique "constitution" of the material, hence

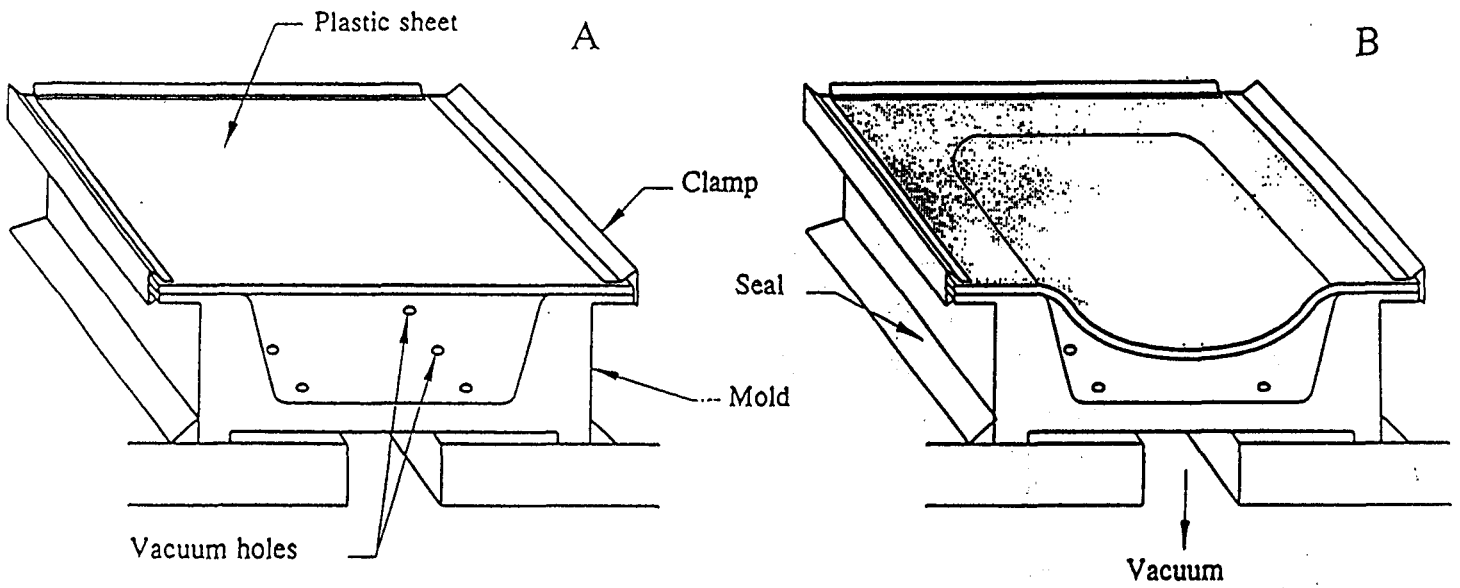

Figure 1.3: Vacuum Forming: (A) preheated clamped sheet over female mold prior to forming; (B) vacuum applied

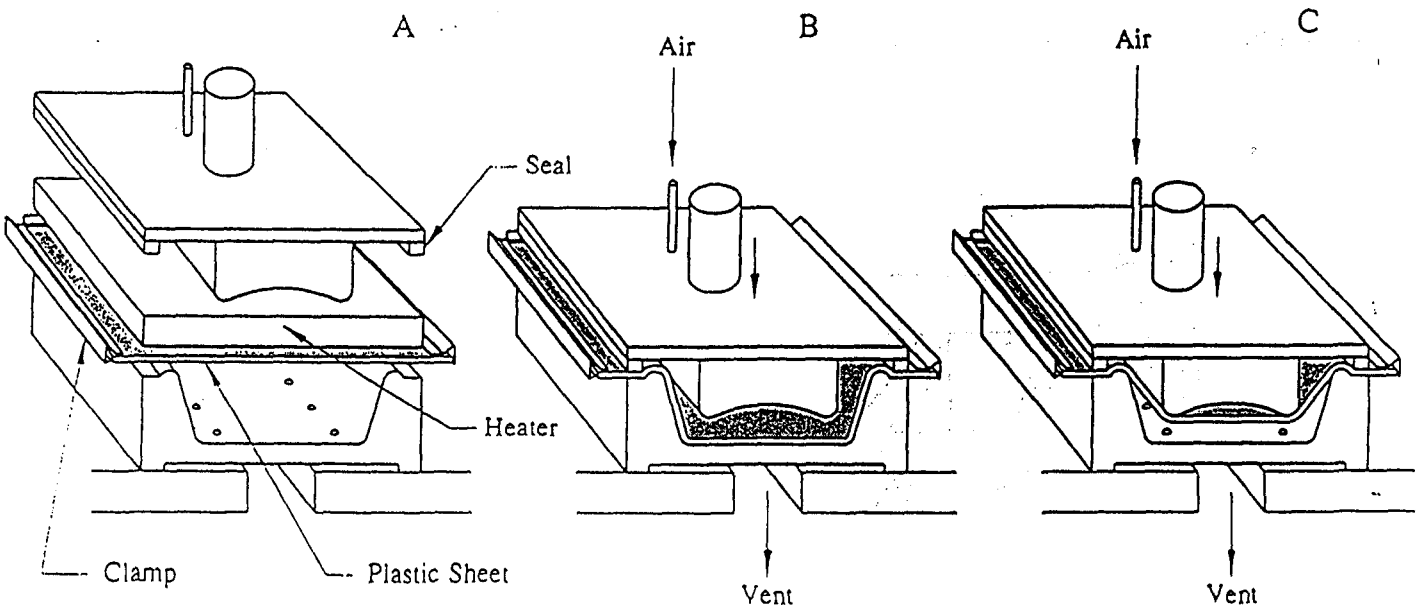

Figure 1.4: Plug-assist thermoforming: (A) preheated, clamped sheet prior to forming; (B) sheet stretched with plug advance; . (C) sheet air-pressure formed into female mold.

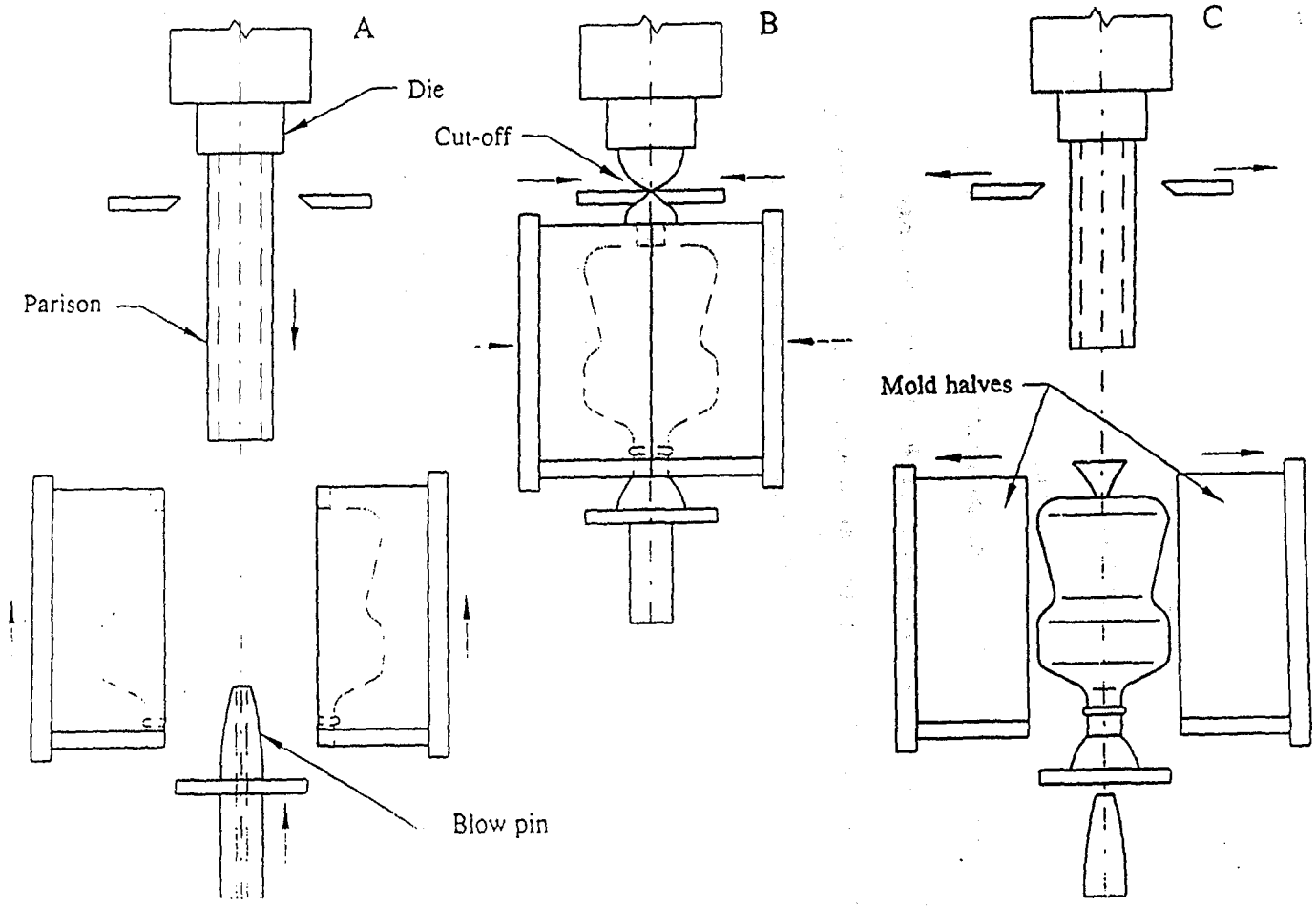

Figure 1.5: Basic extrusion blowmolding process: (A) parison being extruded; (B) compressed air inflates parison; (C) blown container being ejected.

the name "constitutive equations". This relationship is a mathematical one; it allows the calculation of stress in a given material, knowing the details of the applied stimulus, or flow history [7].

Broadly speaking, constitutive models can be classified as either "molecular" or "continuum" models [8]. Molecular models are those that, as a first step, assume or prescribe some shape or attribute to the microscopic molecules of the material, and using physical laws, derive and describe the macroscopic response. While these have had some success with dilute polymer solutions (for example, dumbbell theories [1,9]), they do not accurately describe the response of polymer melts. As a result, constitutive models most often used in describing polymer melts are continuum theories, and are furthermore empirical.

A further classification of continuum models is possible, based on the form of the equations used. There are "rate equations", where the constitutive equations are written in terms which include the rate of stress. An example of this type is the Maxwell fluid. There are also "differential constitutive equations", where the stress is dependent upon the derivative of some function. Examples of this type include the so-called Second-Order Fluid, Reiner-Rivlin Fluid and the Criminale-Eriksen-Filbey (CEF) model. Lastly, there are the "integral constitutive equations", where the stress is considered the integral of some function(s), integrated (usually) over the time domain. Examples of this type include the Lodge rubberlike liquid equation, and the model developed simultaneously by Kaye and Bernstein, Kearsley and Zapas, known as the K-BKZ model [1,10].

1.4 Objectives

While the use of the finite element method in the modeling of polymer processing operations has shown great potential to provide accurate simulations, the results of these simulations are of little worth if the constitutive model used to characterize the physical response of the polymer is inaccurate. However, most of the effort in this field has gone to the production of sophisticated numerical techniques in order to accommodate the very large deformations which arise in the simulations, using a simple hyperelastic constitutive model. While such an approach can be considered valid for processes in which elasticity is dominant, such as very rapid blowmolding, in general a hyperelastic model will be found to be inadequate if it is applied to processes in which viscoelasticity plays a significant role, such as thermoforming.

A short search through any standard text on constitutive modeling will provide the reader with a myriad of constitutive equations for polymer melts, all of which have their unique strengths and weaknesses. It is not the purpose of this thesis to provide a comprehensive review of the field of rheology and its available constitutive equations; there are currently textbooks in which this material appears ([7,9]). Rather, it is the aim of this work to compare some common constitutive equations used in simulating polymer processing operations, with regards to their ability to mimic the physical response of polymers in uniaxial and biaxial deformation, at varying strain rates and temperatures. The constitutive models will be evaluated with respect to their ability to match the observed stress-strain response, and also on the relative ease of their parameter fitting and implementation. In addition, the ability of the models to predict

biaxial response using parameters fit to uniaxial data will be investigated, in order to determine the possibility of foregoing the need for expensive, difficult biaxial tests.

1.5 Outline

Chapter 2: This chapter provides a general background and development of the constitutive models used in this thesis. The underlying assumptions upon which each model is based are described, and the general form of the constitutive equations are presented.

Chapter 3: This chapter provides the details of the equations used. It describes the general testing conditions (as provided by the industrial source), the importance of the constant strain rate versus the constant cross head velocity test, and provides the physical definitions and notation used later in the equations. It next provides the explicit equations used for the two deformation types, and describes the performance of each model, for both polymers, for both types of deformation. Also presented are the results of using uniaxially fitted parameters to predict equibiaxial response. Lastly is a discussion of the problems associated with fitting the parameters of the K-BKZ model, and a short description of the search technique used.

Chapter 4: A summary of the main results is presented in this chapter. The main advantages and disadvantages of each model are discussed, and the models are compared to one another regarding their ability to match the observed data and their ease of implementation. Some recommendations for future work are also provided.

CHAPTER 2

BACKGROUND AND DEVELOPMENT OF MODELS

2.1 Mooney-Rivlin Model Formulation

The model proposed by Mooney [11], and later developed further by Rivlin [12,13] is described in this section. The model is a phenomenological one; that is, it does not make any attempt to convey information about the molecular nature of the materials (as opposed to, for example, statistical models, dumbbell models or reptation theory). Mooney's model is one of the earliest in this field, and also one of the most widely used. The original theory attempted to relate stress-strain response for rubberlike materials in conditions of simple shear, using a hyperelastic formulation.

In the development of the theory two assumptions were made: the first, applicable to the more specialized form of the theory, was that Hooke's Law was valid in a state of simple shear; the second assumption was that, in common with most other constitutive models used for this purpose, is that the material is incompressible and isotropic in the unstrained state.

In the restricted form of the theory (the general form of the theory will not be discussed in this thesis, since almost all published work makes use of the restricted form), the strain energy function can be expressed as

$$W = A_{10}\left(\lambda_1^{\,2} + \lambda_2^{\,2} + \lambda_3^{\,2} - 3\right) + A_{01}\left(\lambda_1^{\,-2} + \lambda_2^{\,-2} + \lambda_3^{\,-2} - 3\right) \qquad (2.1)$$

or, $$W = A_{10}(I_1 - 3) + A_{01}(I_2 - 3) \tag{2.2}$$

where λ_i (i=1,2,3) are the principal stretch ratios of the specimen, and I_1 and I_2 are the first and second invariants of the Finger tensor.

With this form of the strain energy function, the corresponding stress-strain relations are given by the derivatives of the strain energy with respect to I_1 and I_2 and are of the form

$$\sigma_1 - \sigma_2 = 2 \cdot \left(\lambda_1^{\,2} - \lambda_2^{\,2}\right) \cdot \left[\frac{\partial W}{\partial I_1} + \lambda_3^{\,2} \frac{\partial W}{\partial I_2}\right] \tag{2.3}$$

The exact expressions for the stress for the strain cases being considered (uniaxial and equibiaxial tension) will be developed in a section 3.3.1.

2.2 Ogden Model Formulation

The model proposed by Ogden [14] is one of the most easily understood and most used models. It was originally prompted by the need for a constitutive model which provided an accurate representation of the stress-strain response of highly elastic materials up to large stretch ratios, and yet was simple enough to be easily analyzed mathematically.

The model was an attempt to represent, mathematically, the isothermal mechanical behaviour of highly elastic, so called "rubberlike" materials. The term "rubberlike" is used to describe materials which are very nearly perfectly elastic for large quasi-static deformations from some ground (undisturbed) state, and, as a consequence, hysteresis effects are small. If such is the case, then one can postulate the existence of a strain-energy function by which their mechanical response can be

characterized. In other words, the materials are considered to be hyperelastic, like the Mooney-Rivlin Model.

In contrast with viscoelastic, viscoplastic and other models which take the time or strain history of the material into account, in the model Ogden proposed there is no such time dependence. In Ogden's model, the strain energy function (and thus the mechanical response) depends solely on the end states of strain and in no way upon the strain (or time) history; it is a path independent state function. The state of strain of each material element is specified completely (relative to some reference configuration) by the three principal stretches, hereafter denoted λ_1, λ_2 and λ_3.

In order to simplify the analysis (and borne by experience), the material is assumed to be isotropic; that is, there is no change in material properties with direction. Furthermore, the material is assumed to be incompressible; this has been shown to be the case for rubberlike solids, except in extreme circumstances.

With isotropic elastic solids, the strain energy function, denoted by ϕ, depends on the principal stretches λ_1, λ_2 and λ_3 relative to some "ground state". In Ogden's treatment, he took as the ground state the stress free, undistorted state, and all strains (or stretches) are measured relative to this ground state. If the constraint of incompressibility is assumed to hold, then the principal stretches are related through

$$\lambda_1 \cdot \lambda_2 \cdot \lambda_3 = 1 \tag{2.4}$$

to maintain the original volume of the specimen.

Previous to Ogden, when attempts were made to reproduce the stress-strain behaviour of rubberlike solids, a strain energy function was hypothesized which depended on some invariants of the strain tensor. These invariants are symmetric with

respect to λ_1, λ_2 and λ_3, and maintain or reinforce the idea of isotropy. However, the use of these invariants serves to complicate the mathematical analysis, in particular the calculation of "instantaneous" moduli of elasticity [15]. By using reference to the principle stretches, one retains the simplicity and elegance of isotropic elasticity.

Ogden's model evolved based on experiments performed by Treloar [16]. In these experiments, Treloar used three samples from a single sheet of vulcanized rubber, and subjected these samples to three distinct deformation types: uniaxial extension, equibiaxial elongation and pure shear.

The strain energy function proposed by Ogden is a function of the terminal states of strain only, and in no way depends upon the time to arrive at these terminal states. It assumes the material is isotropic, incompressible, and that the deformations occur at constant temperature, in other words, isothermally.

The strain measures which are considered (and which are coaxial with the Lagrangian strain ellipsoid), are

$$\varepsilon_i = \begin{cases} \dfrac{\left(\lambda_i^{\alpha} - 1\right)}{\alpha} & (\alpha \neq 0) \\ \ln\left(\lambda_i\right) & (\alpha = 0) \end{cases} \tag{2.5}$$

where α is any positive or negative real number. The first invariants of these strain measures are expressible as

$$\phi(\alpha) = \begin{cases} \dfrac{\left(\lambda_1^{\,2} + \lambda_2^{\,2} + \lambda_3^{\,2} - 3\right)}{\alpha} & (\alpha \neq 0) \\ \ln\left(\lambda_1 \lambda_2 \lambda_3\right) & (\alpha = 0) \end{cases} \tag{2.6}$$

which are symmetric in λ_1, λ_2 and λ_3. Henceforth $\alpha=0$ is excluded from consideration.

The strain energy function that Ogden proposed is a linear combination of the invariants above, and is denoted

$$\Phi = \sum_r \mu_r \phi(\alpha_r) \tag{2.7}$$

where the μ_r's are constants. The number of terms used cannot be determined *a priori*; rather a comparison with experimental data is necessary to determine how many terms are needed to achieve the desired response. In most cases, however, a three-term strain energy function is used to fit the data.

If the strain energy function, ϕ, is used, then the assumptions stated previously (elastic, isotropic and incompressible) allow the principal Cauchy stresses (σ_1, σ_2 and σ_3) to be written as

$$\sigma_i = \lambda_i \frac{\partial \phi}{\partial \lambda_i} - p \qquad (i = 1,2,3) \tag{2.8}$$

where p is an arbitrary hydrostatic pressure that is introduced due to the constraint of incompressibility.

When the above differentiation is carried out, the principal Cauchy stresses that result are given by

$$\sigma_i = \sum_r \mu_r \lambda_i^{\alpha_r} - p \qquad (i = 1,2,3) \tag{2.9}$$

2.3 G'Sell Model Formulation

One of the most useful phenomenological constitutive equations is one proposed by G'Sell [17,18,19]. The model was originally prompted by the need for a constitutive law which explicitly accounted for the variation of stress with strain rate. By "strain rate" it is meant the local true strain rate, as opposed to the engineering (or nominal) strain rate. The engineering strain rate is referenced to the original cross-sectional area, while the true strain rate is referenced to the current cross-sectional area (precise definitions of these terms are provided in Section 3.2). The model is capable of taking into account non-linear elastic, viscous and hardening phenomena (as well as softening, with the modified G'Sell model discussed later).

In the development of the model's original form, G'Sell and Jonas [20] examined the stress-strain response of HDPE and PVC, and arrived at a model of the form

$$\sigma = K \cdot \exp\left[\left(\frac{\gamma_\varepsilon}{2}\right)\varepsilon^2\right] \cdot \dot{\varepsilon}^m \tag{2.10}$$

where stress, σ, is expressed as a function of the constants K and γ_ε, and the rate sensitivity, m. It can be seen that with the rate sensitivity expressed in a single term, the modeling of the variation of stress with this term is greatly facilitated.

The original model of G'Sell is, however, of limited use when applied to the flow of molten (or semi-molten) polymers. Accordingly, in the later model of G'Sell, stress is expressed as a simple function of temperature, strain and strain rate.

The model is developed as follows:

$$\bar{\sigma}\left(T,\bar{\varepsilon},\dot{\bar{\varepsilon}}\right) = K(T) \cdot f[\bar{\varepsilon}] \cdot g\left[\dot{\bar{\varepsilon}}\right] \tag{2.11}$$

where $\bar{\sigma}$ is the "equivalent" stress, $\bar{\varepsilon}$ is the "equivalent" strain, $\dot{\bar{\varepsilon}}$ is the "equivalent" strain rate and K(T) is an Arrhenius-type function (shown in its final form here) to account for decrease in stress with increasing temperature:

$$K(T) = A \cdot \exp\left[-b\left(T - T_0\right)\right] \tag{2.12}$$

and $f[\bar{\varepsilon}]$ is a function which accounts for both yielding (in the initial viscoelastic domain), and hardening found with most polymer materials.

The function $f[\bar{\varepsilon}]$ can itself be expressed as a combination of two separate functions which account for the yielding and hardening separately. Thus

$$f[\bar{\varepsilon}] = V[\bar{\varepsilon}] \cdot D[\bar{\varepsilon}] \tag{2.13}$$

where

$$\begin{aligned} V[\bar{\varepsilon}] &= 1 - \exp[-w\bar{\varepsilon}] \\ D[\bar{\varepsilon}] &= \exp\left[h\bar{\varepsilon}^2\right] \end{aligned} \tag{2.14}$$

The usefulness of the separation of the strain dependent function becomes evident when considering the shape of most true stress/true strain curves for polymers. With judicious choice of the parameters, the function $V[\bar{\varepsilon}]$ will tend rapidly towards unity, just as the function $D[\bar{\varepsilon}]$ becomes dominant. Thus one is able to separate and deal individually with the phenomena of yielding and hardening.

The last term in the model, $g\left[\dot{\bar{\varepsilon}}\right]$, is to account for the variation in stress with strain rate. Since the model was developed from, and used with, extensional flow, $g\left[\dot{\bar{\varepsilon}}\right]$accommodates the increase in stress with strain rate (in contrast to shear flow, which shows a decrease in stress with strain rate). Thus

$$g\left[\dot{\bar{\varepsilon}}\right] = \dot{\bar{\varepsilon}}^{m} \tag{2.15}$$

where m is a term to account for rate sensitivity.

In summation, the model of G'Sell used in this thesis can be written

$$\bar{\sigma} = K(T)\cdot\left[1-\exp(-w\bar{\varepsilon})\right]\cdot\exp\left[h\bar{\varepsilon}^{2}\right]\cdot\dot{\bar{\varepsilon}}^{m} \tag{2.16}$$

As will be shown in Section 3.3.2.1, the separation of terms which account for the phenomena of yielding, hardening, temperature and strain rate variation greatly facilitates both the clear understanding of the model and its fitting to experimental data.

2.4 Two-Term Polynomial Model Formulation

Upon examination of the shape of the stress-strain curves considered in this thesis, it is evident that while strain hardening is evident when dealing with rubbery elastic materials, the dominant high strain feature for the polymers considered is strain softening. The G'Sell model discussed in the previous section is very successful in mimicking the viscoelastic, strain-rate sensitivity and hardening characteristics of polymer melts; however, it is in adequate when considering materials which exhibit softening at high strains. A modification of the G'Sell model, denoted the Two-term Polynomial model, is proposed and described in this section, on a purely phenomenological basis. It will be shown in Section 3.3.4 to be capable of modeling the strain softening behaviour mentioned above, as well as all of the other aspects that make the G'Sell model an appealing one, namely viscoelasticity, temperature dependence and strain rate sensitivity.

The modification of the G'Sell model occurs in the strain hardening term; instead of modeling the high-strain characteristics with only one second-order term in the exponential, a linear term is added to increase its versatility. Thus in the equation, instead of using a $\exp(h\varepsilon^2)$ term, the term used is $\exp(h_1\varepsilon^2+h_2\varepsilon)$, and the constitutive equation can be written

$$\bar{\sigma}(T,\bar{\varepsilon},\dot{\bar{\varepsilon}}) = K(T)\left[1-\exp(-w\bar{\varepsilon})\right]\exp\left(h_1\bar{\varepsilon}^2+h_2\bar{\varepsilon}\right)\dot{\bar{\varepsilon}}^m \tag{2.17}$$

This equation is identical to that of the G'Sell model, except for the above mentioned modification. For data which exhibits strain hardening, by setting $h_2=0$, the equation reduces to that of G'Sell. In general, the equation is no more difficult to fit than the G'Sell, and follows the same parameter fitting process, described in Section 3.3.3.

2.5 K-BKZ Model Development

Turning now to an entirely different type of constitutive model, we consider the K-BKZ type of equation. It was developed independently by Kaye [21] and Bernstein, Kearsley and Zapas [22]. In its development by Bernstein, Kearsley and Zapas [22] it is proposed to model the flow of fluids which strongly exhibit the kind of elastic recovery associated with rubbery solids.

Previous to the emergence of this type of equation, attempts were made to model the viscoelastic material behaviour by essentially one of two very simple ways. On the one hand, viscous terms can be added to an elastic solid model (this is known as the Voigt solid), while on the other hand, elastic terms can be added to a viscous fluid model (as in the elementary Maxwell model). In this manner, one can obtain

theories to describe the linear viscoelastic phenomena, however when the material exhibits nonlinear characteristics, these essentially solid or essentially fluid models do not suffice.

The model itself is an integral model, which in practical applications can make it difficult to work with, particularly in finite element method simulations; however, its excellent predictive ability somewhat justifies its limitations.

The original development of the K-BKZ class of equations was based on ideas found in rubber elasticity theory. Rather than be limited to a certain model for rubber, however, Kaye and Bernstein, Kearsley and Zapas instead considered the most general strain energy, which is a function of the elastic strain imposed. In the presentation of the K-BKZ constitutive model, it is instructive to examine the original theory from which it evolved (taken from [7]).

In classical rubber elasticity theory, there exists a strain energy function, given by

$$W = \frac{1}{2} G \cdot tr\, \underline{\underline{C}}^{-1} \tag{2.18}$$

where G is a material constant and $\underline{\underline{C}}^{-1}$ is the Finger strain tensor (defined in Section 3.2).

Letting the dependence of W on the strain be general, the equation above becomes

$$W = W\left(\underline{\underline{C}}^{-1}\right) \tag{2.19}$$

Since the principle of frame invariance must be held to apply, W can only depend on those properties of $\underline{\underline{C}}^{-1}$ which are independent of rotation; in other words, the invariants of $\underline{\underline{C}}^{-1}$. These invariants are written as:

$$\begin{aligned} I_1 &= tr\,\underline{\underline{C}}^{-1} \\ I_2 &= \frac{1}{2}\left[\left(tr\,\underline{\underline{C}}^{-1}\right)^2 - tr\,\underline{\underline{C}}^{-2}\right] \\ I_3 &= \det \underline{\underline{C}}^{-1} \end{aligned} \tag{2.20}$$

Also, due to the assumption of incompressibility (which all the constitutive models discussed herein have in common), $\det\underline{\underline{C}}^{-1}=1$. From the Cayley-Hamilton theorem,

$$\underline{\underline{C}}^{-3} - I_1\underline{\underline{C}}^{-2} + I_2\underline{\underline{C}}^{-1} - I_3\underline{\underline{I}} = 0 \tag{2.21}$$

it can be shown that $I_2=tr\underline{\underline{C}}$, and thus

$$W = W\left(I_1, I_2\right) \tag{2.22}$$

From the above argument it is seen that the strain energy function is a function of the first and second invariants only.

In order to obtain a useful theory from this fact, we now consider a unit cube of the rubber in question, and subject it to some extensional deformation. If, for the moment, the incompressibility constraint is relaxed, then W is a function of the three strain invariants, or equivalently, the three principle stretch ratios λ_1, λ_2 and λ_3.

Consider an incremental deformation $d\lambda_1$, with the other two stretch ratios held fixed. The increment of work performed by this deformation is

$$dW = f_1 \cdot d\lambda_1 \tag{2.23}$$

where f_1 is the normal force on the side of the cube to which the force is applied. The stress on this face of the cube is

$$\sigma_{11} = \frac{f_1}{A} = \frac{dW}{d\lambda_1} \cdot \frac{1}{A} \tag{2.24}$$

where A is the area of the face in question, $A=\lambda_2 \cdot \lambda_3$. If we now consider incremental deformations in all directions, we find

$$\sigma_{ii} = \frac{\partial W}{\partial \lambda_i} \cdot \lambda_j^{-1} \cdot \lambda_k^{-1} \tag{2.25}$$

where $i \neq j \neq k$. At this point the incompressibility constraint is invoked, and thus $\lambda_j^{-1} \cdot \lambda_k^{-1} = \lambda_i$. This gives

$$\sigma_{ii} = \frac{\partial W}{\partial \lambda_i} \cdot \lambda_i = \frac{\partial W}{\partial \varepsilon_i} \tag{2.26}$$

where ε_i is the so-called "Hencky strain"; $\varepsilon_i = \ln \lambda_i$.

Now, for an extensional deformation,

$$\underline{\underline{\varepsilon}} = \begin{bmatrix} \ln \lambda_1 & 0 & 0 \\ 0 & \ln \lambda_2 & 0 \\ 0 & 0 & \ln \lambda_3 \end{bmatrix} \tag{2.27}$$

If, however, the Hencky strain tensor is not in an extensional frame, it must undergo a rotation transformation to an extensional frame, and then rotated back. In other words, the operation

$$\hat{\underline{\underline{\varepsilon}}} = \underline{\underline{Q}}^T \cdot \underline{\underline{\varepsilon}} \cdot \underline{\underline{Q}} \tag{2.28}$$

must be performed, where Q is the rotation matrix.

We are now in the position to combine the form of the strain energy, W, with the strain tensors $\underline{\underline{C}}^{-1}$ and $\underline{\underline{C}}$. In an extensional deformation frame,

$$\frac{\partial W}{\partial \varepsilon_i} = \frac{\partial W}{\partial I_1}\frac{\partial I_1}{\partial \varepsilon_i} + \frac{\partial W}{\partial I_2}\frac{\partial I_2}{\partial \varepsilon_i} \tag{2.29}$$

However,

$$I_1 = \sum_i \lambda_i^{\,2} = \sum_i \exp(2\varepsilon_i) \tag{2.30}$$

$$I_2 = \sum_i \lambda_i^{\,-2} = \sum_i \exp(-2\varepsilon_i) \tag{2.31}$$

And so,

$$\frac{\partial I_1}{\partial \varepsilon_i} = 2\exp(2\varepsilon_i) \tag{2.32}$$

$$\frac{\partial I_2}{\partial \varepsilon_i} = -2\exp(-2\varepsilon_i) \tag{2.33}$$

leading to

$$\frac{\partial W}{\partial \varepsilon_i} = 2\frac{\partial W}{\partial I_1}\cdot\exp(2\varepsilon_i) - 2\frac{\partial W}{\partial I_2}\cdot\exp(-2\varepsilon_i)$$

$$= 2\frac{\partial W}{\partial I_1}\cdot\lambda_i^{\,2} - 2\frac{\partial W}{\partial I_2}\cdot\lambda_i^{\,-2} \tag{2.34}$$

which can be denoted in tensor form as

$$\underline{\underline{\sigma}} = \frac{\partial W}{\partial \underline{\underline{\varepsilon}}} = 2\frac{\partial W}{\partial I_1}\cdot\underline{\underline{C}}^{-1} - 2\frac{\partial W}{\partial I_2}\cdot\underline{\underline{C}} \tag{2.35}$$

This equation gives the stress in an incompressible elastic body subjected to extensional strain, to within an isotropic term. In the classical theory of rubber elasticity, $W=\frac{1}{2}GI$, and the above equation gives $\underline{\underline{\sigma}} = 2G\underline{\underline{C}}^{-1}$, as expected.

It is at this point that the K-BKZ class of equations differs from those of rubber elasticity. In the K-BKZ theory, elastic energy and stress are allowed to relax. W depends on the history of I_1 and I_2; it is assumed empirically that W is a history integral over a function of I_1, I_2 and t-t', and is written

$$W = \int_{-\infty}^{t} u(I_1, I_2, t-t')dt' \tag{2.36}$$

With this form of W, the stress is

$$\underline{\underline{\sigma}} = \int_{-\infty}^{t} \left[2\frac{\partial u}{\partial I_1}\underline{\underline{C}}^{-1}(t,t') - 2\frac{\partial u}{\partial I_2}\underline{\underline{C}}(t,t') \right] dt' \tag{2.37}$$

where $\underline{\underline{C}}^{-1}(t,t')$ and $\underline{\underline{C}}(t,t')$ are the relative Finger and Cauchy strain tensors respectively. This equation allows for great variation of stress with strain; a specific constitutive equation can be obtained by choosing a particular form for $u(I_1,I_2,t-t')$, along with some parameters.

Wagner's Equation

The specific form of the K-BKZ equations used in this thesis is that proposed by Wagner [23,24,25,26]. In Wagner's treatment, the effect of time and strain are shown to be independent of each other; that is, time-strain separability applies. Furthermore, the dependence of stress on the Cauchy tensor, $\underline{\underline{C}}(t,t')$, is omitted, and a damping function $h(I_1,I_2)$ is used to account for non-linear response.

Unfortunately, the omission of the $\underline{\underline{C}}(t,t')$ term, while simplifying the model and facilitating its use, introduces several drawbacks into Wagner's equation, namely:

1) the equation predicts a zero second normal stress difference in shear, N_2. This is in disagreement with observation, which has shown N_2 to be negative and approximately 20% that of the first normal stress difference, N_1.

2) Unless h is a function of I_1 only (which leads to a poor fit), then $h(I_1,I_2)\,\underline{\underline{C}}^{-1}(t,t')$ is not derivable from a potential function $u(I_1,I_2)$. The consequence of this is that for deformations rapid enough that relaxation does not occur, the equation can predict a net production of work done on the environment by the material as it is subjected to cyclic strain - a result that is in violation of the Second Law of Thermodynamics. It is due to this drawback that Wagner's equation should only be used for non-cyclic deformations.

In its form used in this thesis, Wagner's equation is

$$\sigma_{ij}(t) = \int_{-\infty}^{t} \mu(t-t') \cdot h(I_1,I_2) \cdot C_{ij}^{-1}(t,t')dt' \qquad (2.38)$$

where $\mu(t-t')$ is a linear viscoelastic memory function, t' is the previous time, t is the present time, $h(I_1,I_2)$ is the damping function to account for non-linear response and $C_{ij}^{-1}(t,t')$ is the relative Finger strain tensor.

The form of $\mu(t-t')$ is approximated by a series of exponential functions which are related to the material relaxation spectrum. The number of terms to be used in not known *a priori*; however usually 6 to 8 terms are used. The memory function is written

$$\mu(t-t') = \sum_{k=1}^{N} \frac{a_k}{\Gamma_k} \cdot \exp\left\{\frac{-(t-t')}{\Gamma_k}\right\} \tag{2.39}$$

where a_k are the relaxation modulus coefficients, Γ_k are the relaxation times (usually with an order of magnitude separating them) and N is the number of terms used.

Although there are many different forms possible for the damping function, $h(I_1,I_2)$, the one used in this theses is of the form proposed by Wagner and Demarmels [26]. It has been found to give excellent result within experimental limits for both uniaxial and equibiaxial flow. It is written as

$$h(I_1,I_2) = \frac{1}{1+A\sqrt{(I_1-3)(I_2-3)}} \tag{2.40}$$

where A is a material constant, and I_1 and I_2 are the first and second invariants of the relative Finger strain tensor, $\underline{\underline{C}}^{-1}(t,t')$. When A=0, the damping function $h(I_1,I_2)$ is equal to unity, and the equation becomes that of the Lodge rubberlike liquid. The damping function is used to account for non-linear viscoelastic response which is not predictable by the rubberlike constitutive equation; the rubberlike equation over-predicts the stress. Consequently, the damping tends to unity at small strains and decreases for larger strains.

It is interesting to note that in including a damping function in his equation, Wagner pointed out that the original rubberlike constitutive equation is unable to predict the observed non-linear shear response of polymers, i.e. shear thinning at higher strain rates. Thus, he observes, "the deviation of material behaviour from theoretical prediction is not one of strain hardening, but of strain thinning" [24].

CHAPTER 3

DESCRIPTION AND PERFORMANCE OF MODELS IN EXTENSION

3.1 Introduction

In this Chapter, a general background of the type of tests commonly performed will be provided, along with some topics to consider when modeling the data. Following that, relevant physical definitions are presented. Lastly, the explicit equations for each of the models are written, and the performance of each model is discussed for each polymer and deformation state considered.

3.1.1 Background

The polymers whose extensional behaviour is described, analyzed and modeled in this thesis are Acrylonitrile-butadiene-styrene (ABS) and High Density Polyethylene (HDPE). They are examples of thermoplastics; that is, they can be melted down, hardened, and melted down again, without affecting their basic nature. This is in contrast with thermoset polymers, which react at a given temperature to form very stiff cross-linked networks.

The data presented is from an industrial source, and show the results of tests performed for uniaxial and equibiaxial elongation, over a temperature range from 150°C to 190°C, and at various constant strain rates. For the uniaxial elongational measurement, a Meissner-type rheometer was used, at the following constant strain

rates (sec^{-1}): 0.008, 0.042, 0.082, 0.5 and 1.0 for ABS, and 0.00983, 0.03, 0.097, 0.29, and 0.602 for HDPE.

For the equibiaxial elongation tests, the equipment used was a Polymics Co., MARS-III rheometer. The tests were performed at 190°C at constant strain rates (sec^{-1}) of 0.01, 0.03, 0.1 and 0.3 for ABS, and at 0.03,0.1 and 0.3 for HDPE. In addition, in order to investigate the variation of stress with temperature, equibiaxial measurements were made for ABS at temperatures of 150°C and 170°C at constant strain rates of 0.3 sec^{-1}.

In the uniaxial case, the experimental operation is fairly straight forward; a cylindrical shaped specimen is loaded in such a manner (exponentially increasing cross-head velocity) so as to obtain a constant true strain rate. However, in the case of equibiaxial elongation, the procedure is not so simple, and there are many different techniques and apparatus available commercially to accomplish these tests [27]. To perform the experiments, one uses a disc-shaped specimen, and either pulls in the planar directions, or alternatively, one can subject the specimen to uniaxial compression in the axial direction. If proper care is taken, the deformation history of the specimen is the same in either case, and through proper understanding of the mechanics involved, the two types can be considered essentially identical. For the data presented in this work, the second type of test method (uniaxial compression) was used, with silicone oil of proper viscosity used as a lubricant between the specimen and the pressurizing plate, to ensure no erroneous frictional forces evolved, which would introduce a radial shear component of stress.

The two types of tests are shown schematically in Figures 3.1 and 3.2.

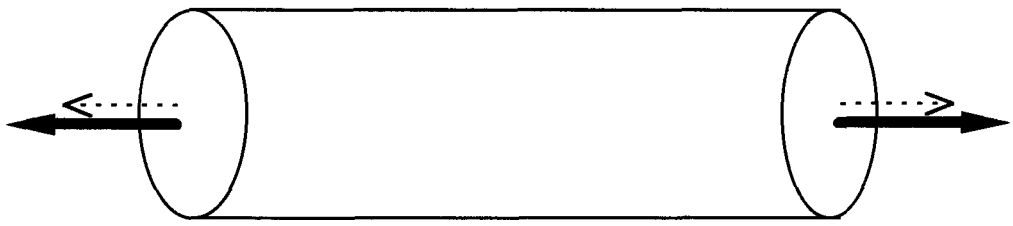

Figure 3.1: Uniaxial Test Schematic

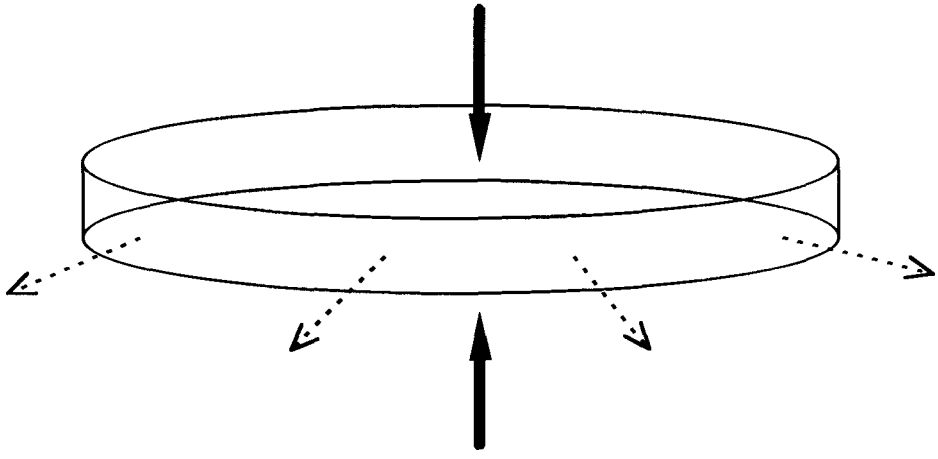

Figure 3.2: Equibiaxial Test Schematic

(Solid lines indicate faces to which stress is applied; dotted lines indicate direction of material deformation)

3.1.2 Constant Strain Rate versus Constant Cross-Head Velocity

In this section, the two types of elongational tests commonly used are examined, in the uniaxial framework for simplicity. The easier of the two tests to perform is the constant cross-head velocity test, in which the clamped ends of the specimen are pulled apart at a constant rate. Thus the specimen elongation rate, $\dot{L} = dL/dt$ is held constant. The data of concern are then the load, P, applied to the specimen and the amount of elongation, $(L-L_0)$, where L is the current length and L_0 the initial length of the specimen. While the data reported in previous works are all essentially of the same nature, various authors have used different approaches to analyze the data. For example, Cross and Haward [28] use a load-extension curve, obtained directly from the test; Oberst and Retting [29] and Andrews and Ward [30] report the so-called "engineering" or "nominal" stress and strain by dividing the primary variables P and $(L-L_0)$ by the original cross-sectional area, A_0, and the original length, L_0, respectively; while still others such as Jäckel [31], Lazurkin [32], Utsuo and Stein [33], Haward *et. al.* [34] and Pezzin *et. al.* [35] utilize curves simply labeled "stress" and "strain", without any precise definition of the terms.

The use of the engineering stress and strain is widespread in the consideration of traditional civil engineering materials such as steel and concrete. The reason for this is the magnitude of the deformations, or strains, that are common with these materials are much smaller than unity, and so small deformation theory is applied. However, the size of the deformations found with traditional civil engineering materials is much less than those routinely found in the processing of polymers, by several orders of magnitude. While experimentally straight forward, conventional testing methods do not

adequately describe the physical behaviour of polymers, because they are referred to the initial cross-section and length of the specimen, and not the current values. This can lead to incorrect conclusions regarding the magnitude of yield drops, the rate of strain hardening, etc. [20].

In order to properly model the large deformations that commonly occur in polymer processing, one must instead examine the "true" stress-strain behaviour. By "true" stress and strain it is meant the instantaneous values, which can be defined as

$$\sigma = \frac{P}{A} \tag{3.1}$$

$$\varepsilon = \lim_{l_0 \to 0}\left[\ln\left(\frac{l}{l_0}\right)\right] \tag{3.2}$$

where l_0 and l are the initial and current lengths of a small slice of the specimen where σ and ε are defined. In practical terms, the limit of $l_0 \to 0$ can be dropped, if necking is not too extensive, and one is left with simply

$$\varepsilon = \ln\left(\frac{l}{l_0}\right) \tag{3.3}$$

or,

$$\varepsilon = \ln(\lambda) \tag{3.4}$$

where λ is the stretch ratio In the direction of elongation.

One main advantage of using data from constant strain rate tests is that the constitutive modeling becomes much easier to accomplish. This is because, as in the G'Sell model discussed in this work, the variation of the stress, σ, with the strain rate, $\dot{\varepsilon}$, can be accounted for explicitly, with the use of some rate-sensitive coefficient. By

accounting for the strain rate explicitly, one can separate the strain-sensitive effects (such as yielding and strain-hardening) from the rate-sensitive effect, although the rate-sensitivity coefficient does, to a small extent, depend on ε. This can be seen in Figure 3.3, which shows the typical response of two polymers, in this case polyvinylchloride (PVC) and polyethylene (PE), at different strain rates, where it is seen that the separation between the curves (which is due to solely to strain rate) varies with strain (from [20]).

3.2 Physical Definitions and Development of Tensor Notation

The physical properties of interest in this work are stress and strain, and their relation to each other. For both of these properties, what is of primary concern is the so-called "true" stress and "true" strain, in contrast to the sometimes-quoted "engineering" (or nominal) stress or strain. While the difference is largely one of choice for stress, for strain it is extremely important to differentiate between the two, and to conduct experiments and analysis accordingly.

In the description of the motion or deformation of a material, one has the choice of using one of either the so-called Lagrangian or Eulerian descriptions. While the choice between the two is arbitrary (since both should give identical results), certain deformations (and processes) are more easily described by one or the other. The Eulerian description can be visualized as follows: if $Ox^1x^2x^3$ is a fixed (in space) coordinate system relative to which a motion or continuum is studied, then we can study the "flow" of material past a small "volume" of observation around some point x. In effect, this method describes the motion of a continuum from the viewpoint of an

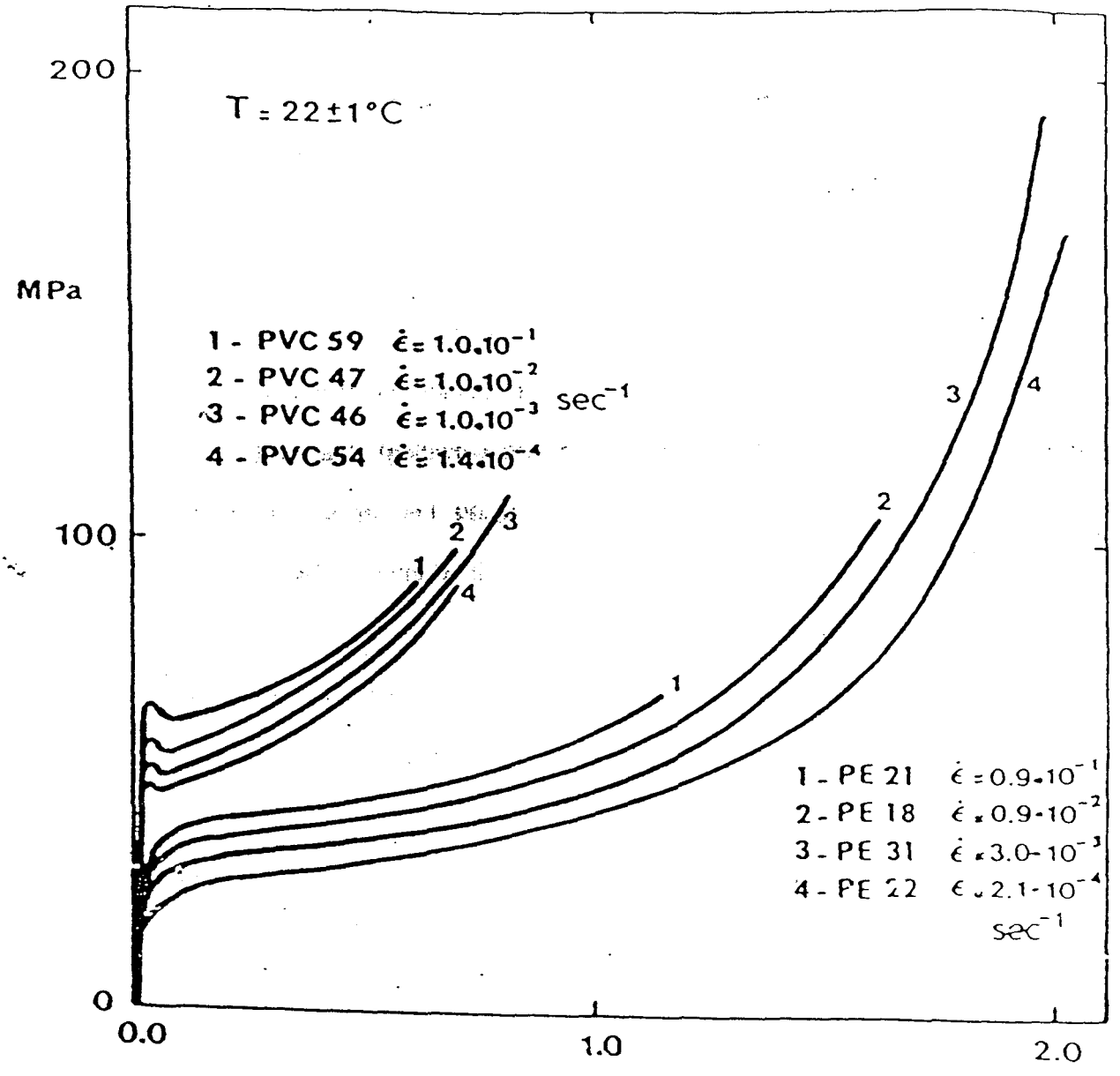

Figure 3.3: Typical true stress versus true strain curves for polymers PVC and PE tested at constant true strain rate

observer fixed in space. In contrast, if we describe the material motion in terms of a coordinate system $O\xi^1\xi^2\xi^3$ which deforms and rotates along with the material, this is called the Lagrangian description [36,37]. Although both descriptions will give identical results, the transformation from one to the other can become complicated for some flows, and thus it is convenient to choose the description which is most convenient for the process in question. When studying the deformation of elastic or viscoelastic solids, where the distance between arbitrary points is limited for the time frame considered (as in processes like thermoforming and blowmolding), the Lagrangian description is more convenient. However, when studying the flow of liquids, and in particular their steady state flows (as in processes like fibre spinning or film casting), the Eulerian description is the method of choice.

In the simple deformations described and modeled in this work, the Lagrangian description is used, although, as stated above, the Eulerian description would give identical results.

The most important properties considered herein are the true stress, σ, and the true strain, ε. The true stress on a face of a block of material is defined as the force per unit area, or

$$\sigma = \frac{P}{A} \qquad [3.1]$$

where A is the *current* area, as opposed to the original area, of the face. The true strain is sometimes called the Hencky (or logarithmic) strain, and can be defined as follows: if a cube of material is stretched in one direction, say the x-direction, by an infinitesimal amount dL, then the corresponding infinitesimal strain, $d\varepsilon$, is defined as

$$d\varepsilon_{xx} = \frac{dL_{xx}}{L_{xx}} \tag{3.5}$$

where L is the current length of the cube in the direction of the elongation. The total strain that has occurred is then the summation, or integral, of all the infinitesimal strains,

$$\varepsilon_{xx} = \int_{L_{0xx}}^{L_{xx}} \frac{dL_{xx}}{L_{xx}} = \ln\left(\frac{L_{xx}}{L_{0_{xx}}}\right) = \ln\lambda_1 \tag{3.6}$$

where λ_1 is called the "stretch ratio" in the direction of elongation, in this case the x (or 1) direction, thus it is denoted λ_1.

Similar definitions apply in the y and z directions, and so we can define the strain tensor ε_{ij};

$$\varepsilon_{ij} = \begin{bmatrix} \varepsilon_{xx} & 0 & 0 \\ 0 & \varepsilon_{yy} & 0 \\ 0 & 0 & \varepsilon_{zz} \end{bmatrix} = \begin{bmatrix} \ln\lambda_1 & 0 & 0 \\ 0 & \ln\lambda_2 & 0 \\ 0 & 0 & \ln\lambda_3 \end{bmatrix} \tag{3.7}$$

(Note this is for extensional deformations only. Shear is not considered)

Another useful definition is the deformation gradient tensor, which for elongational flows is defined as:

$$\underline{\underline{F}}^{-1} = \begin{bmatrix} \lambda_1 & 0 & 0 \\ 0 & \lambda_2 & 0 \\ 0 & 0 & \lambda_3 \end{bmatrix} \tag{3.8}$$

and the condition of incompressibility can be expressed as $\det \underline{\underline{F}}^{-1} = 1$.

Since polymers act like both a fluid and a solid, it is important to also define the velocity gradient, for which the rate of strain must be defined. If we consider a cylinder

of material that is being extended at one end at a rate of $\dot{L} = dL/dt$, then by the chain rule of calculus,

$$\dot{\varepsilon} = \frac{d\varepsilon}{dt} = \frac{d\varepsilon}{dL}\frac{dL}{dt} \tag{3.9}$$

but the strain gradient is

$$\frac{d\varepsilon}{dL} = \frac{1}{L} \tag{3.10}$$

and thus

$$\dot{\varepsilon} = \frac{1}{L}\frac{dL}{dt} \tag{3.11}$$

With this definition, the velocity gradient can be defined as

$$\underline{\underline{\nabla v}} = \begin{bmatrix} \dot{\varepsilon}_{xx} & 0 & 0 \\ 0 & \dot{\varepsilon}_{yy} & 0 \\ 0 & 0 & \dot{\varepsilon}_{zz} \end{bmatrix} \tag{3.12}$$

where $\dot{\varepsilon}_{ij}$ is the velocity gradient, $\partial v/\partial x_i$ in the direction i.

Because of the assumption of isotropy, the stress and strain tensors used in the constitutive models must be frame invariant; that is, they must not demonstrate different properties when regarded from different frames of reference. The manner by which this is accomplished is to consider a strain measure which has had the effect of rotation removed, and only retains the stretching nature of the deformation. Thus we have the stress tensor, $\underline{\underline{\sigma}}$, depend not on $\underline{\underline{F}}^{-1}$, but on the so-called Finger tensor, $\underline{\underline{C}}^{-1}$, defined as

$$\underline{\underline{C}}^{-1} = \left(\underline{\underline{F}}^{-1}\right)^T \cdot \underline{\underline{F}}^{-1} \tag{3.13}$$

In the integral-type constitutive model discussed herein, the Finger tensor used is the "relative" Finger tensor. To examine this, consider the one-dimensional case: if the stretch ratio at the current time, t, is written $\lambda(t)$, and the stretch ratio at some past time, t', is written $\lambda(t')$, then the "relative" stretch ratio is defined as

$$\lambda(t,t') = \frac{\lambda(t)}{\lambda(t')} \tag{3.14}$$

and the relative Finger tensor is written as

$$\underline{\underline{C}}^{-1}(t,t') = \begin{bmatrix} \lambda_1(t,t') & 0 & 0 \\ 0 & \lambda_2(t,t') & 0 \\ 0 & 0 & \lambda_3(t,t') \end{bmatrix} \tag{3.15}$$

For the two types of deformations considered in this work, the deformation gradient tensors and the Finger tensors are as follows:

Uniaxial elongation:

$$\underline{\underline{F}}^{-1} = \begin{bmatrix} \lambda & 0 & 0 \\ 0 & \lambda^{-1/2} & 0 \\ 0 & 0 & \lambda^{-1/2} \end{bmatrix} \; ; \; \underline{\underline{C}}^{-1} = \begin{bmatrix} \lambda^2 & 0 & 0 \\ 0 & \lambda^{-1} & 0 \\ 0 & 0 & \lambda^{-1} \end{bmatrix} \tag{3.16}$$

Equibiaxial elongation:

$$\underline{\underline{F}}^{-1} = \begin{bmatrix} \lambda & 0 & 0 \\ 0 & \lambda & 0 \\ 0 & 0 & \lambda^{-4} \end{bmatrix} \; ; \; \underline{\underline{C}}^{-1} = \begin{bmatrix} \lambda^2 & 0 & 0 \\ 0 & \lambda^2 & 0 \\ 0 & 0 & \lambda^{-4} \end{bmatrix} \tag{3.17}$$

Also used in constitutive modeling to maintain frame invariance are the invariants of the Finger tensor. The invariants of the Finger tensor for uniaxial and equibiaxial elongation are;

Uniaxial:

$$I_1 = \sum_i \lambda_i^2 = \lambda^2 + 2\lambda^{-1} \tag{3.18}$$

$$I_2 = \sum_i \lambda_i^{-2} = \lambda^{-2} + 2\lambda \tag{3.19}$$

Equibiaxial:

$$I_1 = \sum_i \lambda_i^2 = 2\lambda^2 + \lambda^{-4} \tag{3.20}$$

$$I_2 = \sum_i \lambda_i^{-2} = 2\lambda^{-2} + \lambda^4 \tag{3.21}$$

In each case, I_3 is equal to unity due to the incompressibility constraint.

3.3 Performance of Models in Extension

3.3.1 Mooney-Rivlin Model

Mooney-Rivlin Model Equations

The Mooney-Rivlin [11,12,13] model is based upon a postulated strain-energy function, W. It is supposed that W is a function of the two independent strain invariants, I_1 and I_2. In its most general form, W is as follows

$$W = \sum_{i=0}^{m} \sum_{j=0}^{n} A_{ij} (I_1 - 3)^i (I_2 - 3)^j \tag{3.22}$$

where m and n are to be determined, based on the number of terms needed to obtain an adequate fit to the experimental data, and A_{ij} are determined by comparison with the data. The so-called "standard" version of this model (the one that is almost exclusively quoted in the literature) is limited to two unknown constants A_{10} and A_{01} corresponding to m=1,0 and n=0,1 respectively. Thus the standard version is represented by

$$W = A_{10}(I_1 - 3) + A_{01}(I_2 - 3) \qquad [2.2]$$

and due to the incompressibility assumption, the stresses are related to the strain energy function by

$$\sigma_i = \lambda_i \cdot \frac{\partial W}{\partial \lambda_i} - p \qquad (3.23)$$

The form of the stress-stretch ratio function used in this work is that used by Rivlin in his extension of Mooney's work [12,13]. The relationship is determined by the derivatives of the strain energy function with respect to the strain invariants I_1 and I_2, and is of the form

$$\sigma_i - \sigma_j = 2\left(\lambda_i^2 - \lambda_j^2\right)\left[\frac{\partial W}{\partial I_1} + \lambda_k^2 \frac{\partial W}{\partial I_2}\right] \qquad (3.24)$$

But, due to the form of W,

$$\frac{\partial W}{\partial I_1} = A_{10} \quad \textit{and} \quad \frac{\partial W}{\partial I_2} = A_{01} \qquad (3.25)$$

therefore,

$$\sigma_i - \sigma_j = 2\left(\lambda_i^2 - \lambda_j^2\right)\left[A_{10} + \lambda_k^2 A_{01}\right] \qquad (3.26)$$

For the case of uniaxial elongation, the above equation becomes, with i=1, j=2 and k=3 (σ_2=0)

$$\sigma_1 = 2\left(\lambda^2 - \frac{1}{\lambda}\right)\left[A_{10} + \frac{1}{\lambda} A_{01}\right] \qquad (3.27)$$

For the case of equibiaxial extension, we can use i=1, j=3 and k=2, and since $\lambda_1=\lambda_2=\lambda$, and $\lambda_3=\lambda^{-2}$, the stress equation becomes (σ_3=0)

$$\sigma_1 = \sigma_2 = \sigma = 2\left(\lambda - \lambda^{-4}\right)\left[A_{10} + \lambda^2 A_{01}\right] \qquad (3.28)$$

Mooney-Rivlin Performance

ABS Uniaxial

The Mooney-Rivlin model for ABS uniaxial elongation was fitted to data for a strain rate of 1 sec^{-1}. As seen in Figure 3.4, its fit is adequate over the strain range in question since it captures all of the general trends exhibited by the experimental data. However, when the data is extended significantly past the strain range over which it was fitted, one of the two major drawbacks of the model becomes evident; the predicted stress decreases rapidly, and in fact becomes negative when the strain become large enough (this phenomenon is displayed more clearly in the biaxial case). As with the Ogden model, more accuracy would be possible by retaining more terms in the general strain energy function, W. However, because of the form of W used, the higher powered terms tend to greatly diminish the ease of fitting the parameters, as well as complicating the understanding of the model.

The Mooney-Rivlin parameters used for uniaxial elongation of ABS are listed in Table 3.1, presented at the end of this Section.

ABS Equibiaxial

For this case, the model was fit to strain rate data of 0.3 sec^{-1}. As can be seen in Figure 3.5, the fit is inadequate at nearly all strain levels. The reason for this lack of fit is that the Mooney-Rivlin model was originally developed for rubber-like materials which exhibited strain hardening. For the data presented in this work, strain softening is dominant, and when the Mooney-Rivlin model is used to account for this softening, it

Figure 3.4: Uniaxial Elongational True Stress as a Function of Stretch Ratio, ABS, 190 deg. C, Strain Rate 1/sec
Showing Performance of M-R and Ogden Models

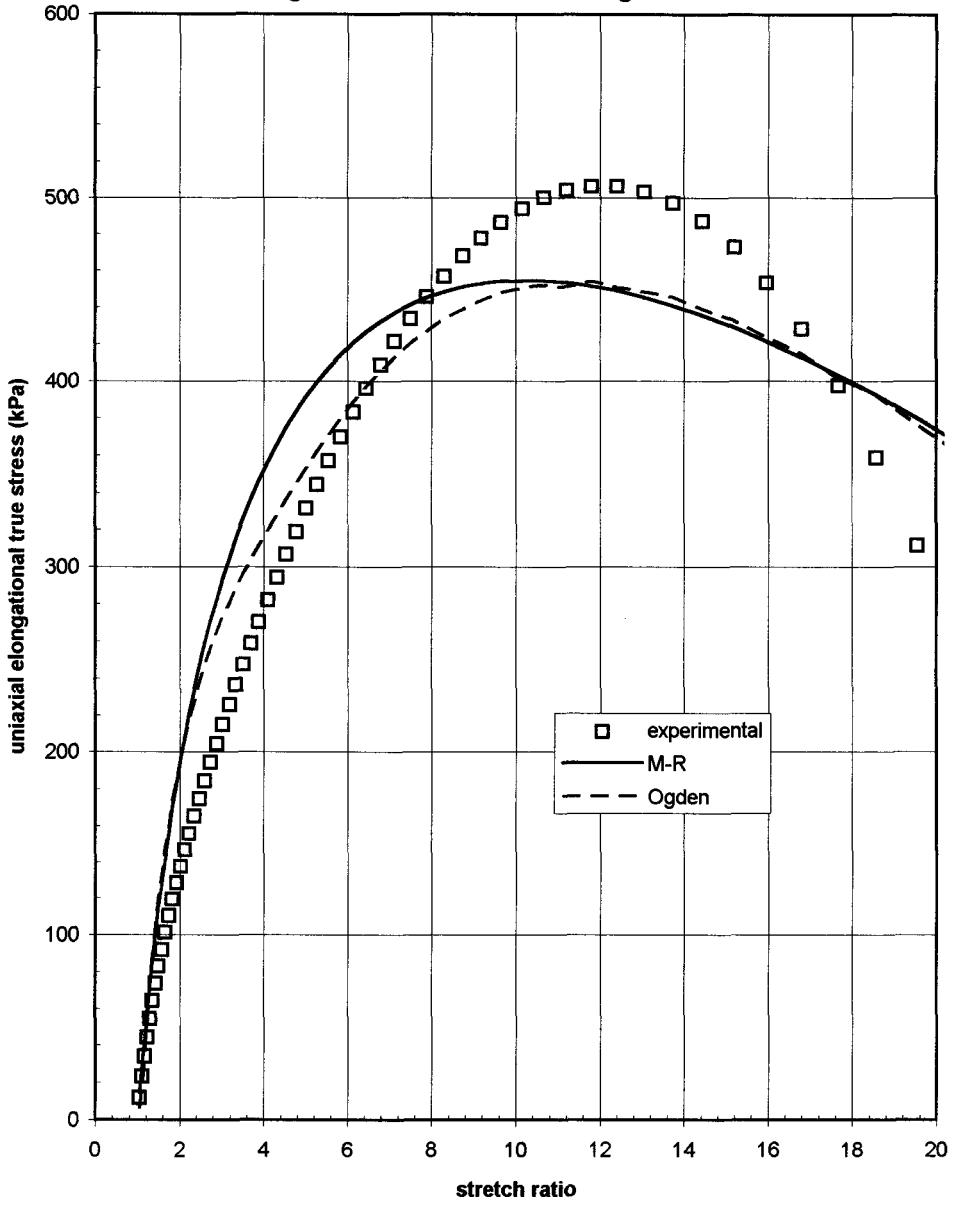

Figure 3.5: Equibiaxial Elongational True Stress as a Function of Stretch Ratio, ABS, 190 deg. C, Strain Rate 0.3/sec
Showing Performance of M-R and Ogden Models

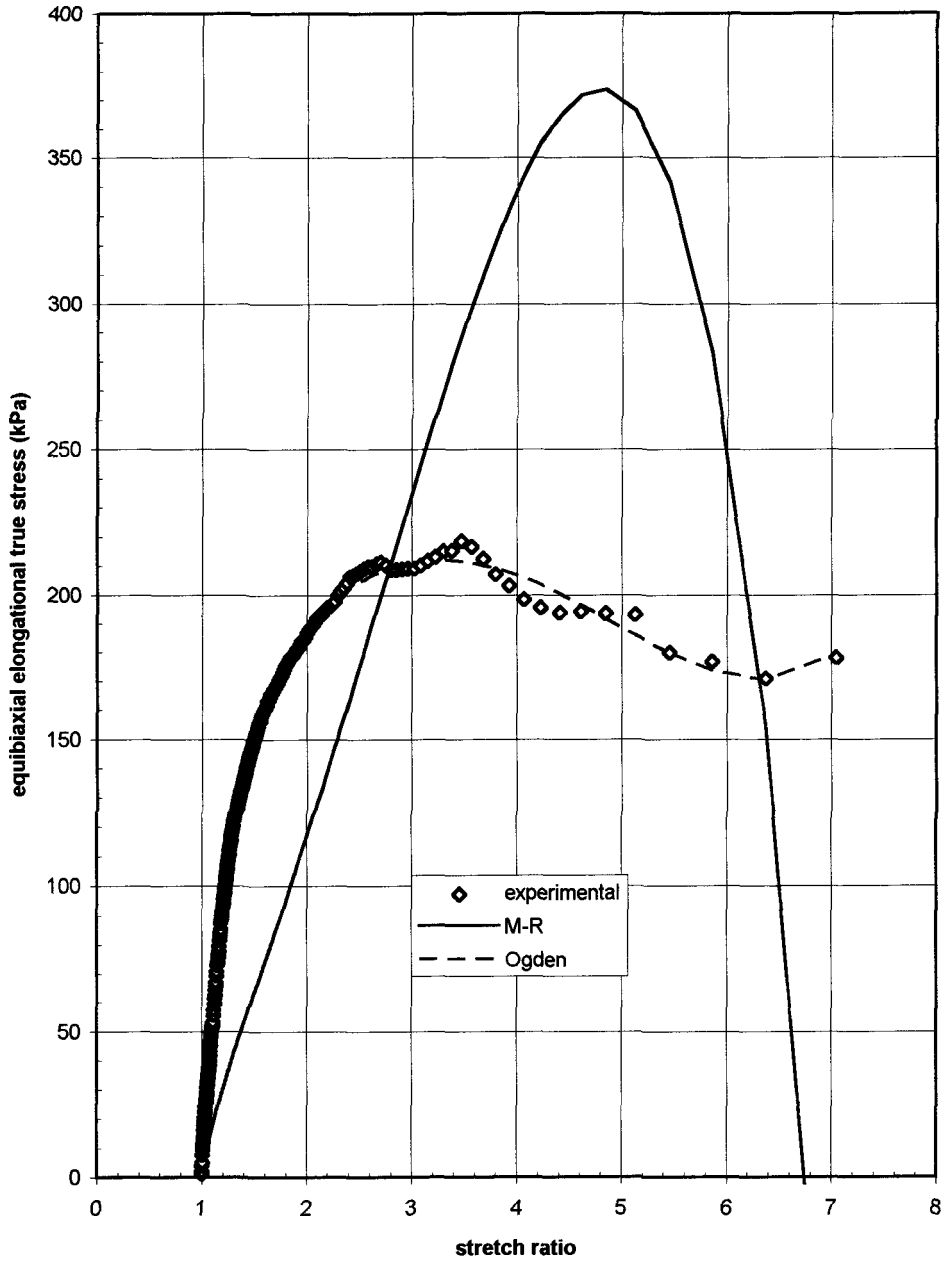

tends to over-compensate, making the stress decrease rapidly at higher strain, eventually becoming negative.

The Mooney-Rivlin parameters used for the equibiaxial elongation of ABS are listed in Table 3.1.

HDPE Uniaxial

For this case, the model was fit to strain rate data of 0.6 sec^{-1}. As seen in Figure 3.6, the fit is adequate over the strain range; however, as mentioned in Section 3.3.1.2.1., if the data is extended much beyond this range, the stress drops off rapidly, eventually becoming negative.

The Mooney-Rivlin parameters used for HDPE uniaxial elongation are listed in Table 3.1.

HDPE Equibiaxial

For this case, the model was fit to data of strain rate 0.3 sec^{-1}. As can be seen in Figure 3.7, the fit is adequate at low strains (stretch ratio less than 2.4), but rapidly deteriorates for higher strains. In fact, the model predicts negative stress at stretch ratios higher than approximately 6.6, which is clearly inadmissible.

As well as the above drawback, the Mooney-Rivlin model has another failing that, in fact, it shares with the Ogden model (and indeed any other model based on strain hardening rubbers). This is its inability to account for, in any manner, the (sometimes large) variation of stress with strain rate. As can readily be seen by examination of both the uniaxial and equibiaxial data used in this work, there is a great degree of variation of stress with strain rate.

Figure 3.6: Uniaxial Elongational True Stress as a Function of Stretch Ratio, HDPE, 190 deg. C, Strain Rate 0.6/sec
Showing Performance of M-R and Ogden Models

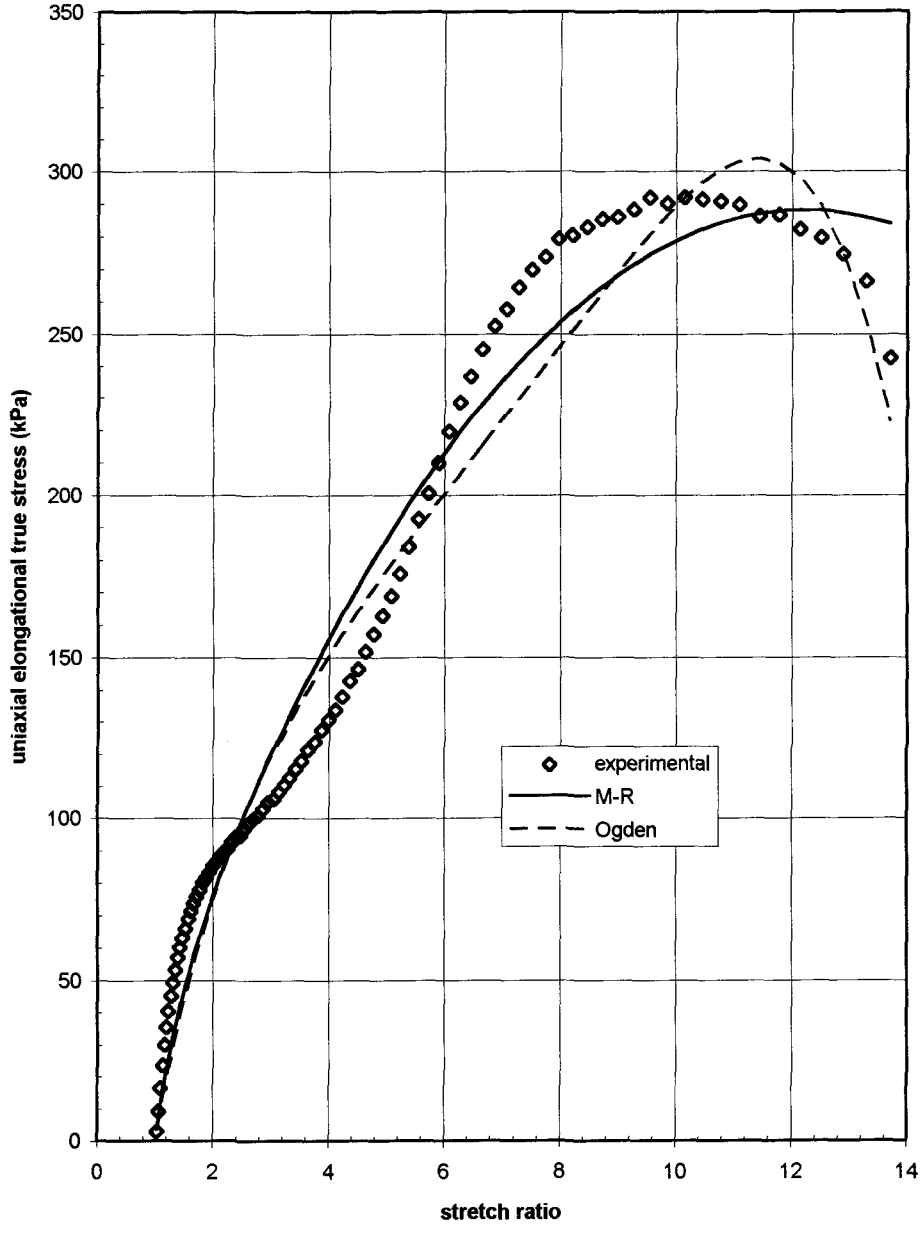

Figure 3.7: Equibiaxial Elongational True Stress as a Function of Stretch Ratio, HDPE, 190 deg. C, Strain Rate 0.3/sec Showing Performance of M-R and Ogden Models

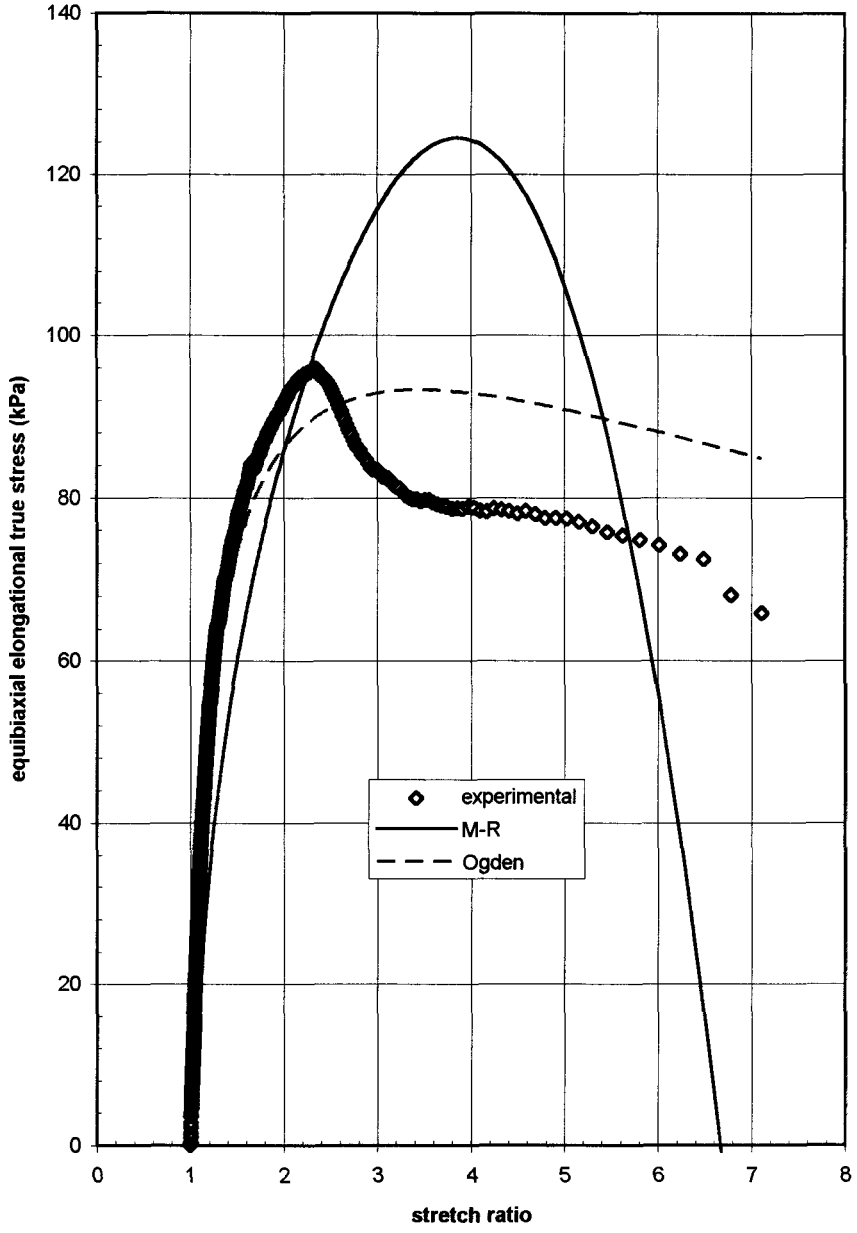

These two failings raise several important points which should be considered when using models such as the Mooney-Rivlin or Ogden models: first, care should be taken when implementing these models into a computer program, to ensure that the strains under consideration are within the parameters' range of applicability; second, the parameters should be fitted using data which is as close as possible to the strain rate of the real process in question, to reduce the error associated with the models' lack of strain rate variation. It should be borne in mind, however, that the data used in the present work covers a large range of strain rates, in some cases approximately two orders of magnitude.

The Mooney-Rivlin parameters used for HDPE equibiaxial elongation are shown in Table 3.1.

Table 3.1 Mooney-Rivlin Model Parameters

	Deformation Type			
	Uniaxial		Equibiaxial	
Polymer	ABS	HDPE	ABS	HDPE
A_{10}	-1.74	-0.97	16.24	24.25
A_{01}	42.03	23.65	-0.35	-0.54

3.3.2 Ogden Model

Ogden Model Equations

In common with the Mooney-Rivlin model, the Ogden model [14] is based upon the response of a homogeneous, isotropic, incompressible elastic solid. The form of the strain energy function, Φ, is

$$\Phi = \sum_r \mu_r \phi(\alpha_r) \qquad [2.7]$$

The form of the model used in this work is the 3-term model (r=1,2,3). This form was used by Ogden in his original work and gives the best fit with the lowest number of parameters; it can, with appropriately chosen parameters, account for initial yielding and eventual strain hardening. The form of Φ is

$$\Phi = \mu_n \left[\frac{\left(\lambda_1^{\alpha_1} + \lambda_2^{\alpha_1} + \lambda_3^{\alpha_1} - 3\right)}{\alpha_1} + \frac{\left(\lambda_1^{\alpha_2} + \lambda_2^{\alpha_2} + \lambda_3^{\alpha_2} - 3\right)}{\alpha_2} + \frac{\left(\lambda_1^{\alpha_3} + \lambda_2^{\alpha_3} + \lambda_3^{\alpha_3} - 3\right)}{\alpha_3} \right] \tag{3.29}$$

with the principal Cauchy stresses given by

$$\sigma_i = \lambda_i \frac{\partial \Phi}{\partial \lambda_i} - p \quad (i = 1,2,3) \tag{2.8}$$

In uniaxial elongation, $\lambda_1=\lambda$; $\lambda_2=\lambda_3=\lambda^{-½}$ due to the incompressibility constraint. Also, in the direction of elongation, $\sigma_1=\sigma$, with the other two stresses, σ_2 and σ_3, equal to zero since no lateral forces are applied. Thus, with the forms of Φ and σ_i given above,

$$\begin{aligned} \sigma_1 &= \sigma = \mu_1 \lambda^{\alpha_1} + \mu_2 \lambda^{\alpha_2} + \mu_3 \lambda^{\alpha_3} - p \\ \sigma_2 &= \sigma_3 = \mu_1 \lambda^{-\frac{1}{2}\alpha_1} + \mu_2 \lambda^{-\frac{1}{2}\alpha_2} + \mu_3 \lambda^{-\frac{1}{2}\alpha_3} - p = 0 \end{aligned} \tag{3.30}$$

And elimination of the hydrostatic pressure, p, yields

$$\sigma = \mu_1 \left(\lambda^{\alpha_1} - \lambda^{-\frac{1}{2}\alpha_1} \right) + \mu_2 \left(\lambda^{\alpha_2} - \lambda^{-\frac{1}{2}\alpha_2} \right) + \mu_3 \left(\lambda^{\alpha_3} - \lambda^{-\frac{1}{2}\alpha_3} \right) \quad (uniaxial) \tag{3.31}$$

In equibiaxial extension, $\lambda_1=\lambda_2=\lambda$, $\lambda_3=\lambda^{-2}$, and the principal Cauchy stresses in the two directions of extension are $\sigma_1=\sigma_2=\sigma$. The stress on the third, unloaded, face is zero. With a similar development to that for the uniaxial case, it can be shown that

$$\sigma = \mu_1 \left(\lambda^{\alpha_1} - \lambda^{-2\alpha_1} \right) + \mu_2 \left(\lambda^{\alpha_2} - \lambda^{-2\alpha_2} \right) + \mu_3 \left(\lambda^{\alpha_3} - \lambda^{-2\alpha_3} \right) \quad (equibiaxial) \tag{3.32}$$

Ogden Model Performance

ABS Uniaxial

The 3-term Ogden model for ABS uniaxial extension was fitted to a strain rate of 1 sec^{-1}. As can be seen in Figure 3.4, the fit is quite good over the entire strain range. However, the performance of the model in this case is open to question, since, strictly speaking, each pair of Ogden parameters (α_r, μ_r) should be both positive or both negative (that is, their product should be positive), and the parameters used here are not. This criterion is sufficient (but not necessary) to ensure that the general strain energy function, Φ, is positive for all strains [14]. In the present analysis, this criterion is not met, and thus the applicability of the present parameters is questionable when applied outside the strain range shown here.

In fact, the Ogden model, while very successful in predicting stresses for problems in rubber elasticity, in which strain hardening occurs, is incapable of modeling the softening shown in this case. This is because, for strain softening to occur, the slope of the stress-strain (or stress-stretch ratio) curve must be negative,

$$\frac{d\sigma}{d\lambda} < 0 \tag{3.33}$$

But

$$\frac{d\sigma}{d\lambda} = \sum_r \alpha_r \mu_r \left(\lambda^{\alpha_r - 1} + \frac{1}{2} \lambda^{-\frac{1}{2}\alpha_r - 1} \right) \quad \textit{for uniaxial extension} \tag{3.34}$$

$$\frac{d\sigma}{d\lambda} = \sum_r \alpha_r \mu_r \left(\lambda^{\alpha_r - 1} + 2\lambda^{-2\alpha_r - 1} \right) \quad \textit{for equibiaxial extension} \tag{3.35}$$

The terms in parentheses are always positive, and if the $\alpha_r \cdot \mu_r > 0$ criterion holds, then the above derivatives are always positive (except in the trivial case when they are zero). Thus, it can be concluded that if the condition of positivity of Φ holds, then strain softening can not be accounted for by the Ogden model.

The Ogden parameters for ABS uniaxial elongation are shown in Table 3.2.

ABS Equibiaxial

The parameters for this case were fitted to a strain rate of 0.3 sec^{-1}. As can be seen in Figure 3.5, the fit is very good over the entire strain range. Yielding and strain softening are both modeled quite well; however the applicability of the success with strain softening must be taken with caution, following the above discussion regarding the positivity of the strain energy function Φ.

The Ogden parameters for ABS equibiaxial extension are listed in Table 3.2.

HDPE Uniaxial

For this case the Ogden parameters were fit to a strain rate of 0.6 sec^{-1}. As seen in Figure 3.6, the fit is satisfactory over the strain range in question, with a relative error between predicted and observed stress never more than about 15%. However, it must be noted that while the magnitude of error is relatively small, the predictions do not in fact clearly mimic the trends of the data, including yielding, hardening and eventual softening. The predicted stress simply follows the general trend of the experimental data, without matching its detailed form.

The Ogden parameters for HDPE uniaxial elongation are listed in Table 3.2.

HDPE Equibiaxial

For this case the Ogden parameters were fit using data for a strain rate of 0.3 sec^{-1}. As can be seen in Figure 3.7, the general fit of the model is satisfactory, however as with the uniaxial case of HDPE, the model follows the general trend of the data, but does not capture its details. In HDPE equibiaxial extension, stress overshoot is quite evident, indicated by the significant drop in stress at a stretch ratio of approximately 2.4 in Figure 3.7. The Ogden model is not able to model this phenomenon.

The Ogden parameters for HDPE equibiaxial extension are listed in Table 3.2.

Table 3.2 Ogden Model Parameters

	Deformation Type			
	Uniaxial		Equibiaxial	
Polymer	ABS	HDPE	ABS	HDPE
μ_1	19678.0	14471.5	233.16	12160
α_1	0.01134	0.005	1.594	0.00214
μ_2	-91.19	0.00116	170.65	-25868
α_2	0.7744	5.24	-.8874	-.0003
μ_3	130.8	0.00012	.1008	329.8
α_3	0.322	-12.26	4.21	-.205

Unlike the G'Sell and K-BKZ models described in the following sections, the method of fitting the Mooney-Rivlin and Ogden models was accomplished by judicious selection of the appropriate parameters, to yield reasonable results over the regions of interest. While standard optimization techniques can be used, they must be used with a clear understanding of the influence of each term in the equations.

3.3.3 G'Sell Model

G'Sell Model Equations

The model proposed by G'Sell [17] and described in Chapter 2, is one of the easiest models to fit, and based on the present analysis, is also one of the most useful. Its ease in fitting is accomplished by separating the various stress-strain effects, and by accounting for each with a different function in the equation. Thus, there are four parameters to determine, one for each of the following functions:

- temperature dependence, $K(T) = A \cdot e^{-b(T-T_0)}$
- "viscoelastic" effects, $\left[1-\exp\left(-w\bar{\varepsilon}\right)\right]$
- strain hardening, $\exp\left(h\bar{\varepsilon}^2\right)$
- rate-sensitivity, $\dot{\bar{\varepsilon}}^m$

The measures of stress and strain used in the model are the "effective" stress and strain [18]; this allows for one equation to be used, and no special manipulation is needed to incorporate tensors (besides the initial definitions), as is necessary in the K-BKZ model discussed herein.

The effective stress and strain are defined as follows:

$$\bar{\sigma} = \frac{1}{\sqrt{2}}\sqrt{\left[\sigma_{xx}-\sigma_{yy}\right]^2+\left[\sigma_{xx}-\sigma_{zz}\right]^2+\left[\sigma_{yy}-\sigma_{zz}\right]^2} \tag{3.36}$$

$$\bar{\varepsilon} = \int \dot{\bar{\varepsilon}}\, dt = \int \sqrt{\frac{2}{3}\dot{\varepsilon}:\dot{\varepsilon}}\, dt \tag{3.37}$$

where

$$\dot{\varepsilon}:\dot{\varepsilon} = \dot{\varepsilon}_{ij}\dot{\varepsilon}_{ji}\ , \text{or}\ \ \dot{\varepsilon}:\dot{\varepsilon} = \underline{\underline{\dot{\varepsilon}}}\cdot\underline{\underline{\dot{\varepsilon}}}^T \tag{3.38}$$

If these definitions are applied to the deformations in question, the results are as follows:

Uniaxial: in this case $\sigma_x=\sigma$; $\sigma_y=\sigma_z=0$,

$$\bar{\sigma} = \frac{1}{\sqrt{2}}\sqrt{[\sigma_{xx}-0]^2+[\sigma_{xx}-0]^2} = \sigma_{xx} = \sigma \tag{3.39}$$

also,

$$\dot{\varepsilon}_{ij} = \begin{bmatrix} \dot{\varepsilon} & 0 & 0 \\ 0 & -\frac{\dot{\varepsilon}}{2} & 0 \\ 0 & 0 & -\frac{\dot{\varepsilon}}{2} \end{bmatrix} \quad \text{(since det } \dot{\varepsilon}_{ij}=0\text{)} \tag{3.40}$$

so

$$\dot{\varepsilon}:\dot{\varepsilon} = \dot{\varepsilon}^2 + \frac{\dot{\varepsilon}^2}{4} + \frac{\dot{\varepsilon}^2}{4} = \frac{3}{2}\dot{\varepsilon}^2 \tag{3.41}$$

and

$$\dot{\bar{\varepsilon}} = \sqrt{\frac{2}{3}\cdot\left(\frac{3}{2}\dot{\varepsilon}^2\right)} = \dot{\varepsilon} \tag{3.42}$$

Thus, $\bar{\varepsilon} = \int \dot{\varepsilon}\, dt = \dot{\varepsilon}\, t = \varepsilon$, for constant strain rate tests, and the constitutive equation for uniaxial elongation is

$$\sigma = A\cdot e^{-b(T-T_0)}\left[1-\exp(-w\varepsilon)\right]\exp\left[h\varepsilon^2\right]\dot{\varepsilon}^m \tag{3.43}$$

Equibiaxial: in this case $\sigma_{xx}=\sigma_{yy}=\sigma$; $\sigma_{zz}=0$, and thus,

$$\bar{\sigma} = \frac{1}{\sqrt{2}}\sqrt{[\sigma-\sigma]^2+[\sigma-0]^2+[\sigma-0]^2} = \sigma \tag{3.44}$$

and,

$$\dot{\varepsilon}_{ij} = \begin{bmatrix} \dot{\varepsilon} & 0 & 0 \\ 0 & \dot{\varepsilon} & 0 \\ 0 & 0 & -2\dot{\varepsilon} \end{bmatrix} \quad \text{(since det } \dot{\varepsilon}_{ij}=0\text{)} \tag{3.45}$$

so,

$$\dot{\varepsilon} : \dot{\varepsilon} = \dot{\varepsilon}^2 + \dot{\varepsilon}^2 + 4\dot{\varepsilon}^2 = 6\dot{\varepsilon}^2 \tag{3.46}$$

and,

$$\bar{\dot{\varepsilon}} = \sqrt{\frac{2}{3} \cdot \left(6\dot{\varepsilon}^2\right)} = 2\dot{\varepsilon} \tag{3.47}$$

Thus, $\bar{\varepsilon} = \int \bar{\dot{\varepsilon}}\, dt = \int 2\dot{\varepsilon}\, dt = 2\dot{\varepsilon}\, t = 2\varepsilon$, for constant strain rate tests, and the constitutive equation for equibiaxial elongation is

$$\sigma = A \cdot e^{-b(T-T_0)}\left[1 - \exp\left(-2w\varepsilon\right)\right]\exp\left[4h\varepsilon^2\right]\left(2\dot{\varepsilon}^m\right) \tag{3.48}$$

Of course, the rigorous definition of equivalent stress and strain, and their use in the constitutive equation is an attempt to account for all deformation types (uniaxial elongation, biaxial extension, shear) with one constitutive model. The ultimate success of the model hinges upon its being able to predict the stress in all deformations, regardless of what type of deformation the parameters were fitted to. If this is not the case, and biaxial data must be used to obtain biaxial parameters (for example) then the "extra" numerical factors in the above equation (the factors of 2 and 4 not found in the uniaxial equation) are not necessary, since they are merely part of the constants to be determined. The topic of using uniaxial (inexpensive) tests to obtain parameters to mimic equibiaxial (expensive) data is discussed in section 3.4.

The next section will describe the method by which the 4 parameters for this model are fitted; uniaxial notation is used for simplicity.

Method of Fitting Parameters (from [18])

Calculation of strain-rate sensitivity, m:

When one considers data points for several different strain rates, at the same temperature, T, and effective strain, ε, the dependence of stress on strain rate can be written:

$$\ln\sigma = m\ln\dot{\varepsilon} + const\cdot(T,\varepsilon) \tag{3.49}$$

from which one can obtain m, the slope of the $\ln\sigma$ *vs.* $\ln\dot{\varepsilon}$ line.

Calculation of h:

For values of strain greater than 0.6, $\left[1-\exp(-w\varepsilon)\right]$ is approximately unity. In this case, the constitutive equation reduces to

$$\sigma = K(T)\cdot\exp\left(h\varepsilon^2\right)\dot{\varepsilon}^m \tag{3.50}$$

or, written another way,

$$\ln\left[\frac{\sigma}{\dot{\varepsilon}^m}\right] = \ln K(T) + h\varepsilon^2 \tag{3.51}$$

If one then plots $\ln\left[\frac{\sigma}{\dot{\varepsilon}^m}\right]$ *vs.* ε^2, one can find the slope, h, of this line.

Calculation of w:

Once the parameters m and h are found, one can then determine the last non-temperature parameter, w. By manipulation of the equation, one can obtain

$$\ln\left[1-\frac{\sigma}{K(T)\exp\left[h\varepsilon^2\right]\dot{\varepsilon}^m}\right] = -w\varepsilon \tag{3.52}$$

and one can obtain the slope, w, by plotting the left side of the above equation versus ε.

In G'Sell's original work, and in other work that has used his model, the strain-rate parameter, m, was found to vary with temperature (as well as strain). In the present work, m was taken to be a constant; it was determined at a temperature of 190°C, and not changed when calculating the stress at any other temperature. In other words, all of the effects of temperature were accounted for by the K(T) function. This was modeled by an Arrhenius-type function as follows: data points for the (roughly) same strain value and strain rate were plotted at the three temperatures for which data was obtained, namely 150, 170 and 190°C. From this data, the slope of the ln K(T) versus T curve was found, and fitted to the equation

$$K(T) = A \cdot e^{-b(T-T_0)} \tag{3.53}$$

where b is the slope, T is the temperature the stress is to be calculated at, and T_0 is some reference temperature, in this case 190°C.

G'Sell Model Performance

ABS Uniaxial

For this case the parameters were fitted to a strain rate of 1 sec^{-1}. As shown in Figure 3.8, the fit of the predicted stress in not adequate to predict all of the characteristics of the experimental data. Whereas the experimental data shows clear indications of strain softening, the predicted stress shows hardening. This discrepancy is because the softening occurs at a relatively high strain, and the term in the G'Sell

Figure 3.8: Uniaxial Elongational True Stress as a Function of Stretch Ratio, ABS, 190 deg. C, at High Strain Rates
Showing Performance of G'Sell and 2-Term Polynomial Models

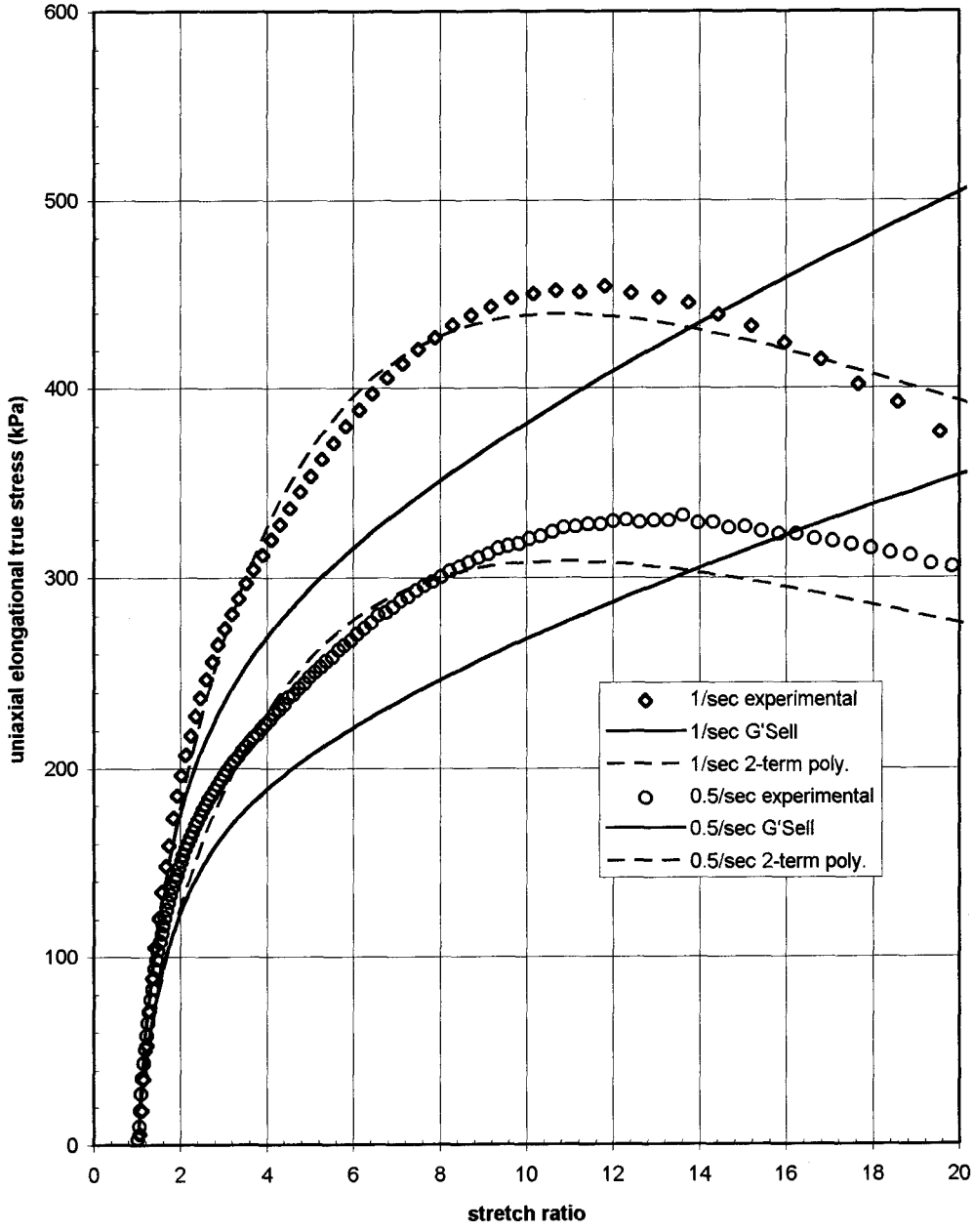

model which accounts for high strain behaviour, $\exp(h\varepsilon^2)$, becomes dominant at approximately ε=0.6, which is quite low for this data.

With the exception of the lack of hardening modeling, the model does perform adequately for this case, within an error of approximately 30%. The variation in stress with strain rate is modeled satisfactorily, as can be seen in Figures 3.8 and 3.9.

The G'Sell model parameters used for ABS uniaxial elongation are shown in Table 3.3, presented at the end of this Section.

ABS Equibiaxial

For this case the parameters were fitted to a strain rate of 0.3 sec^{-1}. As shown in Figures 3.10, 3.11 and 3.12, the performance of the models for this case is very good, in all aspects of the strain, strain rate and temperature dependence. The only apparent lack of fit to experimental data occurs at very low strains, where the model underestimates the stress; this occurs at all strain rates.

The G'Sell model parameters for ABS equibiaxial extension are listed in Table 3.3.

HDPE Uniaxial

For this case, the parameters were fit to a strain rate of 0.6 sec^{-1}. As shown in Figures 3.13 and 3.14, the fit of the predicted to the experimental data is not adequate to match the characteristics seen here. The model does not follow the clear yielding, hardening and eventual softening of the data, but merely follow the generally increasing trend.

Figure 3.9: Uniaxial Elongational True Stress as a Function of Stretch Ratio, ABS, 190 deg. C, at Low Strain Rates
Showing Performance of G'Sell and 2-term Polynomial Models

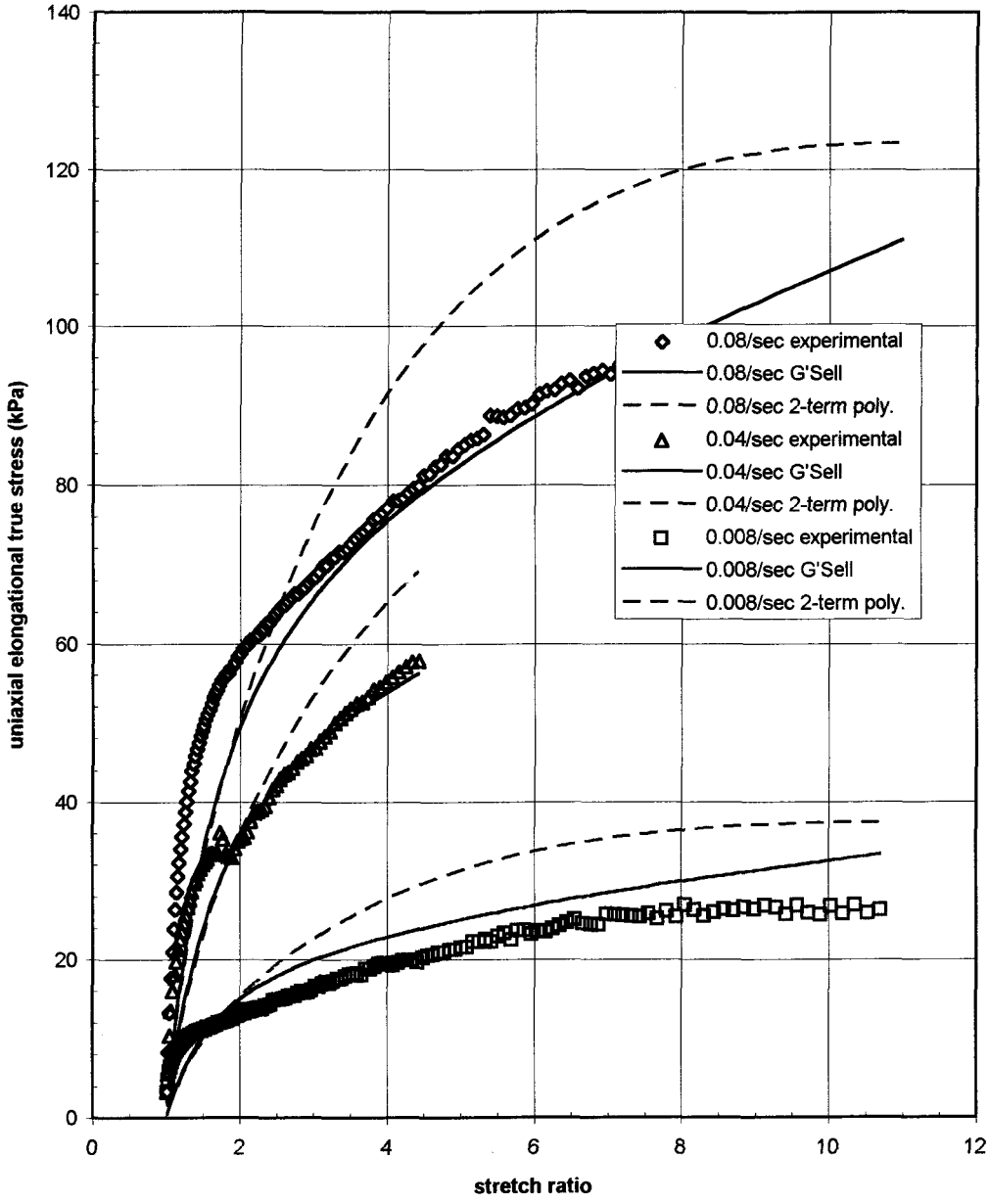

Figure 3.10: Equibiaxial Elongational True Stress as a Function of Stretch Ratio, ABS, 190 deg. C, at High Strain Rates
Showing Performance of G'Sell and 2-term Polynomial Models

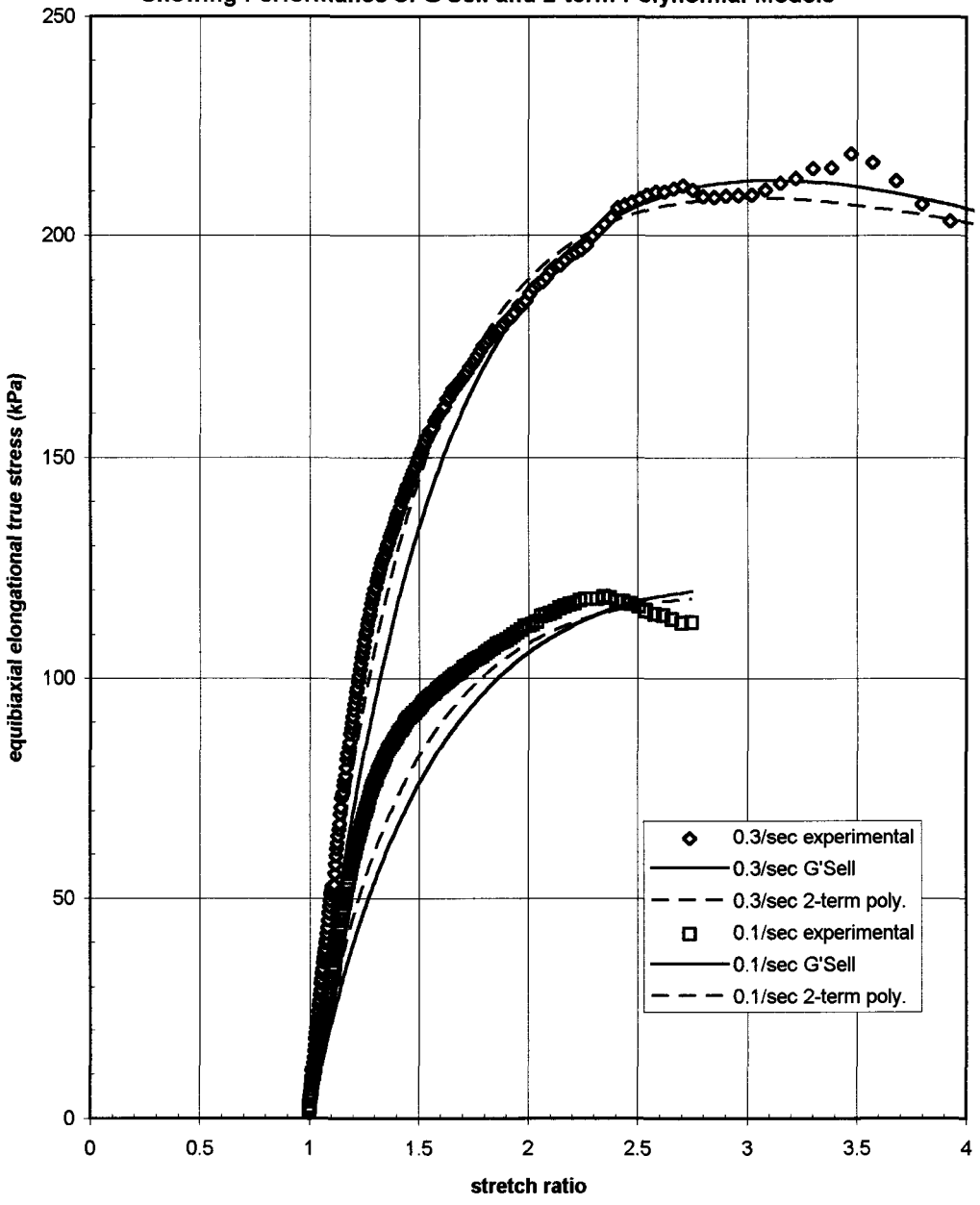

Figure 3.11: Equibiaxial Elongational True Stress as a Function of Stretch Ratio, ABS, 190 deg. C, at Low Strain Rates
Showing Performance of G'Sell and 2-term Polynomial Models

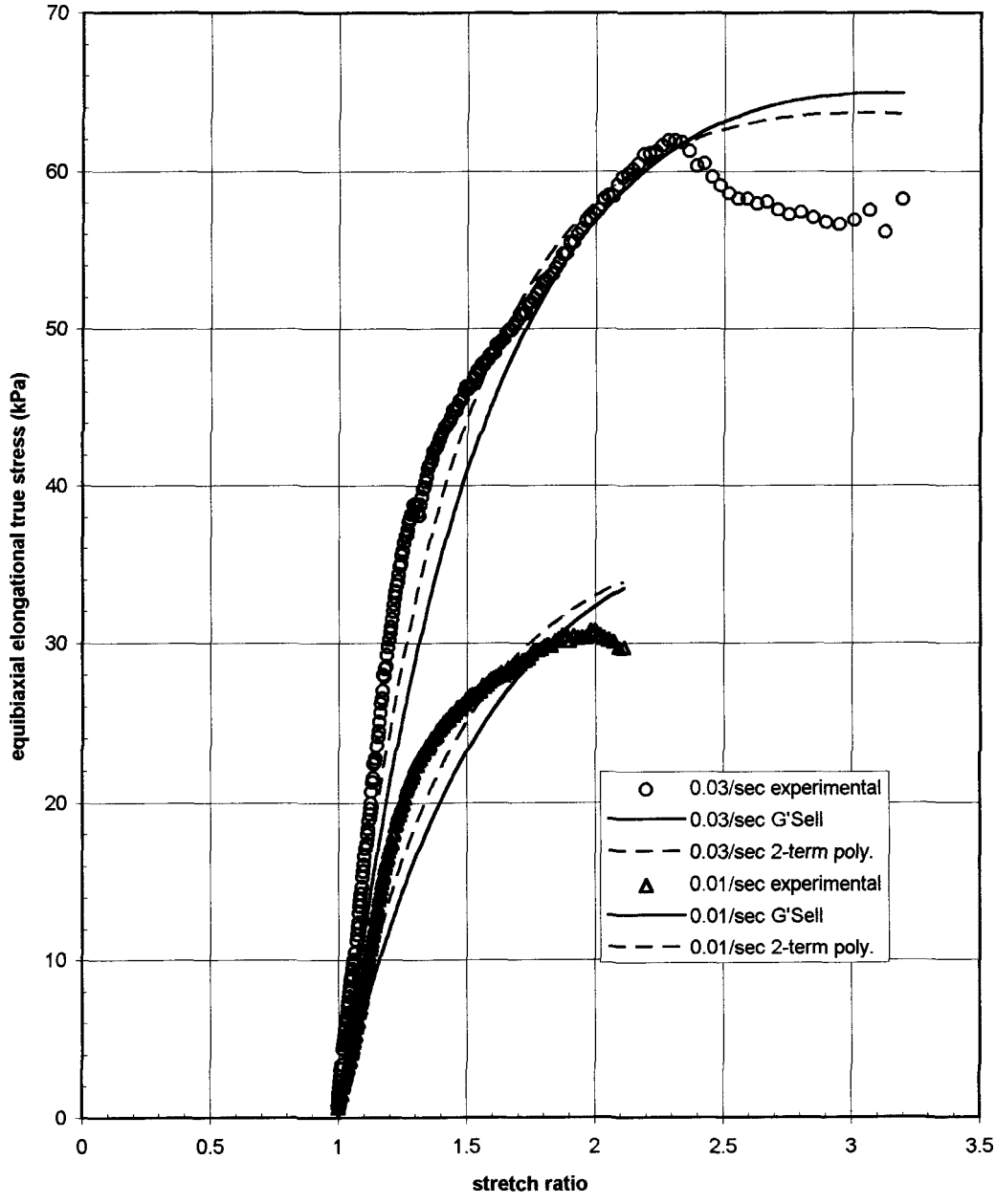

Figure 3.12: Equibiaxial Elongation True Stress as a Function of Stretch Ratio, ABS, Strain Rate 0.3/sec Showing Temperature Variation of G'Sell and 2-Term Polynomial Models

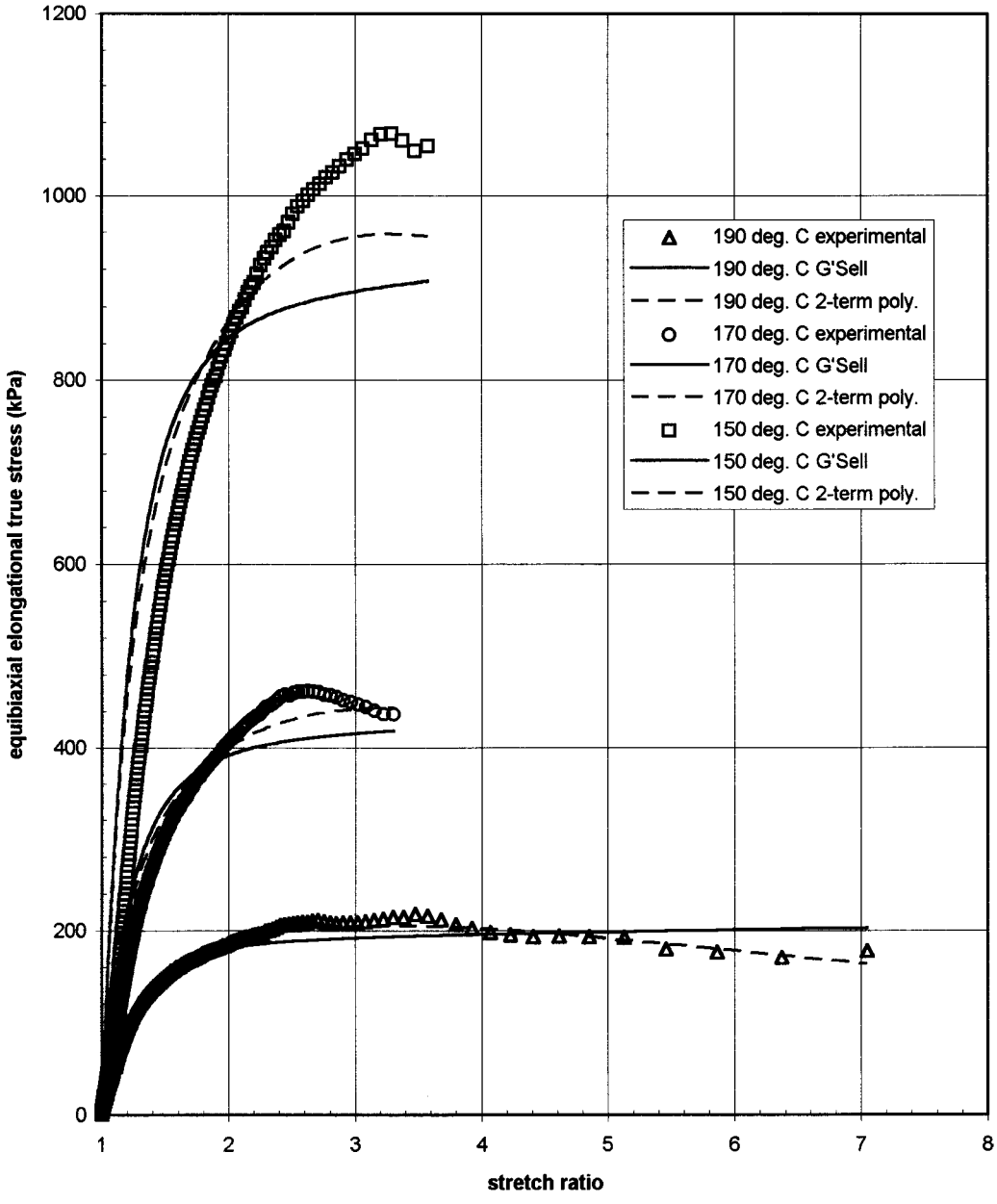

Figure 3.13: Uniaxial Elongational True Stress as a Function of Stretch Ratio, HDPE, 190 deg. C, at High Strain Rates
Showing Performance of G'Sell and 2-Term Polynomial Models

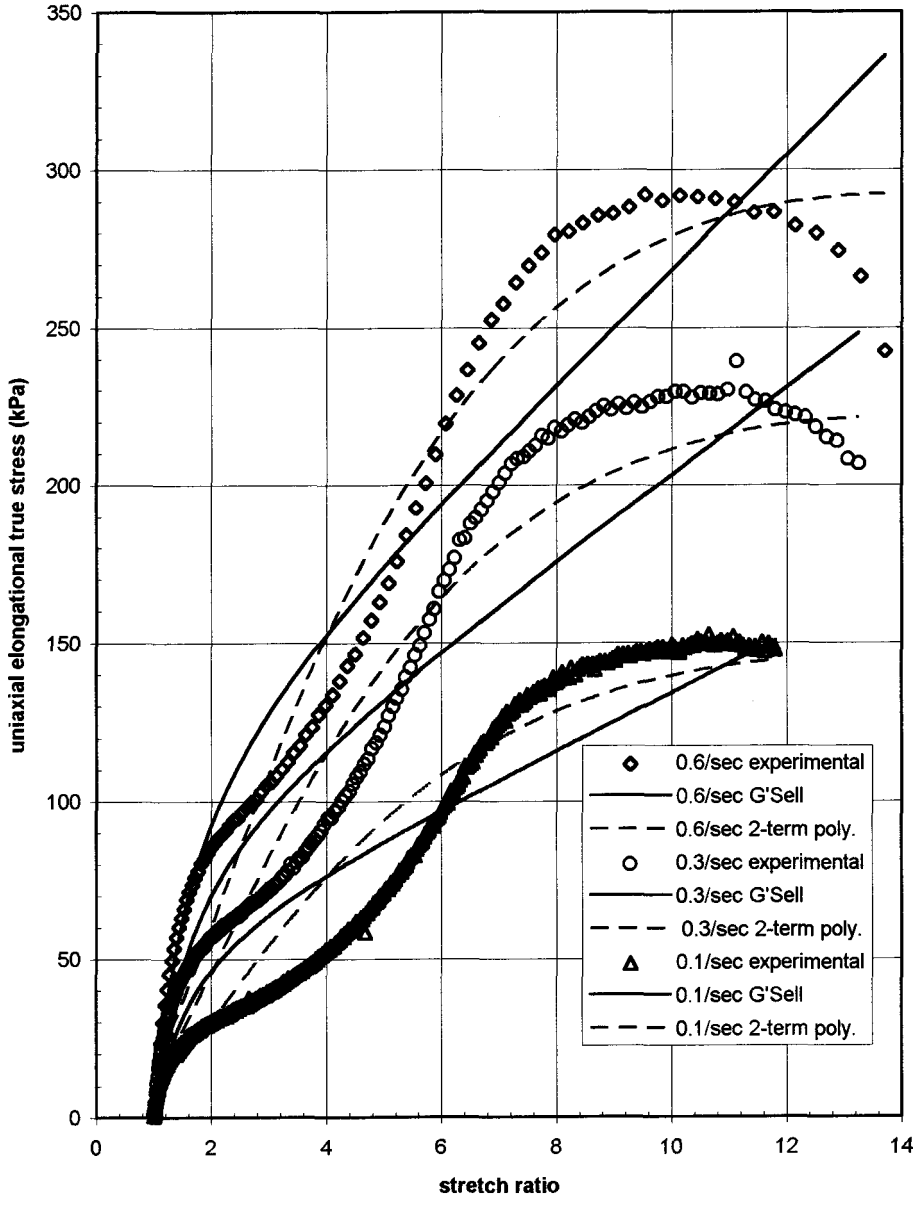

Figure 3.14: Uniaxial Elongational True Stress as a Function of Stretch Ratio, HDPE, 190 deg. C, at Low Strain Rates
Showing Performance of G'Sell and 2-Term Polynomial Models

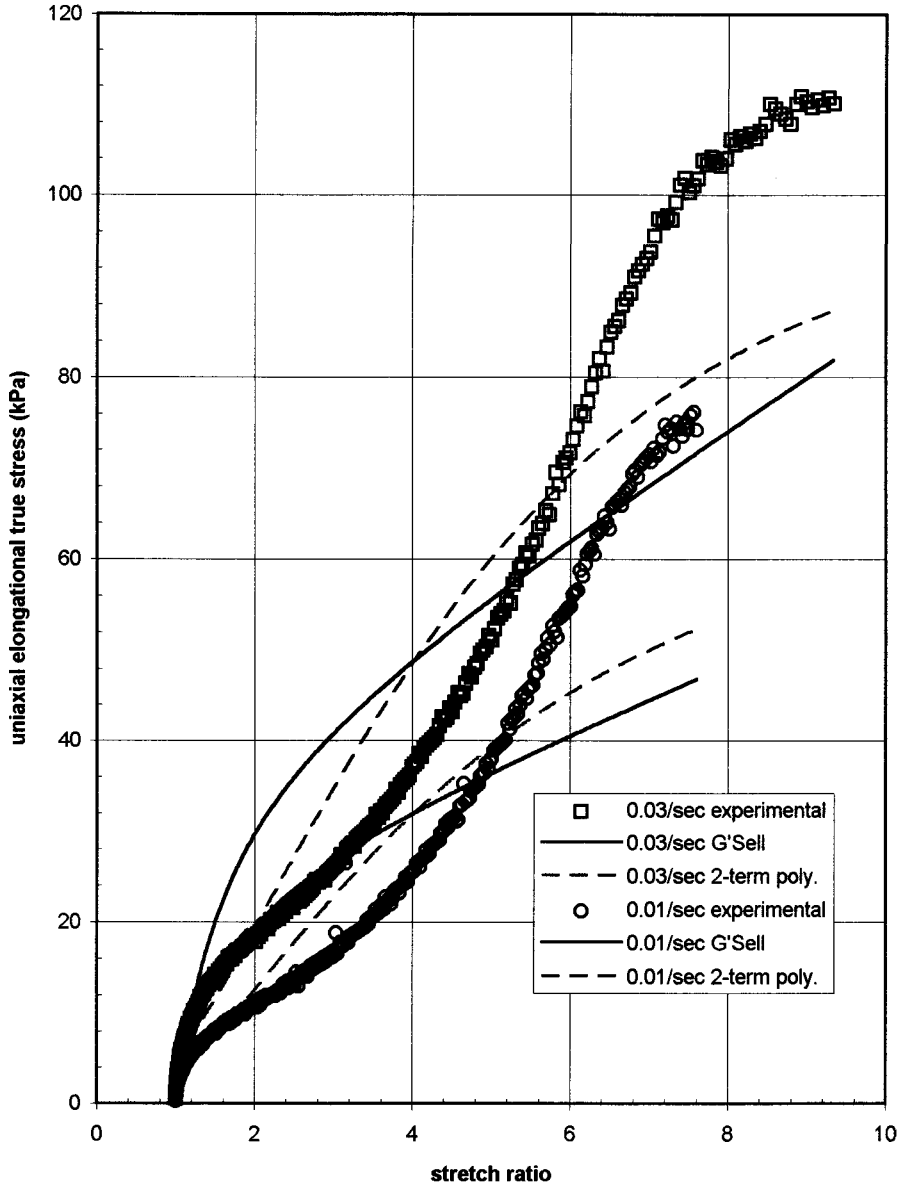

The G'Sell model parameters for HDPE uniaxial extension are listed in Table 3.3.

HDPE Equibiaxial

For this case the data was fitted to a strain rate of 0.3 sec^{-1}. As can be seen in Figure 3.15, the general fit of the model is satisfactory, with the predicted stress modeling the overall trend of the experimental data. However, the model does not seem able to account for the stress overshoot seen in this case; it does, however match the rapid initial increase in stress, and the eventual long slow decline at higher strains, albeit with an error of approximately 20%

The model performs well with respect to the strain rate variation, as shown by the lower two curves in Figure 3.15.

The G'Sell model parameters used for HDPE equibiaxial extension are listed in Table 3.3.

Table 3.3 G'Sell Model Parameters

	Deformation Type			
	Uniaxial		Equibiaxial	
Polymer	ABS	HDPE	ABS	HDPE
A	275.8	162.1	704.01	343.4
b	0.03845	0.03845	0.03845	0.03845
w	1.37	1.507	1.12	0.5877
h	0.0686	0.137	-0.193	-0.127
m	0.508	0.3804	0.5152	0.3804

Figure 3.15: Equibiaxial Elongational True Stress as a Function of Stretch Ratio, HDPE, 190 deg. C, at Various Strain Rates Showing Performance of G'Sell and 2-Term Polynomial Models

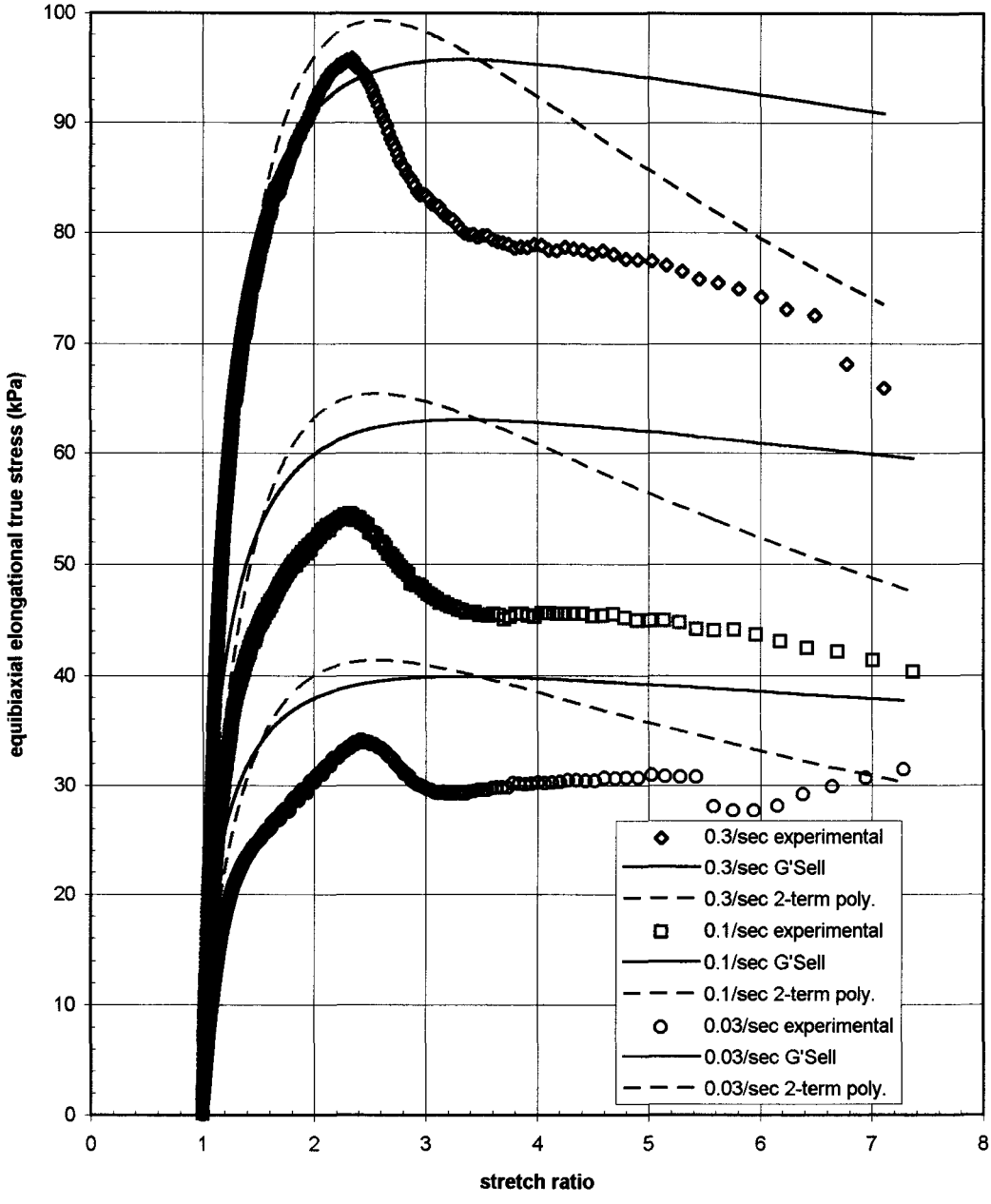

3.3.4 Two-term Polynomial Model

Two-term Polynomial Model Equations

The Two-term polynomial model described in Section 2.4. has a virtually identical development to the G'Sell, which it is a modification of. All of the same definitions and use of equivalent stress and strain apply; the constitutive equations used in the following analysis are written below for reference.

$$\sigma = A \cdot e^{-b(T-T_0)}\left[1-\exp(-w\varepsilon)\right]\exp\left(h_1\varepsilon^2 + h_2\varepsilon\right)\dot{\varepsilon}^m \quad \textit{uniaxial elongation} \qquad (3.54)$$

$$\sigma = A \cdot e^{-b(T-T_0)}\left[1-\exp(-2w\varepsilon)\right]\exp\left(4h_1\varepsilon^2 + 2h_2\varepsilon\right)\left(2\dot{\varepsilon}^m\right) \quad \textit{equibiaxial extension} \qquad (3.55)$$

Two-term Polynomial Model Performance

ABS Uniaxial

For this case the parameters for the Two-term Polynomial model were fitted to a strain rate of 1 sec^{-1}. As shown in Figures 3.8 and 3.9, the fit of the predicted to the experimental data is excellent, over the strain range. All of the data's characteristics are closely matched by the model. The fit of the model's strain rate dependence is satisfactory; some drift occurs for the data for 0.08 sec-1. However, when it is considered that the parameters were fit to strain rate data more than an order of magnitude larger, this fit can be considered satisfactory.

The Two-term polynomial model parameters for ABS uniaxial elongation are listed in Table 3.4.

ABS Equibiaxial

In this case the parameters were fitted to a strain rate of 0.3 sec^{-1}. As can be seen in Figures 3.10 and 3.11, the fit of the model to data is very close to that of the G'Sell model, except that the Two-term Polynomial model shows slightly better matching at the low and high strain ranges.

Also in common with the G'Sell model, the temperature dependence of the Two-term polynomial model is excellent, as shown in Figure 3.12.

The Two-term polynomial model parameters for ABS equibiaxial extension are listed in Table 3.4.

HDPE Uniaxial

For this case, strain rate data for 0.3 sec^{-1} was used to fit the parameters. As can be seen in Figures 3.13 and 3.14, the Two-term model shows much better matching to the experimental data than the G'Sell model; however, it does not mimic the particular characteristics of the data, merely following its general trend. Strain rate sensitivity shows good agreement with the data, for all the strain rates shown here.

The Two-term polynomial model parameters used for HDPE uniaxial elongation are shown in Table 3.4.

HDPE Equibiaxial

For this case, the parameters were fit to the data for strain rate 0.3 sec^{-1}. As illustrated in Figure 3.15, the fit is quite good over the entire strain range, and it is in this plot that the most prominent advantage of the Two-term polynomial model over the G'Sell model becomes evident. Although neither model completely accounts for the

stress overshoot exhibited by the data, the Two-term Polynomial shows greater variation in stress after the initial yielding, much more closely matching the drop in stress seen here. The G'Sell model, because it has only one term to account for either hardening or softening, cannot match the Two-term Polynomial's adaptability and versatility in the high strain regions.

As with the uniaxial case for HDPE, the strain rate sensitivity of the model is quite good, with only a small amount of drift from the experimental data being evident over the order of magnitude difference in strain rates shown here.

The Two-term polynomial model parameters for HDPE equibiaxial extension are listed in Table 3.4.

Table 3.4 Two-Term Polynomial Model Parameters

	Deformation Type			
	Uniaxial		Equibiaxial	
Polymer	ABS	HDPE	ABS	HDPE
A	80.2	19.37	760.5	129.4
b	0.03845	0.03845	0.03845	0.03845
w	4.58	25.04	1.27	0.764
h1	-0.3	-0.42	-0.05	-0.63
h2	1.42	2.2	-0.3	1.32
m	0.508	0.3804	0.5152	0.3804

3.3.5 K-BKZ Model

K-BKZ Model Equations

As described in Chapter 2, the K-BKZ [21,22,23,24,25,26] type of constitutive equation is one of the most used of the integral-type. It tends to give good results, however it can prove to be difficult to both implement into a computer code, as well as being difficult to fit to experimental data. In the present work, the K-BKZ equation,

modified by the inclusion of a Wagner damping function, was used to model experimental data. This section will develop and describe the equations used, as well as illustrate their performance in the comparison with the experimental data.

For the purpose of the present analysis, the K-BKZ equation with Wagner damping function can be written in general terms as

$$\underline{\underline{\sigma}}(t) = \int_{-\infty}^{t} \mu(t'-t) \cdot h(I_1, I_2) \cdot \underline{\underline{C}}^{-1}(t,t')dt' + P\underline{\underline{\delta}} \tag{3.56}$$

where $\mu(t'-t)$ is a linear viscoelastic memory function, $h(I_1,I_2)$ is the Wagner damping function, $\underline{\underline{C}}^{-1}(t,t')$ is the relative Finger tensor and $P\underline{\underline{\delta}}$ is an arbitrary hydrostatic pressure, written

$$P\underline{\underline{\delta}} = P\begin{bmatrix} 1 & 0 & 0 \\ 0 & 1 & 0 \\ 0 & 0 & 1 \end{bmatrix} \tag{3.57}$$

In equation 3.56 above, the appropriate Finger tensor for the deformation in question must be used; in the overwhelming majority of cases in thermoforming and blowmolding, it is biaxial extension that occurs. The Finger tensors for the two deformations were described in Section 3.2 and are repeated below:

Uniaxial:

$$\underline{\underline{C}}^{-1} = \begin{bmatrix} \lambda^2 & 0 & 0 \\ 0 & \lambda^{-1} & 0 \\ 0 & 0 & \lambda^{-1} \end{bmatrix}$$

Equibiaxial:

$$\underline{\underline{C}}^{-1} = \begin{bmatrix} \lambda^2 & 0 & 0 \\ 0 & \lambda^2 & 0 \\ 0 & 0 & \lambda^{-4} \end{bmatrix}$$

Since in the general stress equation, there is a term to account for hydrostatic pressure, this term must be eliminated in order to investigate the extra stress caused by deformation. For the purpose of illustration, the uniaxial equation will be examined.

The equation for uniaxial elongation can be written, including the Finger tensor explicitly, as

$$\begin{bmatrix} \sigma_{xx}(t) & 0 & 0 \\ 0 & \sigma_{yy}(t) & 0 \\ 0 & 0 & \sigma_{zz}(t) \end{bmatrix} = \int_{-\infty}^{t} \sum_{k=1}^{N} \frac{a_k}{\Gamma_k} \exp\left(\frac{t'-t}{\Gamma_k}\right) \cdot h(I_1, I_2) \cdot \begin{bmatrix} \lambda^2 & 0 & 0 \\ 0 & \lambda^{-1} & 0 \\ 0 & 0 & \lambda^{-1} \end{bmatrix} dt' + P \begin{bmatrix} 1 & 0 & 0 \\ 0 & 1 & 0 \\ 0 & 0 & 1 \end{bmatrix} \tag{3.58}$$

And since it is known *a priori* that in this type of deformation, $\sigma_{yy}=\sigma_{zz}=0$, these terms must vanish from the equation. This is accomplished by equating the pressure, P, to the negative of the terms for σ_{yy} and σ_{zz}, and in this manner it is found that

$$\sigma_{xx}(t) = \int_{-\infty}^{t} \sum_{k=1}^{N} \frac{a_k}{\Gamma_k} \exp\left(\frac{t'-t}{\Gamma_k}\right) \cdot h(I_1, I_2) \cdot \left[\lambda^2 - \lambda^{-1}\right] dt' \tag{3.59}$$

The next step in the calculation of the stress is to break the integral into two parts: the first, with limits of $-\infty$ to 0, and the second, with limits of 0 to t. The purpose of this step is to facilitate the integration, in that the $-\infty$ to 0 portion can be integrated immediately in closed form; this alleviates the need to numerically integrate the strain history back to some arbitrarily large negative time. The above step assumes that the

deformation begins at time t=0, is positive for all time t>0, and is zero for all times t<0. Again, the uniaxial case will be used for illustrative purposes. We can write

$$\sigma_{xx}(t) = \int_{-\infty}^{0} \sum_{k=1}^{N} \frac{a_k}{\Gamma_k} \exp\left(\frac{t'-t}{\Gamma_k}\right) \cdot h(I_1, I_2) \cdot \left[\lambda^2 - \lambda^{-1}\right] dt' + \int_{0}^{t} \sum_{k=1}^{N} \frac{a_k}{\Gamma_k} \exp\left(\frac{t'-t}{\Gamma_k}\right) \cdot h(I_1, I_2) \cdot \left[\lambda^2 - \lambda^{-1}\right] dt' \tag{3.60}$$

Which upon performing the integration becomes

$$\sigma_{xx}(t) = \sum_{k=1}^{N} a_k \exp\left(\frac{-t}{\Gamma_k}\right) \cdot h(I_1, I_2) \cdot \left[\lambda^2 - \lambda^{-1}\right] + \int_{0}^{t} \sum_{k=1}^{N} \frac{a_k}{\Gamma_k} \exp\left(\frac{t'-t}{\Gamma_k}\right) \cdot h(I_1, I_2) \left[\lambda^2 - \lambda^{-1}\right] dt' \tag{3.61}$$

Because of the stipulation that deformation before t=0 be zero, and after t=0 be positive, the stretch ratios as written in the two parts of the above equation are in fact different. In the original equation, all the stretch ratios are relative stretch ratios, and can be written

$$\lambda(t, t') = \frac{\lambda(t)}{\lambda(t')} \tag{3.62}$$

However, since for time less than zero, $\lambda(t')=1$, we have that

$$\lambda(t, t') = \lambda(t) \qquad (for \ \ t < 0) \tag{3.63}$$

and this stretch ratio is used in both the Finger tensor and the damping function, $h(I_1, I_2)$. For the damping function, the invariants are then

$$I_1(t) = \lambda(t)^2 + 2\lambda(t)^{-1}$$
$$I_2(t) = \lambda(t)^{-2} + 2\lambda(t) \tag{3.64}$$

for the portion t<0. On the other hand, for the portion when t>0, the relative stretch ratios must be used, and the invariants are

$$I_1(t,t') = \left[\frac{\lambda(t)}{\lambda(t')}\right]^2 + 2\left[\frac{\lambda(t)}{\lambda(t')}\right]^{-1}$$
$$I_2(t,t') = \left[\frac{\lambda(t)}{\lambda(t')}\right]^{-2} + 2\left[\frac{\lambda(t)}{\lambda(t')}\right] \tag{3.65}$$

With these considerations in mind, we can write the equation for the stress in the x-direction as

$$\sigma_{xx}(t) = \sum_{k=1}^{N} a_k \exp\left(\frac{-t}{\Gamma_k}\right) \cdot h(I_1(t), I_2(t)) \cdot \left[\lambda(t)^2 - \lambda(t)^{-1}\right]$$
$$+ \int_0^t \sum_{k=1}^{N} \frac{a_k}{\Gamma_k} \exp\left(\frac{t'-t}{\Gamma_k}\right) \cdot h(I_1(t,t'), I_2(t,t')) \cdot \left[\left(\frac{\lambda(t)}{\lambda(t')}\right)^2 - \left(\frac{\lambda(t)}{\lambda(t')}\right)^{-1}\right] dt' \tag{3.66}$$

Using similar arguments, the equation for the stress in the principle stretch directions can be found for the case of equibiaxial extension. In this case,

$$\sigma_{xx}(t) = \sigma_{yy}(t) = \sum_{k=1}^{N} a_k \exp\left(\frac{-t}{\Gamma_k}\right) \cdot h(I_1(t), I_2(t)) \cdot \left[\lambda(t)^2 - \lambda(t)^{-4}\right]$$
$$+ \int_0^t \sum_{k=1}^{N} \frac{a_k}{\Gamma_k} \exp\left(\frac{t'-t}{\Gamma_k}\right) \cdot h(I_1(t,t'), I_2(t,t')) \cdot \left[\left(\frac{\lambda(t)}{\lambda(t')}\right)^2 - \left(\frac{\lambda(t)}{\lambda(t')}\right)^{-4}\right] dt' \tag{3.67}$$

with the appropriate equibiaxial expressions for the invariants I_1 and I_2 being used.

Temperature Dependence of K-BKZ Model

In contrast with the other models discussed herein, the variation of stress with temperature for the K-BKZ equation was not modeled with an Arrhenius-type function. Instead a WLF approach was taken, whereby the decrease in stress with increasing

temperature was accommodated by multiplying the relaxation times of the relaxation spectrum by a shift factor, Θ(T), written

$$\Theta(T) = \exp\left[\frac{-C_1 \cdot (T - T_0)}{C_2 + (T - T_0)}\right] \tag{3.68}$$

where C_1 and C_2 are constants, T_0 represents the reference temperature, and T is the temperature at which the stress is to be calculated. For the data presented, the reference temperature, T_0, is 160°C, and the values of C_1 and C_2 were found to be 20 and 169, respectively. Thus the final form of Θ(T) used was

$$\Theta(T) = \exp\left[\frac{-20 \cdot (T - 160)}{169 + (T - 160)}\right] \tag{3.69}$$

Choice of Parameters

As with any constitutive model, the worth of its predictions are dependent not only on its physical or thermodynamic admissibility, but also on its ability to accurately mimic the trends shown by the experimental data. This, in turn, depends on the parameters chosen for use in the equations. For the K-BKZ equations used in this thesis, there are a total of nineteen independent parameters which may be chosen in order to fit the predicted to the observed stress. These parameters consist of: the relaxation spectrum, a_k and Γ_k; the damping parameter, A; and the parameters used in the WLF temperature dependence function, C_1 and C_2. As previously mentioned, C_1 and C_2 were relatively easy to fit, by judicious choice, and were found to be 20 and 169 respectively. Similarly, the damping parameter A was relatively easy to fit, since its optimization only involved one parameter, and was found to fit best using a value of 0.045.

The relaxation moduli and times, on the other hand, proved to be fairly difficult to fit. For all cases considered, the parameters were fit to the highest strain rate data.

When approaching this problem, one of several different methods can be adopted: one can either arbitrarily set the moduli and fit the relaxation times; arbitrarily set the relaxation times and fit the moduli; or not set any values in the spectrum, and fit them all. By and large, any method is adequate (there are no inherent advantages of one over the other), providing that any parameters that are set beforehand are done so wisely. Various authors have used different methods [23,38,39,40,41,42]; in the present analysis, the relaxation times were arbitrarily set, separated by an order of magnitude, from 0.001 to 1000 seconds, and the relaxation moduli were fitted by minimizing the following function

$$\Phi = \sum_{n=1}^{m} \left(\sigma_{pred.} - \sigma_{obs.} \right)^2 \tag{3.70}$$

where m is the number of data points, $\sigma_{pred.}$ is the predicted stress and $\sigma_{obs.}$ is the experimentally observed stress. The search method used is briefly described in section 3.5.

The problem of minimization is a very complex one. The function to be minimized is highly non-linear, and for each new iteration an entirely new set of data must be generated. For data sets with a large number of points, beyond one hundred or so, the task is quite cumbersome and time consuming. Moreover, because of its high degree of non-linearity, the final "solution" found is largely dependent upon the initial conditions; that is, the initial guesses for the moduli. This would indicate that the solution is in fact only a local minimum, and a different solution would be obtained with

different starting values, and that there is almost certainly no unique "best" set of parameters to be found.

K-BKZ Model Performance

ABS Uniaxial

The parameters were fitted to the experimental data for strain rate 1 sec^{-1}. As shown in Fig 3.16, the predicted stress exhibits most of the characteristics of the observed data, yet falls short in one significant respect: the predicted stress could not be made to exhibit the strain softening seen at high strains (ε>2.5). While at first this may seem to be a fatal flaw, it must be kept in mind that a true strain of 2.5 corresponds to a stretch ratio of approximately 15, which is quite large.

The next aspect to consider is the model's performance for the other strain rates. Certainly, one could expect that the closeness of fit will deteriorate the further one moves from the strain rate for which it was fitted, and this is true in this case also. As can be seen from Figures 3.16 and 3.17, the predictions are of the some order of accuracy for the 0.5 sec^{-1} data as for the fitted 1 sec^{-1} data. However, for the three lowest strain rates (0.08, 0.04 and 0.008 sec^{-1}), the predictions become further from the observed data, and can be considered unsatisfactory. For all of the three lowest strains, the observed data is roughly double that of the predicted stress over almost the entire strain range measured.

The K-BKZ model parameters for ABS uniaxial elongation are listed in Table 3.5, presented at the end of this Section.

Figure 3.16: Uniaxial Elongational True Stress as a Function of Stretch Ratio, ABS, 190 deg. C, at High Strain Rates

Showing Performance of K-BKZ Model

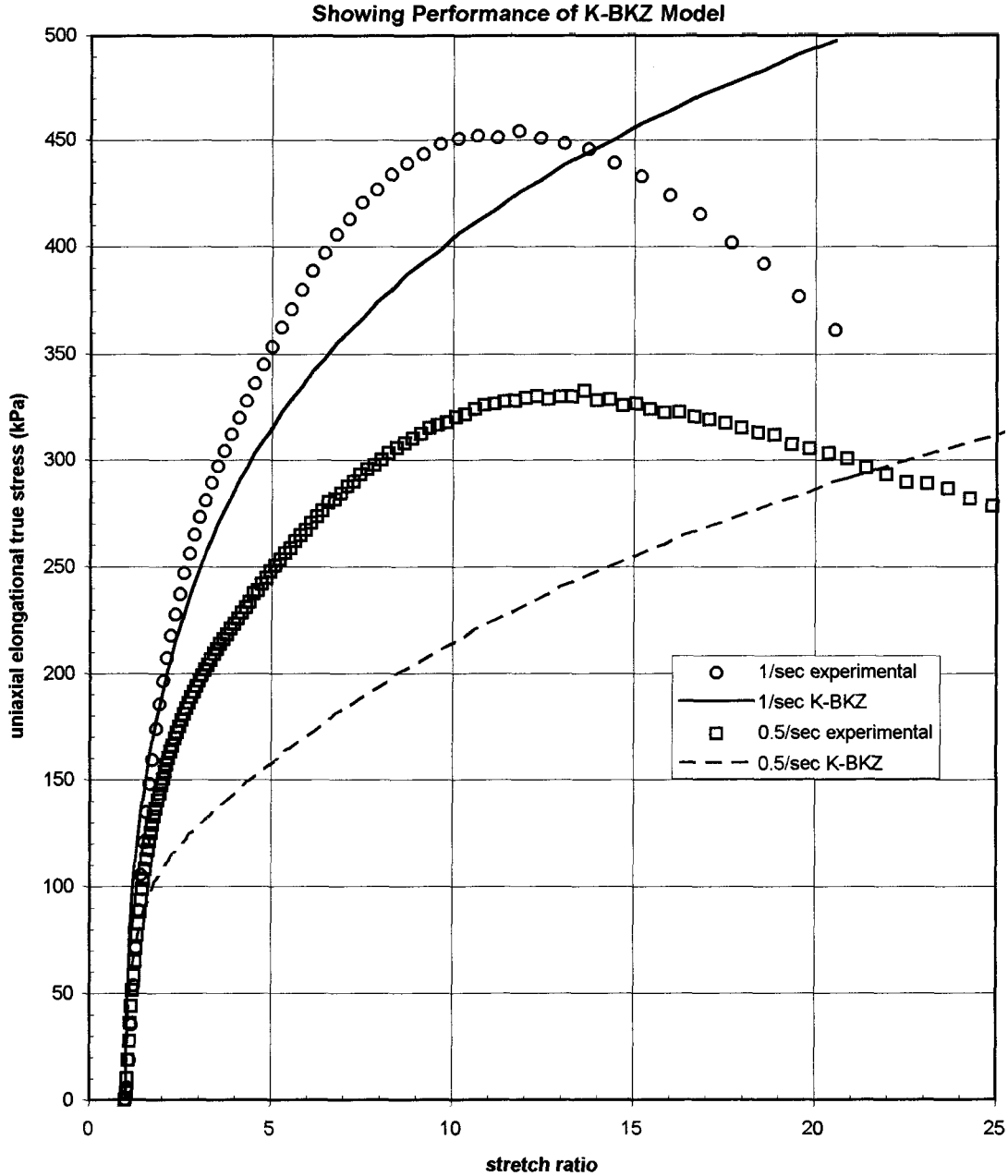

Figure 3.17: Uniaxial Elongational True Stress as a Function of Stretch Ratio, ABS, 190 deg. C, at Low Strain Rates
Showing Performance of K-BKZ Model

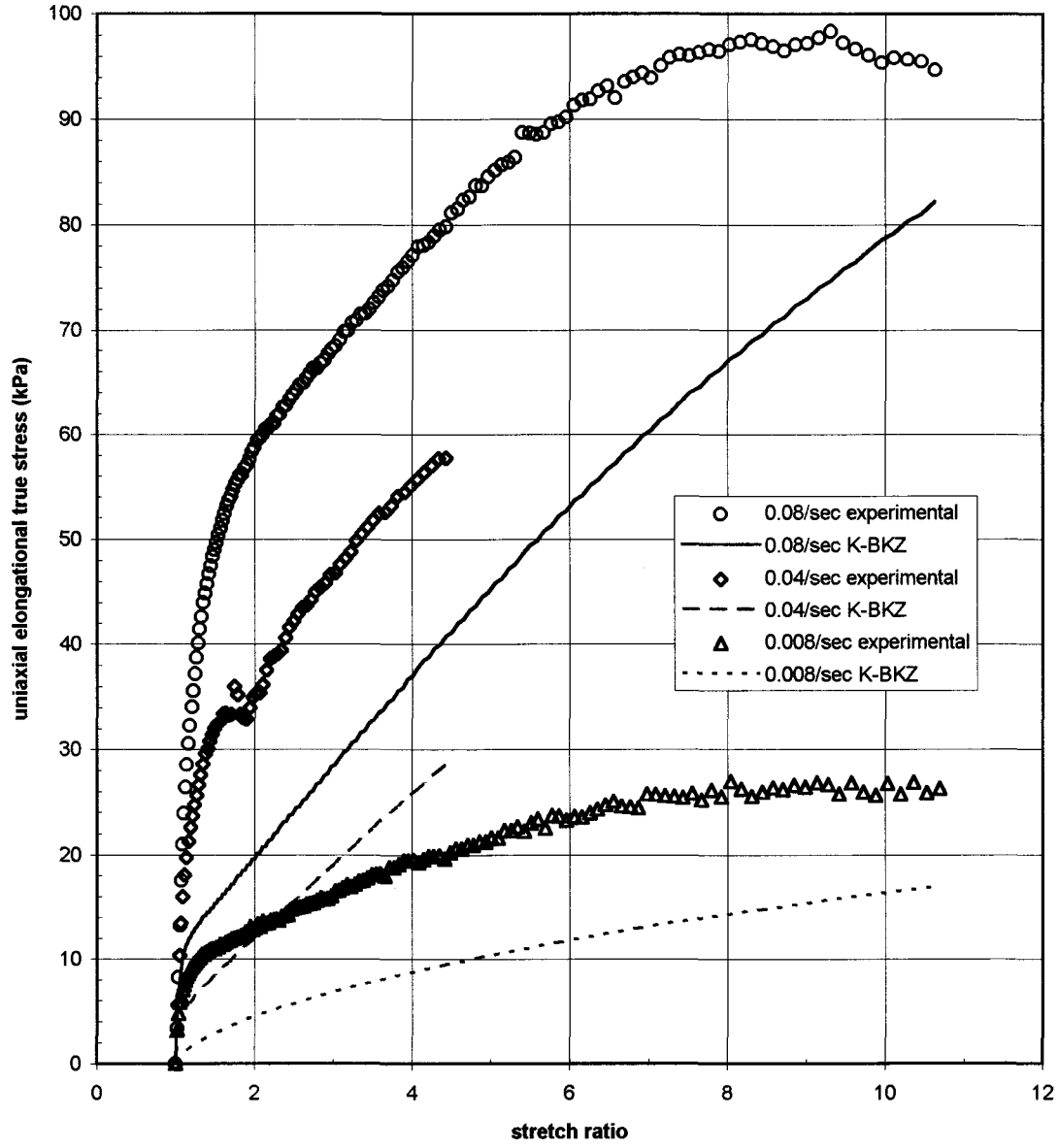

ABS Equibiaxial

The K-BKZ predictions for the case of equibiaxial elongation of ABS are quite good. The parameters were fitted using the 0.3 sec^{-1} strain rate data. As can be seen in Figure 3.18, the model very closely matches the experimental data over the entire strain range (this graph was truncated at a stretch ratio of four, in order to more clearly show the data for the lower strain rates; the data for $\dot{\varepsilon}$=0.3 sec^{-1} actually extend to a stretch ratio of approximately seven, and is shown in Figure 3.19).

For the lower three strain rates (0.1, 0.03 and 0.01 sec^{-1}) the predictions also show good agreement with the experimental data. Besides an initial over-estimation of the stress at low strains, up to about ε=0.2, the predictions very closely match the observed values over the entire strain range.

The K-BKZ model parameters used for ABS equibiaxial extension are listed in Table 3.5.

Temperature Variation

As mentioned in Section 3.3.5, the variation of stress with temperature was accounted for by multiplying the relaxation times, Γ_k, by a WLF shift factor Θ(T). The results are shown in Figure 3.20, and the function Θ(T) is shown in Figure 3.21. In general, the modeling of this phenomenon is quite successful, however there are two major drawbacks of the present analysis:

1) The moduli were fitted at a temperature of 190°C, whereas the parameters used in Θ(T) are referenced to 160°C. Attempts were made to refer Θ(T) to 190°C, but the fit obtained was inferior to that one shown here.

Figure 3.18: Equibiaxial Elongational True Stress as a Function of Stretch Ratio, ABS, 190 deg. C, at Various Strain Rates
Showing Performance of K-BKZ Model, to Stretch Ratio of 4

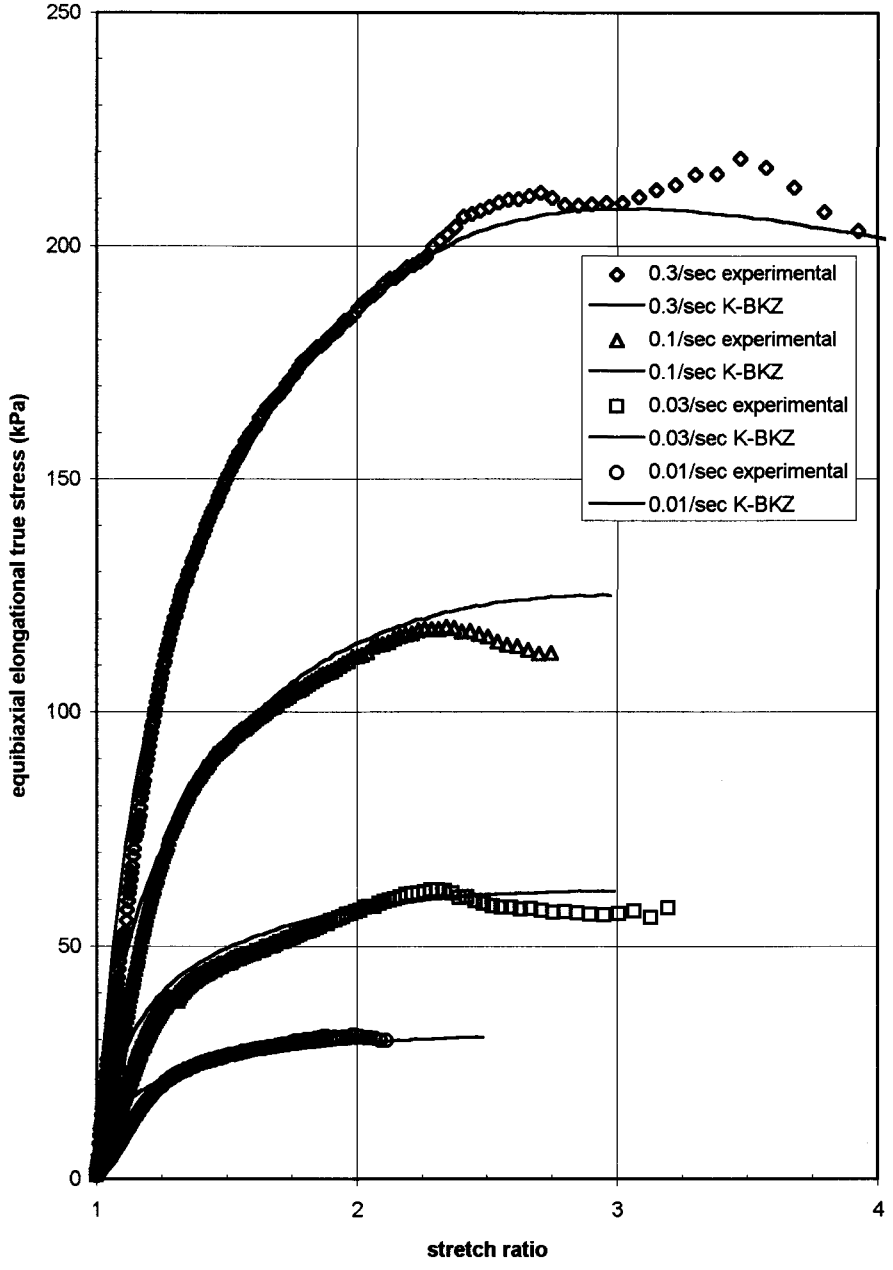

Figure 3.19: Equibiaxial Elongational True Stress as a Function of Stretch Ratio, ABS, 190 deg. C, at Various Strain Rates
Showing Performance of K-BKZ Model, to Stretch Ratio of 8

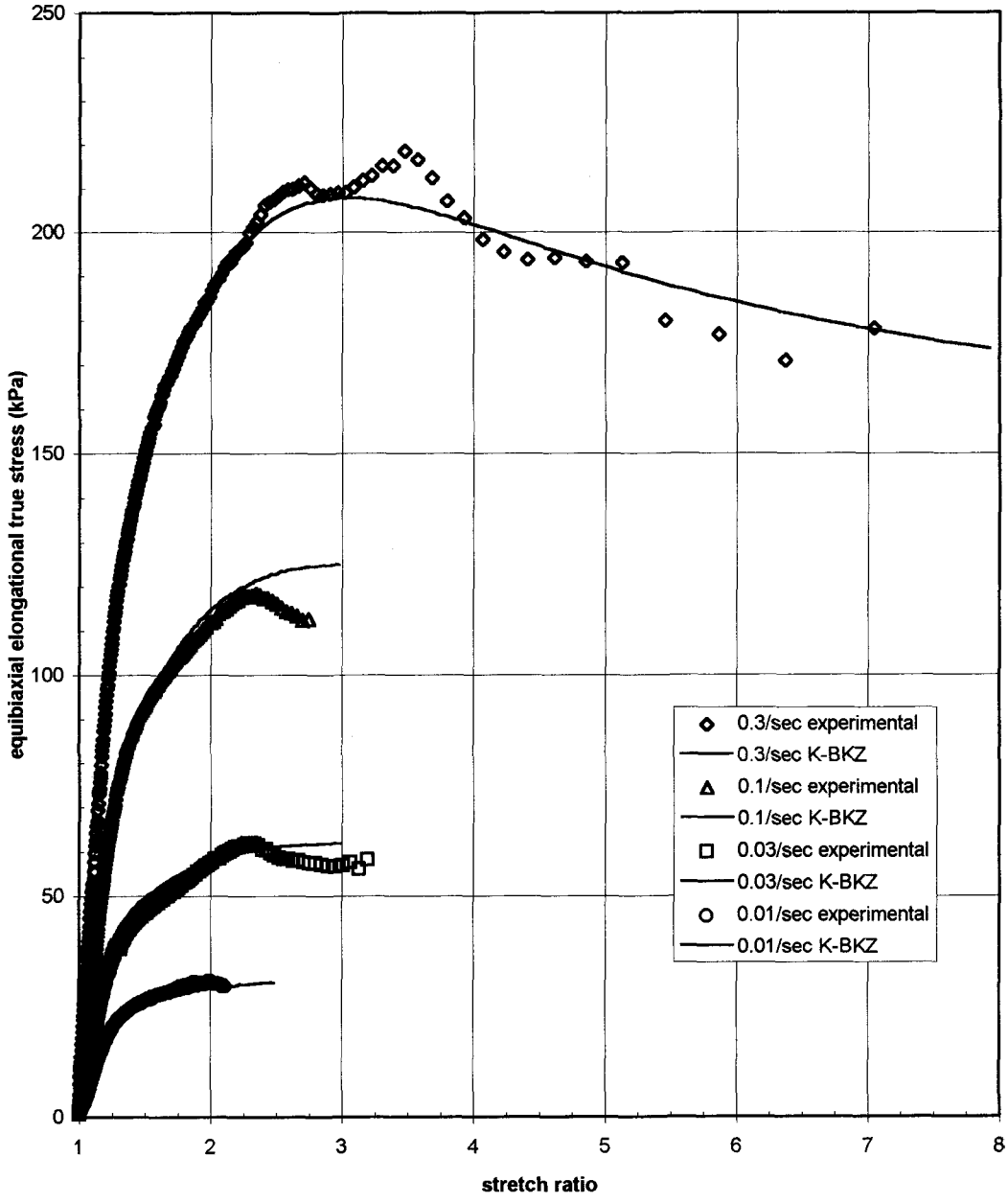

Figure 3.20: Equibiaxial Elongational True Stress as a Function of Stretch Ratio, ABS, Strain Rate 0.3/sec, at Various Temperatures
Showing Performance of K-BKZ Temperature Effect Shift

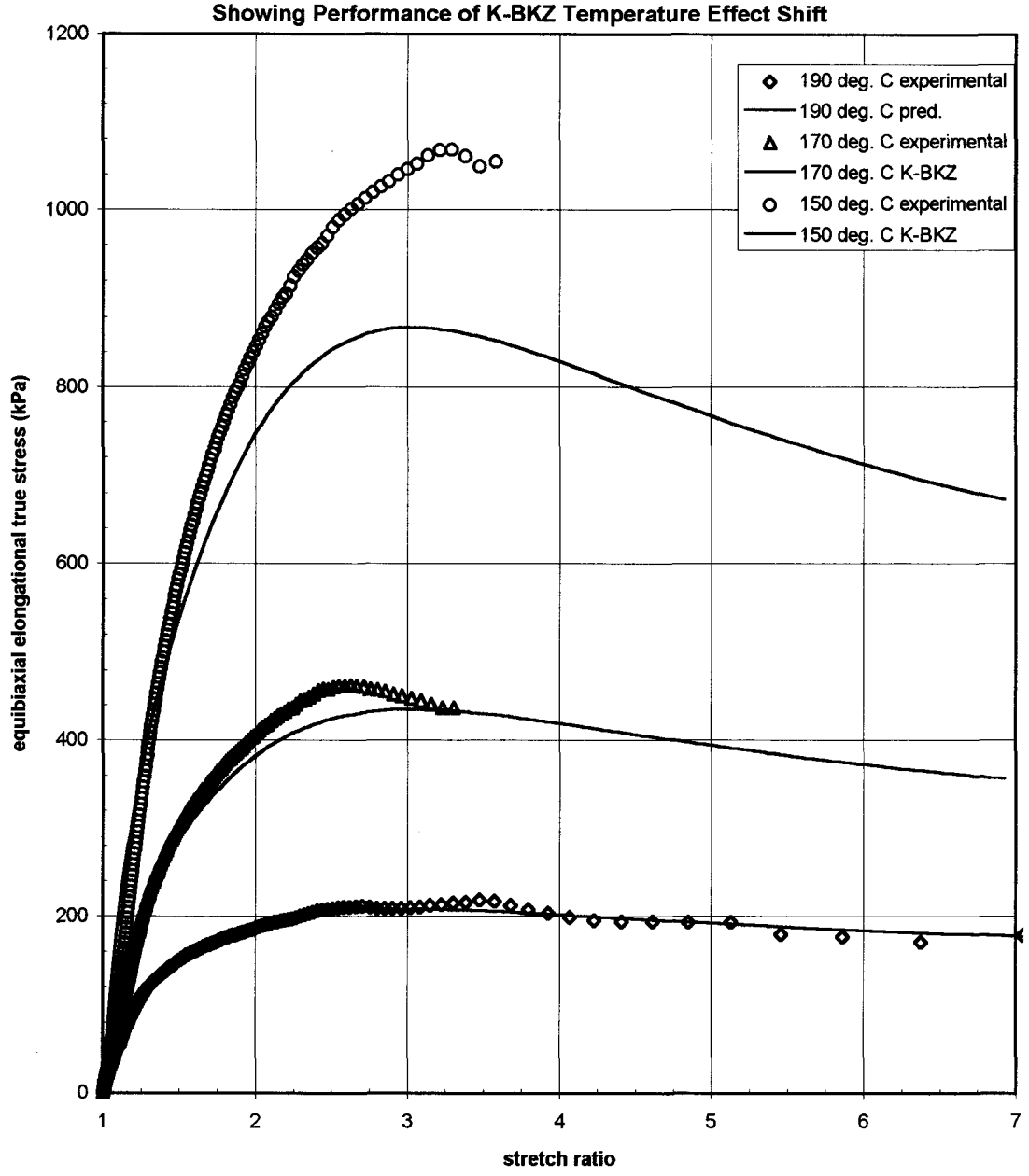

Figure 3.21: WLF Shift Factor as a Function of Temperature

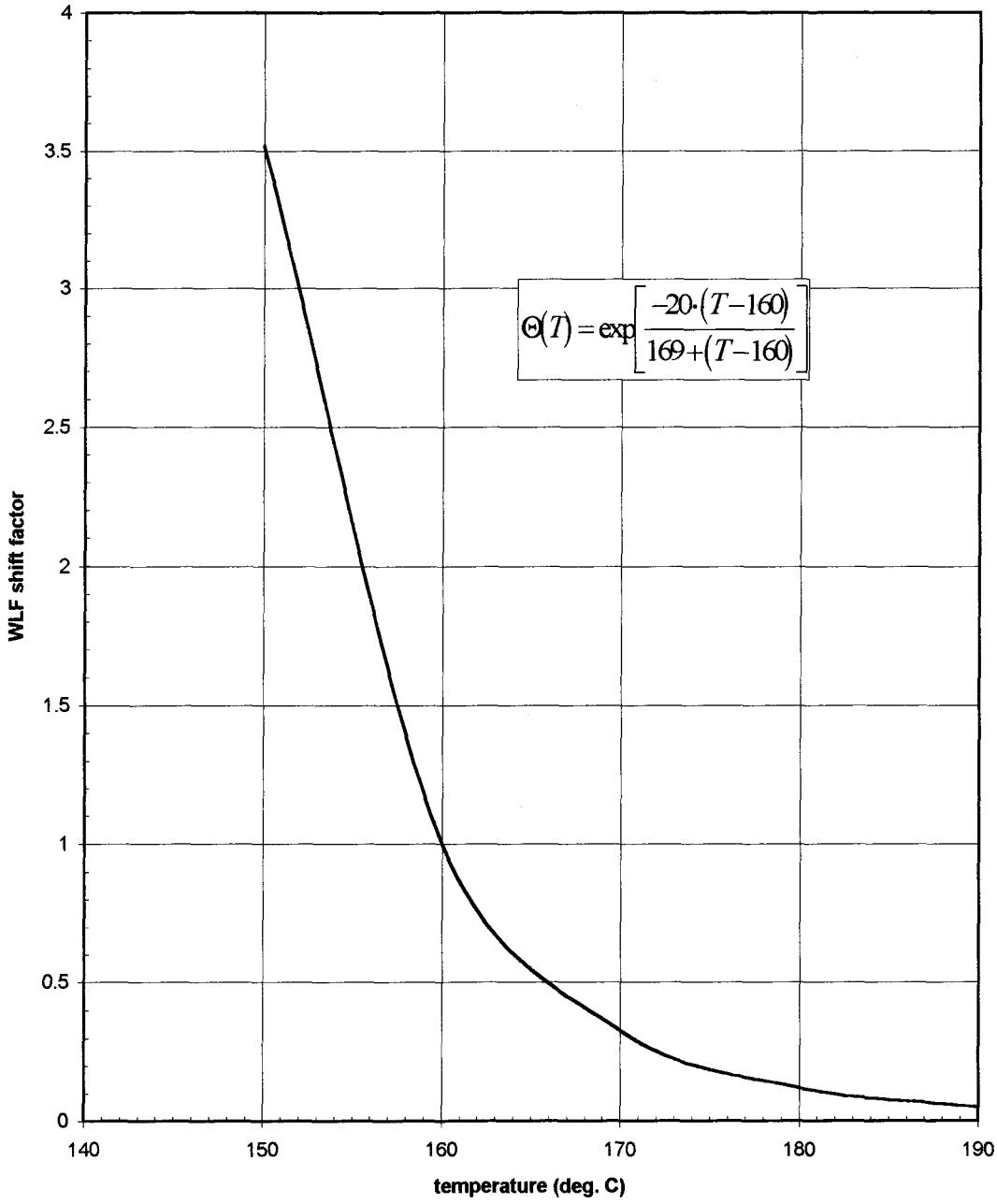

2) No additional data are available for other temperatures for this polymer, and indeed no temperature data at all were available for HDPE. Additional data would allow a more in-depth analysis of the applicability of the WLF function, as well as provide more insight into this phenomenon in general.

HDPE Uniaxial

The parameters for the case of uniaxial elongation of HDPE were fitted at a strain rate of 0.6 sec^{-1}. As can be seen in Figure 3.22, the agreement between the predicted and experimental stress in not good. While the magnitude of error over the strain range is never more than about 30%, the model does not exhibit any of the specific trends shown by the data. The data clearly shows initial yielding (or viscoelastic behaviour) followed by strain hardening, and lastly exhibits final yielding at a stretch ratio of about 12. The model used, however, shows a monotonically increasing stress, albeit with some small amount of negative curvature. Because of the lack of agreement between the predicted and experimental stress, the model, with the parameters used, can be deemed to be unsatisfactory for this case.

With regards to the model's mimicking the decrease of stress with decreasing strain rate, the model does perform adequately, in a general sense. As mentioned above, the originally fitted data does not exhibit the characteristics shown by the experimental data, and thus the lower strain rates could not be expected to match their experimental data either. However, in the amount of decrease of stress at the lower strain rates, the model does exhibit the correct general trend.

Figure 3.22: Uniaxial Elongational True Stress as a Function of Stretch Ratio, HDPE, 190 deg. C, at Various Strain Rates
Showing Performance of K-BKZ Model

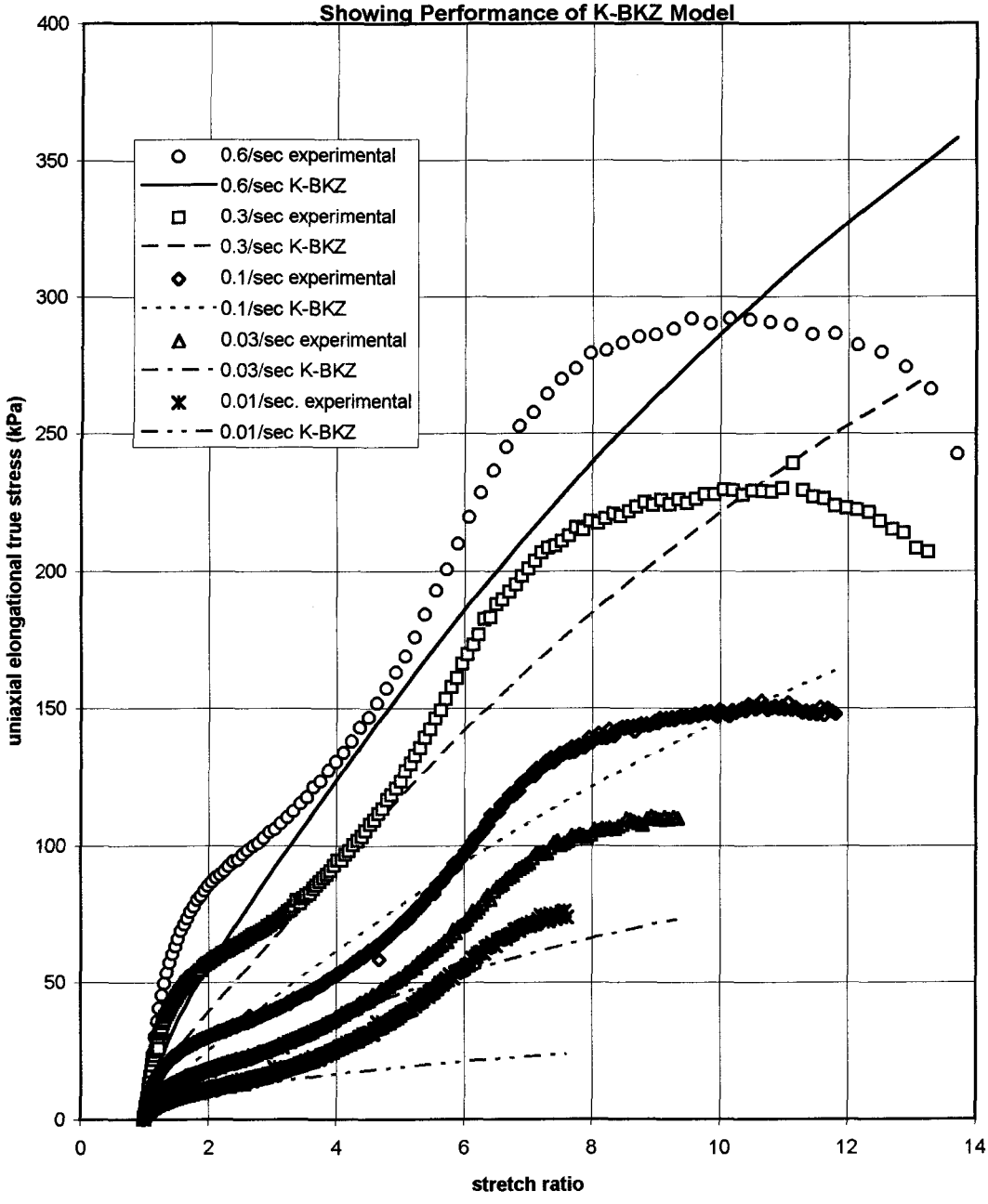

The K-BKZ model parameters used for the HDPE uniaxial predictions are shown in Table 3.5.

HDPE Equibiaxial

In common with the K-BKZ predictions for ABS, the predictions for equibiaxial elongation for HDPE show excellent agreement with the observed data over the entire strain range. The parameters were fitted to the data for a strain rate of 0.3 sec^{-1}. As can be seen in Figure 3.23, the predicted stress exhibits the viscoelastic response seen in the experimental data, as well as the long slow decrease in stress with increasing strain.

The one aspect that is not mimicked by the model is the large drop in stress at a stretch ratio of approximately λ=2.4. This sharp drop after a quick rise in stress can be attributed to stress "overshoot", a common phenomenon in viscoelastic polymers, and its effect can be more easily seen in a plot of stress versus time, as in Figure 3.24. This plot illustrates and underscores the difference in the time frames considered in the three tests. Whereas for the lowest strain rate (0.03 sec^{-1}), the time extends to a value of almost 70 seconds, for the highest strain rate (0.3 sec^{-1}) the test is terminated at less than 7 seconds. Indeed, the stress overshoot is much less evident in the 0.03 sec^{-1} data, as expected. Furthermore, in the method used for fitting the parameters, all data points considered have equal importance, or weight, when minimizing the error. Thus, when the data exhibits a long slow decline in stress, these data points, while important, perhaps are fitted too precisely, taking away somewhat from the importance of the overshoot points. It is believed that with further manipulation of the moduli or perhaps

Figure 3.23: Equibiaxial Elongational True Stress as a Function of Stretch Ratio, HDPE, 190 deg. C, at Various Strain Rates
Showing Performance of K-BKZ Model

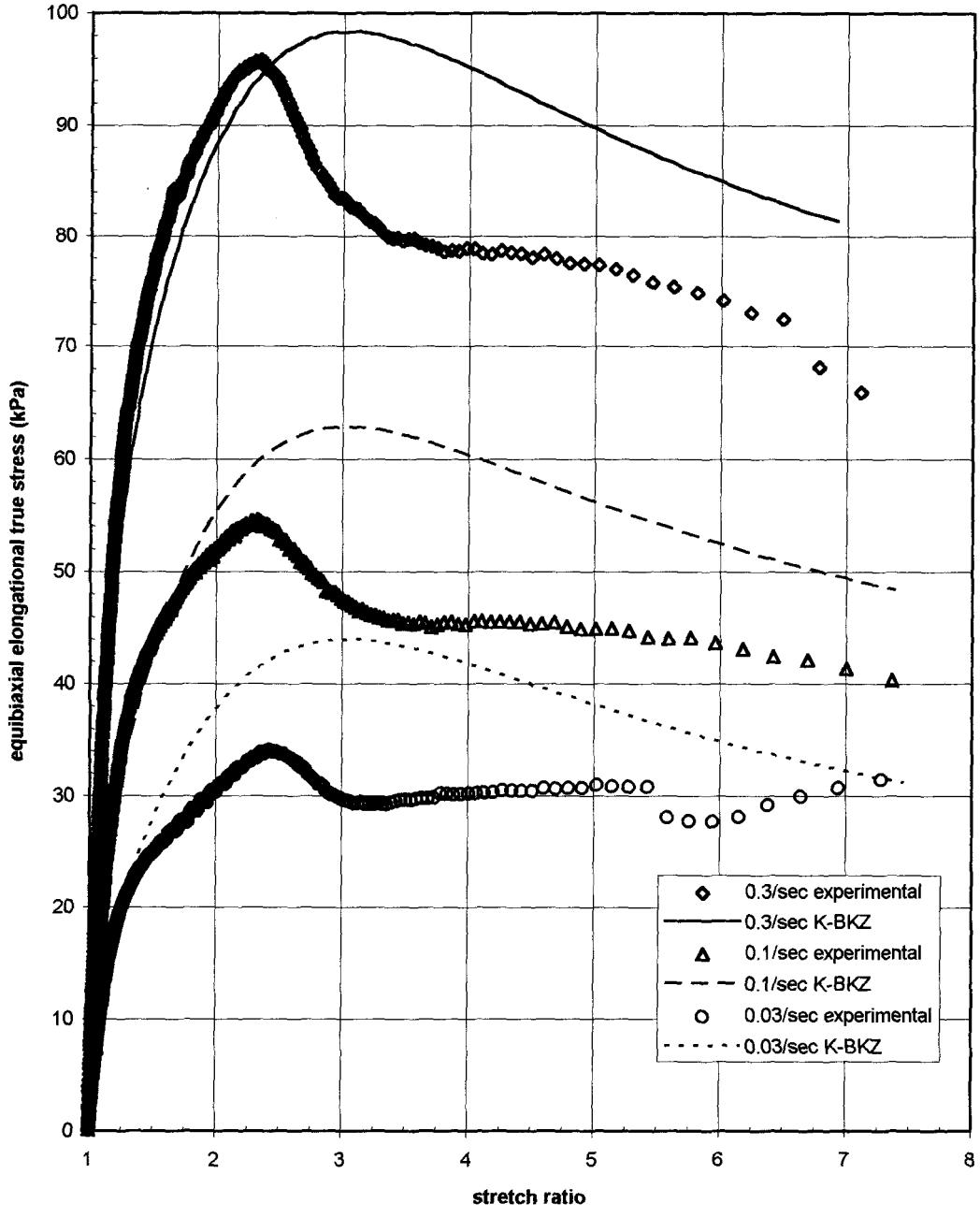

Figure 3.24: Equibiaxial Elongational True Stress as a Function of Time, HDPE, 190 deg. C, at Various Strain Rates
Showing Performance of K-BKZ Model

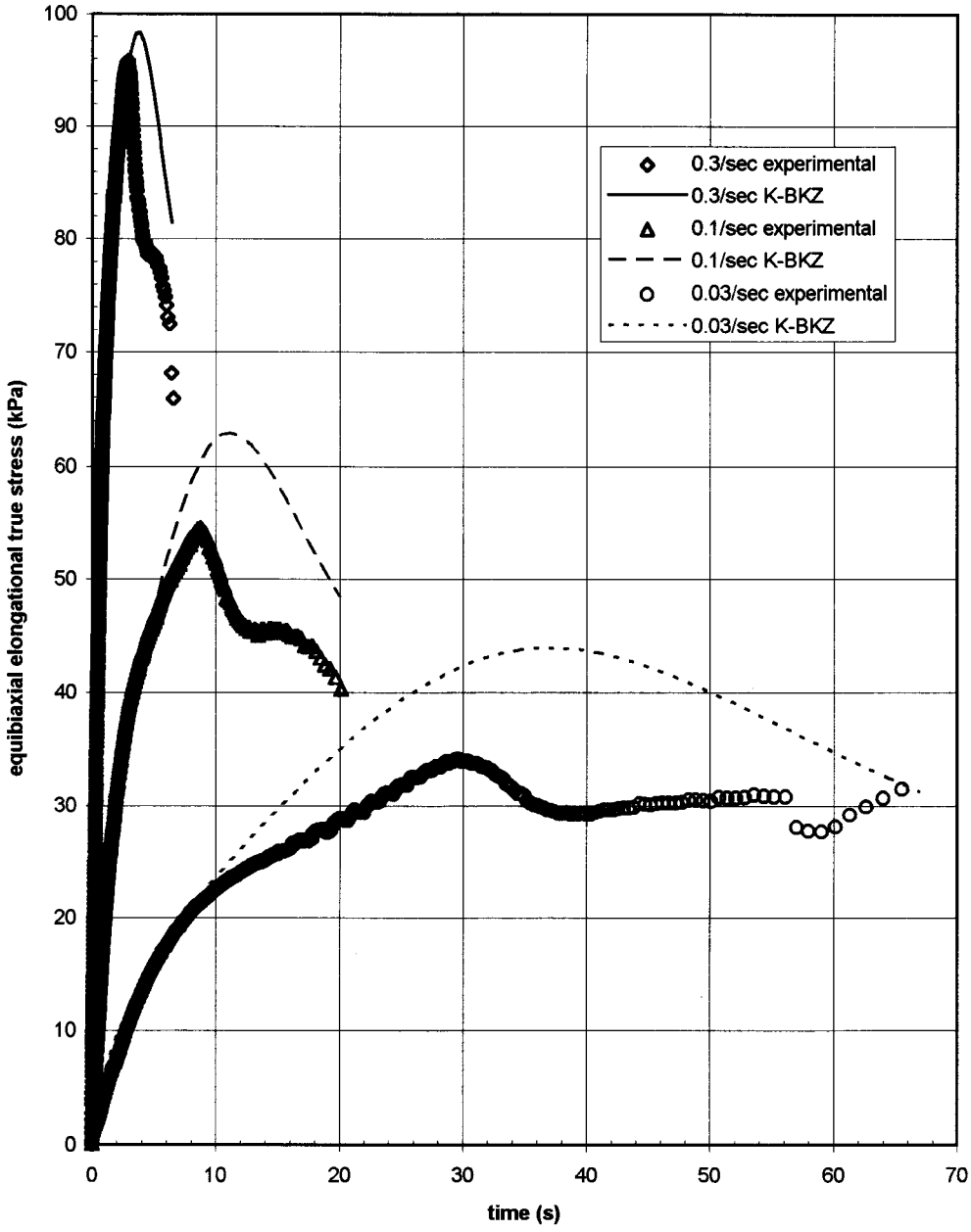

the damping parameter, one could more closely model the overshoot phenomenon (although this might have the additional effect of decreasing the accuracy of the predictions at high strains).

The parameters used the HDPE equibiaxial elongation analysis are shown in Table 3.5.

Table 3.5 K-BKZ Model Parameters

	Deformation Type			
	Uniaxial		Equibiaxial	
Polymer	ABS	HDPE	ABS	HDPE
a_1	494	497.5	830	7500
a_2	2009.8	4370	9018	8420
a_3	1200	4100	38740	48100
a_4	70400	24300	79800	67000
a_5	475600	28800	134000	121700
a_6	976400	68800	156000	517000
a_7	4976000	288000	144000	867000
a_8	9764000	688000	1360000	–
Γ_1	10000	10000	10000	1000
Γ_2	1000	1000	1000	100
Γ_3	100	100	100	10
Γ_4	10	10	10	1
Γ_5	1	1	1	0.1
Γ_6	0.1	0.1	0.1	0.01
Γ_7	0.01	0.01	0.01	0.001
Γ_8	0.001	0.001	0.001	–
C_1	–	–	20	–
C_2	–	–	169	–
A	0.045	0.045	0.045	0.045

3.4 Using Uniaxial Parameters to Predict Biaxial Response

One of the great drawbacks of investing faith in the predictions of numerical simulations of thermoforming and blowmolding is the fact that the rheological parameters used in the computer programs are (normally) obtained from uniaxial tests.

In the overwhelming majority of cases, however, the deformations are of a biaxial (though not necessarily equibiaxial) nature, and this can cause discrepancies with observed results. Indeed, there is no reason to believe that uniaxial parameters can be blindly extended to biaxial deformation, and yet because of the high cost and difficulty involved in obtaining biaxial data, uniaxial parameters are used in almost all simulations [27].

For the present analysis, the equations considered for the conversion from uniaxial to equibiaxial elongation were those of the Ogden, G'Sell, Two-term Polynomial and K-BKZ models. The Mooney-Rivlin model was not considered, due to its poor fit in the equibiaxial case.

It was found that the Two-term Polynomial model performed the best in this regard, followed by the G'Sell, K-BKZ and Ogden models. In fact, the Ogden predictions were very far off the observed values, and hence were omitted from the plots below. It is interesting to note that in Ogden's original work [14], he obtained one set of parameters for his model which satisfactorily fit data for uniaxial elongation, equibiaxial extension and shear. The model's lack of strain rate sensitivity may be partly accountable for the discrepancy shown in the present analysis, since the uniaxial parameters for ABS and HDPE were fitted to a strain rate of 1 sec^{-1} and 0.6 sec^{-1}, respectively, while the equibiaxial data was obtained at a strain rate of 0.3 sec^{-1}.

The K-BKZ predictions are shown in Figure 3.25 for ABS. As can be seen, although the general shape of the response is exhibited by the predicted values, its magnitude is off by a factor of 2 at the higher strain rate, and by a factor of 4 at the lower.

Figure 3.25: Elongational True Stress as a Function of Stretch Ratio, ABS, 190 deg. C

Showing Performance of K-BKZ Model to Predict Biaxial Response Using Uniaxially Fit Parameters

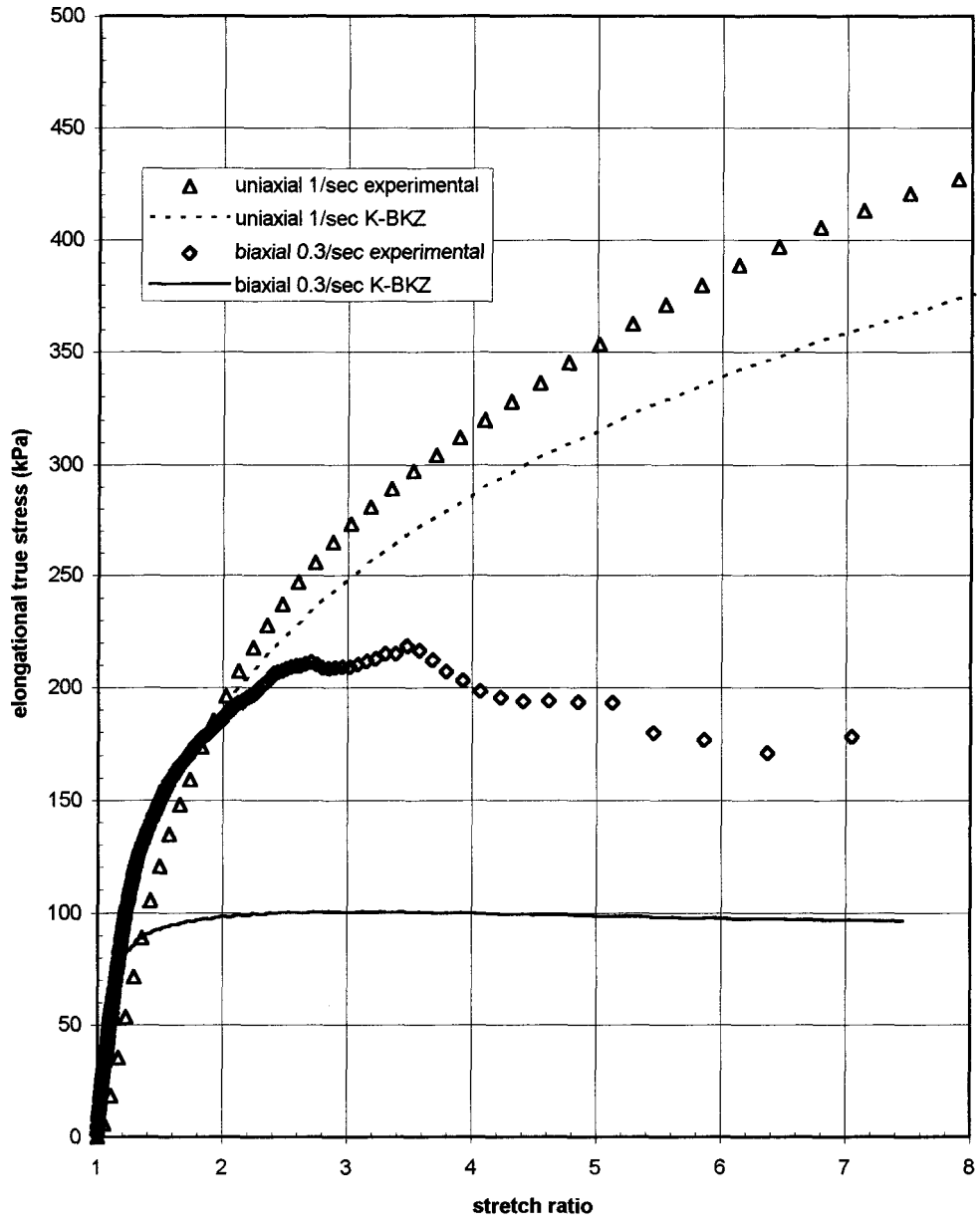

The prediction for the G'Sell model, and its modification, the Two-term Polynomial model, are shown in Figure 3.26 for ABS and Figure 3.27 for HDPE. The G'Sell model in both cases does not appear to give good results, since the strain hardening term becomes too dominant too early.

The best conversion from uniaxial to equibiaxial elongation was provided by the Two-term Polynomial model. In the case of ABS, the predictions are excellent, and with HDPE they follow the correct trend, but are off by a factor of 2 over most of the strain range.

It should be noted that, while most of the models do not appear to perform well in this regard (with the exception of the Two-term Polynomial model), their great sensitivity to the values of their parameters should be kept in mind. In some previous analyses [14,16], the parameters were chosen with the goal of fitting all of the deformation types simultaneously; that is, the equibiaxial response was known *a priori*, and the parameters were accepted or rejected based upon their ability to provide accurate predictions for all of the deformation types. In contrast, the present analysis took the approach that ignored the equibiaxial data in the fitting of the uniaxial parameters, and simply used these parameters in the appropriate equibiaxial equations. The reason this approach was adopted was to realistically test each model's ability to provide useful predictions, without the need perform expensive biaxial rheological tests. While modifying the uniaxial parameters to match known biaxial measurements is useful as an illustration of a model's versatility, if the biaxial data is readily available, it would be easier to simply fit the parameters to this data (ignoring

Figure 3.26: Elongational True Stress as a Function of Stretch Ratio, ABS, 190 deg. C

Showing Performance of G'Sell and 2-Term Polynomial Models to Predict Biaxial Response Using Uniaxially Fitted Parameters

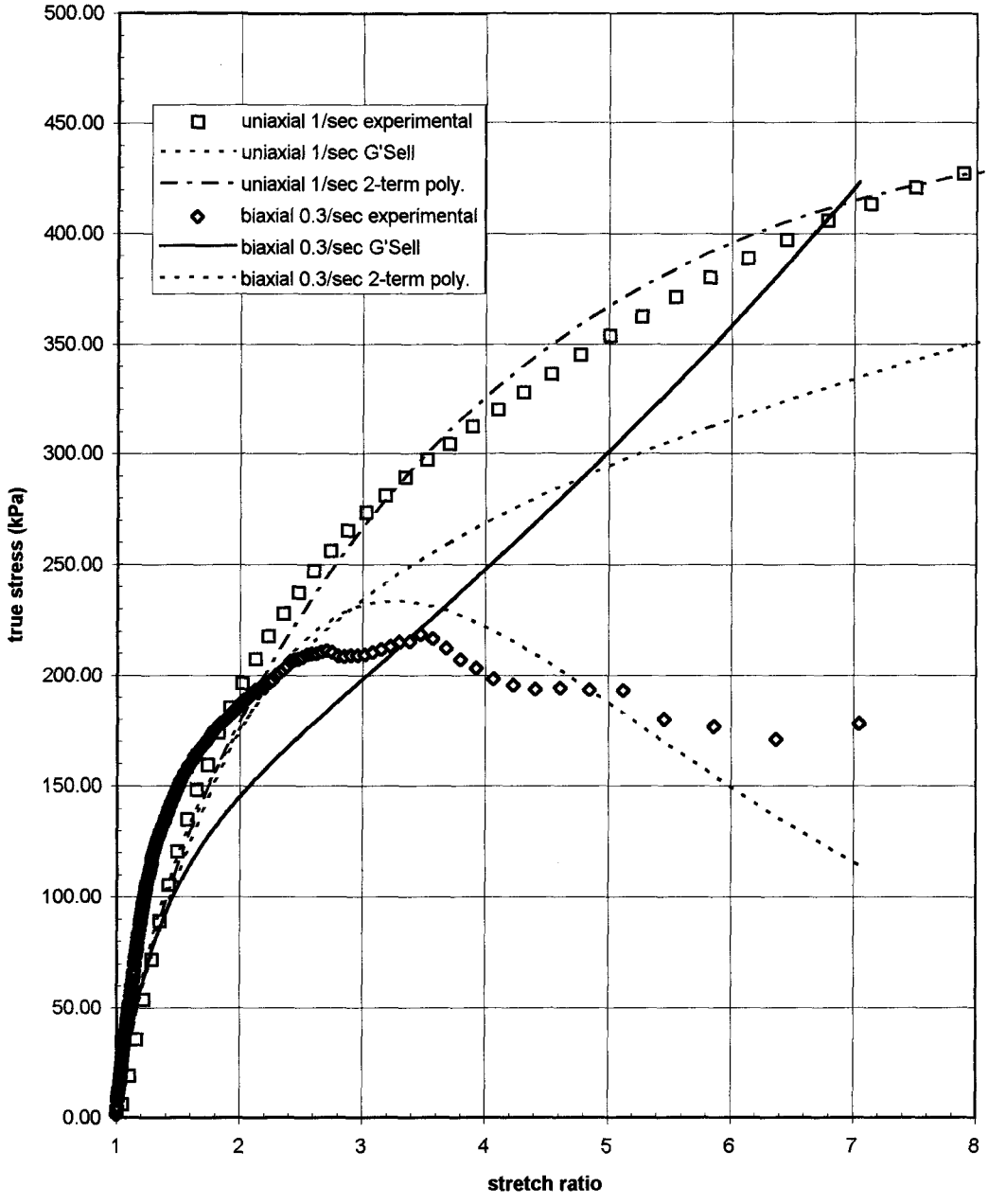

Figure 3.27: Elongational True Stress as a Function of Stretch Ratio, HDPE, 190 deg. C

Showing Performance of G'Sell and 2-Term Polynomial Models to Predict Biaxial Response Using Uniaxially Fitted Parameters

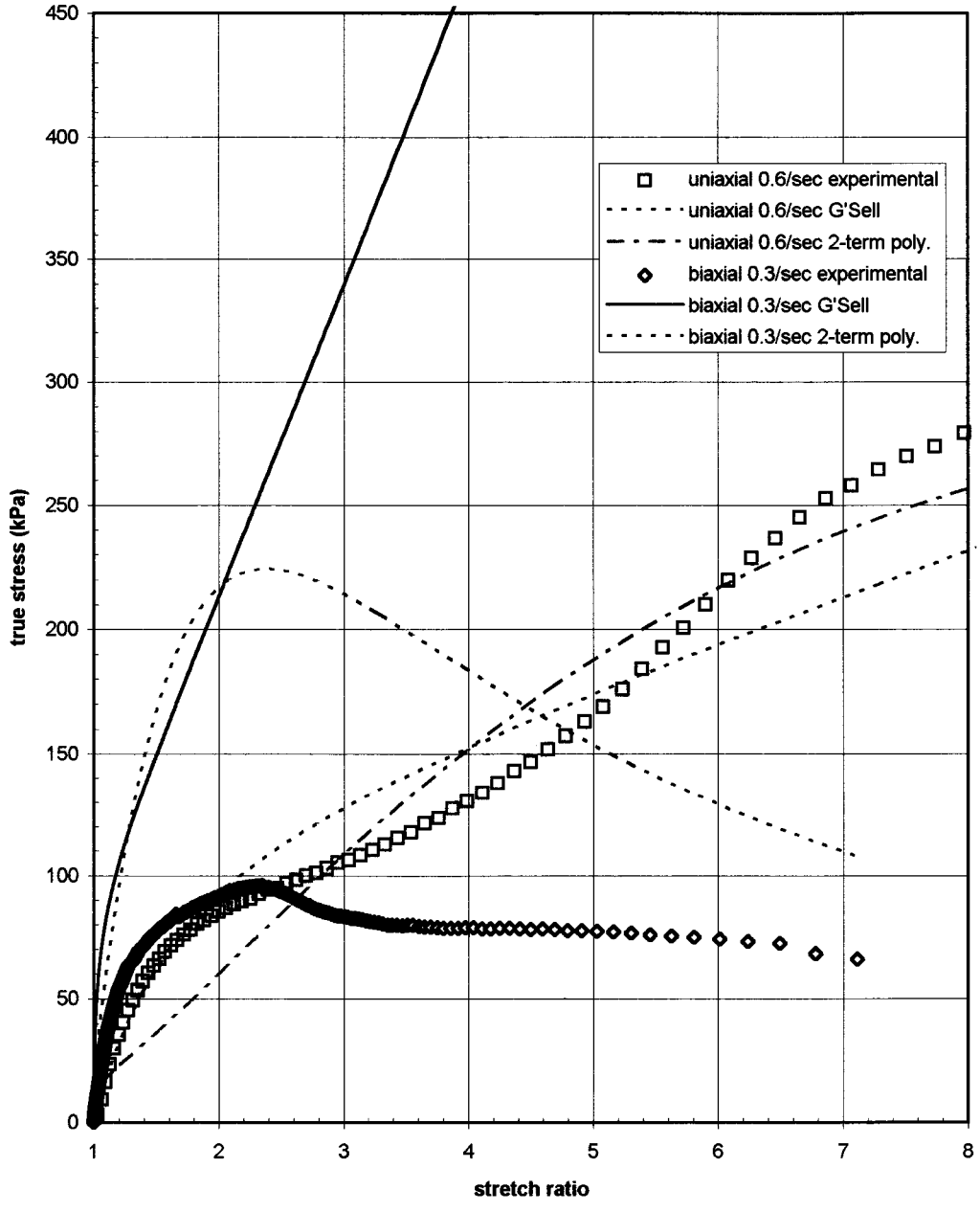

the uniaxial data), since real processes, and thus the numerical simulations of these processes, deal with biaxial deformations, not uniaxial.

3.5 Description of Method Used for K-BKZ Parameter Fit

In order to fit the relaxation moduli used in the K-BKZ constitutive equation, the difference between the observed and predicted stress was minimized in the least squares sense; i.e., the function

$$\Phi = \sum_{n=1}^{m} \left(\sigma_{pred.} - \sigma_{obs.} \right)^2$$

was minimized. There are many different techniques that have been explored in order to accomplish the minimization [43,44,45,46,47]; the method used in this work was the method of steepest descent, whereby the maxima of the error function, Φ, is represented by "hills" of the function, and the minima by the "valleys". The method of steepest descent derives its name from the idea that successive iterations follow the opposite "direction" of the gradient (the direction of steepest increase), eventually reaching a point where an iteration in any possible direction represents a step "up". When this point is reached, the function is at a minimum (local or global), and this is the solution sought [45]. Although there are many other methods that can be used to minimize this function [41,42], the technique employed here has the advantage of being simple to both understand and to implement into a computer code. This simplicity is matched, however, by two major drawbacks: first, the "valley" may be very shallow and long, so that convergence is slow; second, a better solution may lie at the bottom of a narrow "valley" that is completely stepped over in the search routine [45]. It is this second drawback that suffers most highly form the large non-linearity of the

problem, in that in all cases considered, a small change in the initial guesses gave quite different results. This indicated the presence of many local minima, but not necessarily any global minima (at least for the range of parameters considered here).

CHAPTER 4

CONCLUSIONS AND RECOMMENDATIONS

4.1 Conclusions

The numerical simulation of polymer processing operations using the finite element method has shown a great potential to model the type of flow exhibited by polymers, thus aiding in the optimization of processing and design operations [5,27,48,49,50,51]. However, even with state of the art numerical techniques and computer hardware, the simulation results obtained are of little worth if the constitutive models used do not accurately reflect the real physical response of the material. This task, however, is not easily completed, due in large part to the complicated non-linear, non-Newtonian response of polymers under most processing conditions. Indeed, even after many years of extensive research by many workers in this field, there is to date no single constitutive model that adequately represents all of the unique physical responses of viscoelastic polymer melts, and as a result, many constitutive models used in numerical simulations work best with a particular type of flow field. This thesis reports on the performance of five constitutive models (Mooney-Rivlin, Ogden, G'Sell, Two-Term Polynomial and K-BKZ) to represent the stress-strain response of polymer melts in elongational uniaxial and equibiaxial flow, and the variation of this stress with changes in strain rate and temperature.

The models are fitted to experimental data (obtained from an industrial source) over a broad range of strain rates, and a temperature range of 40°C. The data presented are for constant strain rate tests on Acrylonitrile-butadiene-styrene (ABS) and High Density Polyethylene (HDPE), which are commonly used in thermoforming and blowmolding operations.

The first two models considered were the Mooney-Rivlin and Ogden models. In general, these models did not perform as well as the other models considered. Their most attractive attributes include:

- the ease with which their parameters were fitted to the experimental data,
- they are easy to use; incorporating these models into a computer code would present little difficulty, compared with the other models examined in this work.

The disadvantages of these models include:

- their complete inability to account for, in any way, the variation in stress with strain rate,
- the applicability of their predictions is highly suspect outside of the strain range over which their parameters were fit,
- the Ogden model was found to be incapable of modeling strain softening data, while at the same time meeting the sufficient condition that the strain energy function must be always positive.

Because of these drawbacks, it can be concluded that either the Mooney-Rivlin or Ogden models would be inadequate in simulating processes in which viscous effects play a significant part, or which involve very large stretch ratios.

The next models considered were the G'Sell model and its modification, the Two-Term Polynomial model. In general, both models performed adequately over most of the strain range, although the G'Sell model, because of its single high-strain effect term, had difficulty in accounting for the strain softening which occurred at very high strains. The Two-Term Polynomial model, however, has (as the name implies) two terms to account for high-strain effects, and showed marked improvement in this regard over the G'Sell model.

Both the G'Sell and Two-Term Polynomial models performed very well with respect to variations in stress with strain rate and temperature. In addition, the parameters for both were easily fit to experimental data, and both models present little difficulty in their understanding and use.

The last model considered was an integral model, known as the K-BKZ model. Its predictive accuracy was much better in the equibiaxial case as compared to the uniaxial case, for both of the polymers considered. Its poor fit to the experimental data for the uniaxial case serves to illustrate, or underscore, the main drawback of using this model. In particular, the model's predictions are very dependent on the parameters chosen for the relaxation spectrum, and the selection of these parameters involves the optimization of a highly non-linear, seemingly non-unique error function. By this it is meant that very different results can be obtained with different parameters, although the relative "error" of the two different parameter sets is roughly the same. This leads to the conclusion that the search technique used to find the model parameters is an important consideration, and that if enough time is spent in the search, another set of

parameters that fit the data equally good can usually be found, indicating there is most probably no unique "best" set of parameters.

Another drawback of the K-BKZ model, and indeed any integral model, is that in order to carry out the integration, one needs to keep stored in memory the entire deformation history. For a single specimen, or element, this does not present a problem for most cases; however, when the model is implemented in a finite element code in the simulation of an actual three dimensional process, the demands that this places on the computer's memory has the effect of severely limiting the number of elements one can use, which in turn can affect the accuracy of the simulation's predictions. This limitation does not apply to the G'Sell or Two-Term Polynomial models, however; all that is needed for their implementation is the strain and the instantaneous strain rate at that point in order to calculate the stress, and it is this feature that is their main advantage over the K-BKZ model.

Another goal of this thesis was to investigate the possibility of taking uniaxially fitted parameters, and extending their use to equibiaxial deformations. That is, if one can find a set of parameters, fitted to uniaxial data, that would allow a model to accurately predict the stress observed from equibiaxial tests, the outcome would be twofold: first, this would enhance the model's applicability and legitimacy; and second, it would allow one to forego the expense and difficulty involved in obtaining reliable equibiaxial data, an endeavor which is on-going, and has been in general unsatisfactory, although many specialized techniques have been proposed [52,53]. One could perform a quick, inexpensive uniaxial test, and use parameters fit to this data in the simulation of biaxial processing operations. The models for which this was

attempted were the Ogden, G'Sell, Two-Term Polynomial and K-BKZ. The Ogden Model was found to be inadequate for this purpose. The G'Sell model did not perform well in this regard, mainly because the high-strain effect term became too dominant, causing an over-prediction of the stress. The K-BKZ model exhibited the correct shape of the stress-strain curve, but under-predicted the observed stress by about a factor of 2. The Two-Term Polynomial performed the best in predicting biaxial stress using uniaxially parameters, showing very close agreement with the observed data over the entire strain range for ABS, while it over-predicted the stress by a about a factor of 2 for HDPE.

Overall, the prediction of equibiaxial stress using parameters fitted uniaxially was not reliably successful for any of the models considered. While it is possible to find parameters that would adequately match the observed data for both uniaxial and equibiaxial deformation, the main goal of this investigation was to determine the possibility of eliminating the need for expensive equibiaxial testing altogether. Based on the results of this work, it can be concluded that the models considered are incapable of modeling equibiaxial stress-strain response based solely on parameters fitted uniaxially, and thus equibiaxial data is still necessary in order to model processes in which biaxial deformations play a large part.

4.2: Recommendations

In this thesis, five constitutive models were used to characterize the stress-strain response of two polymers commonly used in thermoforming and blowmolding operations, in uniaxial and equibiaxial elongational deformation. The predictions of the

various models were compared to the experimental data over a range of strain rates and temperatures, and conclusions were drawn regarding the apparent worthiness of the models, in terms of their quality of predictions and the ease with which the models are implemented. In addition, the ability of four of the models - Ogden, G'Sell, Two-Term Polynomial and K-BKZ - to predict biaxial response using parameters fit uniaxially was investigated.

To further research the use and application of constitutive models for numerical simulations of polymer processing operations, the following recommendations are made:

1. Further data, with many different polymers, be obtained for both uniaxial and biaxial deformations. These tests should be carried out at constant strain rates to facilitate modeling, and should cover the broad range of strains, strain rates and temperatures found in common processing conditions. Ideally, both the uniaxial and biaxial tests would be conducted at similar strain rates and temperatures, in order to aid in the comparison and modeling of both of the data sets.

2. More work should be conducted in constructing a more accurate constitutive model. This model should be one that is relatively easy to fit to experimental data and implement into a computer code, yet give accurate results, not only for the conditions under which it was fitted, but also over a broad range of strains, strain rates and temperatures. In addition, it would ideally be able to accomplish what none of the models studied herein were able to do; namely, to predict biaxial response based solely on parameters fit to uniaxial data.

3. Further study is needed to characterize the processes to which the models would, and would not, apply. For instance, if a process is a relatively fast one (high strain rate), then viscous effects would play a lesser role, and an elastic model would suffice. However, if viscous effects are found to contribute significantly, a more complicated (and thus more difficult to implement) viscoelastic model would be needed. Foreknowledge of the dominant effect - viscous or elastic - would allow one to choose the appropriate constitutive model, and place more faith in the simulation results, thus reducing the need for expensive prototype fabrication and testing.

REFERENCES

(1). Tadmor, Z., Gogos, C. G., "Principles of Polymer Processing", John Wiley & Sons, New York (1979).

(2). Beer, F., Johnston, E., "Mechanics of Materials", SI Metric Edition, McGraw-Hill Ryerson, Toronto (1985).

(3). Lai, M. O., Holt, D. L., *Journal of Applied Polymer Science*, **19**, 1209 (1975).

(4). Axtell, F. H., Haworth, B., *Plastics, Rubber and Composites Processing and Applications*, **22**, 127 (1994).

(5). Ghafur, M. O., "Comparison of Numerical Simulations and Experimental Results in Thermoforming and Blowmolding", M.Eng. Thesis, McMaster University (1994).

(6). Gruenwald, P. E., "Thermoforming: A Plastics Processing Guide", Technomic, Lancaster (1987).

(7). Larson, R. G., "Constitutive Equations for Polymer Melts and Solutions", Butterworth (1988).

(8). Davies, A. R., "Rheological Fundamentals of Polymer Processing", NATO Advanced Study Institute, Lavor, Portugal (1994).

(9). Bird, R. B., Armstrong, R. C., and Hasseger, O., "Dynamics of Polymeric Liquids, Vol. I, Fluid Mechanics", Wiley, New York (1977).

(10). Astarita, G., Marrucci, G., "Principles of Non-Newtonian Fluid Mechanics", McGraw-Hill, London (1974).

(11). Mooney, M., *Journal of Applied Physics*, **11**, 582 (1940).

(12). Rivlin, R. S., *Phil. Trans. R. Soc. Lond.*, **240**, 459 (1948).

(13). Rivlin, R. S., *Phil. Trans. R. Soc. Lond.*, **241**, 379 (1948).

(14). Ogden, R. W., *Proc. R. Soc. Lond. A.*, **326**, 565 (1972).

(15). Hill, R., "Problems in Mechanics", Novozhilov Anniversary Volume, Leningrad (1970).

(16). Treloar, L. R. G., *Trans. Faraday Soc.*, **39**, 241 (1943).

(17). G'Sell, C., et. al., *Journal of Materials Science*, **30**, 701 (1995).

(18). Vantal, M., "Etude Numerique et Experimentale du Thermoformage de Polymeres", Ph. D. Thesis, L'École Nationale Superieure des Mines de Paris (1995).

(19). G'Sell, C., Leterrier, Y., *Journal of Materials Science*, **23**, 4209 (1988).

(20). G'Sell, C., Jonas, J. J., *Journal of Materials Science*, **14**, 583 (1979).

(21). Kaye, A., College of Aeronautics, Note No. 134, Cranfield (1962).

(22). Bernstein, B., Kearsley, E. A., Zapas, L. J., *Transactions of the Society of Rheology*, **VII**, 391 (1963).

(23). Wagner, M. H., *Rheol. Acta.*, **15**, 136 (1976).

(24). Wagner, M. H., *J. Non-Newtonian Fluid Mech.*, **4**, 39 (1978).

(25). Wagner, M. H., Raible, T., Meissner, J., *Rheol. Acta.*, **18**, 427 (1979).

(26). Wagner, M. H., Demarmels, A., *J. Rheol.*, **24**, 943 (1990).

(27). Isayev, A. I., ed., "Modeling of Polymer Processing: Recent Developments", Hanser, New York (1991).

(28). Cross, A., Haward, R. N., *Journal of Polymer Science*, **11**, 2423 (1973).

(29). Oberst, H., Retting, W., *Journal of Macromol. Sci.- Phys.*, **B5(3)**, 559 (1971).

(30). Andrews, J. M., Ward, I. M., *Journal of Materials Science*, **5**, 411 (1970).

(31). Jäckel, K., *Kolloid Z.*, **137**, 130 (1954).

(32). Lazurkin, Y. S., *Journal of Polymer Science*, **30**, 595 (1958).

(33). Utsuo, A., Stein, R. S., *Journal of Polymer Science*, **5**, 583 (1967).

(34). Haward, R. N., Murphy, B. M., White, E. F. T., *Journal of Polymer Science*, **A2-9**, 801 (1971).

(35). Pezzin, G., Ajroldi, G., Casiraghi, T., Garbuglio, C., Vittadini G., *Journal of Applied Polymer Science*, **16**, 1839 (1972).

(36). Leonov, A. I., Prokunin, A. N., "Nonlinear Phenomena in Flows of Viscoelastic Polymer Fluids", Chapman & Hall, Cambridge University Press (1984).

(37). Mase, G. E., "Theory and Problems of Continuum Mechanics", McGraw-Hill, New York (1970).

(38). Luo, X. L., Mitsoulis, E., *Advances in Polymer Technology*, **10 (1)**, 47 (1990).

(39). Park, H. J., Mitsoulis, E., *J. Non-Newtonian Fluid Mech.*, **42**, 301 (1992).

(40). Kiriakidis, D. G., Mitsoulis, E., *Advances in Polymer Technology*, **12 (2)**, 107 (1993).

(41). Kajiwara, T., Barakos, G., Mitsoulis, E., *Int. J. Polymer Analysis & Characterization*, **1**, 201 (1995).

(42). Barakos, G., Mitsoulis, E., Tzoganakis, C., Kajiwara, T., *Journal of Applied Polymer Science*, **59**, 543 (1996).

(43). Levenberg, K., *Quart. Appl. Math.*, **2**, 164 (1944).

(44). Marquardt, D., *J. Soc. Indust. Appl. Math.* **11 (2)**, 431 (1963).

(45). Smith, A., Hinton, E., Lewis, R., "Civil Engineering Systems Analysis and Design", John Wiley & Sons, New York (1983).

(46). Jeter, M. W., "Mathematical Programming: An Introduction to Optimization", Marcel Dekker, New York (1986).

(47). Kuester, J., Mize, J., "Optimization Techniques With FORTRAN", McGraw-Hill, New York (1973).

(48). Nayak, G. C., Zienkiewicz, O. C., *Int. J. Num. Meth. Eng.*, **5**, 113 (1972).

(49). Zienkiewicz, O. C., Cormeau, I. C., *Archives of Mechanics*, **24 (5-6)**, 873 (1972).

(50). Zienkiewicz, O. C., Cormeau, I. C., *Int. J. Num. Meth. Eng.*, **8**, 821 (1974).

(51). Bellet, M., Massoni, E., Chenot, J. L., *Eng. Comput.*, **7**, 21 (1990).

(52). Schmidt, L. R., Carley, J. F., *Polymer Science and Engineering*, **15 (1)**, 51 (1975).

(53). Chandran, P., Jabarin, S., *Advances in Polymer Technology*, **12 (2)**, 119 (1993).